



ICEBE
IMAGINEERING
NATURE

Master Thesis

Investigation of the presence of minerals on the lactic acid recovery using membrane technology

Carried out for the purpose of obtaining the degree of Master of Science

Diplom-Ingenieur

By

Mohammad Salem

Matr. Nr. 11728321

Under the supervision of

Ao. Univ.Prof. Dipl.-Ing. Dr.techn. Michael Harasek

Senior researcher. Dr.Amal El Gohary Ahmed

Univ.Ass. Dipl.-Ing. Dr.techn. Christian Jordan

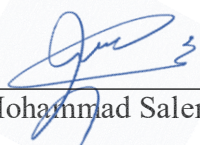
Ph.D. researcher Mayuki Cabrera-González

(E166 Institute of Chemical, Environmental and Bioscience Engineering)

Submitted at Vienna University of Technology

Faculty of Mechanical and Industrial Engineering

Vienna, January 2022


Mohammad Salem



TECHNISCHE
UNIVERSITÄT
WIEN

I confirm that going to press of this thesis needs the confirmation of the examination committee.

Affidavit

In lieu of oath, I declare that I wrote this thesis and performed the associated research myself, using only literature cited in this volume. If text passages from sources are used literally, they are marked as such.

I confirm that this work is original and has not been submitted elsewhere for any examination, nor is it currently under consideration for a thesis elsewhere

Vienna, January 2022


Mohammad Salem

Acknowledgments

First and foremost, I would like to express my heartfelt appreciation to my supervisor, Ao. Univ.Prof. Dipl.-Ing. Dr.techn. **Michael Harasek**, for his continuous encouragement of my master thesis and this research, as well as his patience, inspiration, and vast expertise. His advice was invaluable during the preparation of my thesis. I could not have imagined having a better supervisor and mentor for my study.

A big and heartfelt thanks to my supervisor, senior researcher. Dr.**Amal El Gohary Ahmed**, who stood with me from the beginning to the end of my study, assisted me step by step in the laboratory to conduct all the analyses and measurements required to finish my research. I am very grateful for what she has provided for me. I'd also want to thank her for her compassion and sense of humor. Your encouraging remarks and thoughtful, comprehensive feedback have meant a lot to me.

I am deeply indebted to my supervisor, Univ.Ass. Dipl.-Ing. Dr.techn.**Christian Jordan**, for providing me with the chance to do research and offer important advice during this research. His energy, vision, honesty, and drive have all left an indelible impression on me. He taught me the technique for doing the study and presenting the findings as simply as possible. Working and studying under his supervision was a tremendous pleasure and honor

In addition to my supervisors, I would like to express my heartfelt appreciation to the members of my thesis committee. Ao.Univ.Prof. Dipl.-Ing. Dr.techn.**Andreas Werner** and Ao.Univ.Prof. Dipl.-Ing. Dr.techn.**Franz Winter**.

I am extending my thanks to Ph.D. researcher **Mayuki Cabrera-González** for all she did, her assistance, encouragement, and friendliness. I wish you the best of luck with your Ph.D. study.

I want to express my gratitude to Dipl.-Ing. Dr.techn.**Stefan Beisl**, MSc.**Thomas Jung**, and Univ.Ass. Dipl.-Ing. **Johannes Adamcyk** for their analytical help using the HPLC and ICS equipment.

I'd want to thank my fellow and best friend **Khaled Maamo** for the sleepless nights we spent working together before deadlines, as well as for all the fun we've had during our Master's study in TU Wien over the past two years.

Thank is also extended to the members of the Institute of Chemical, Environmental, and Bioscience Engineering. They supplied me with all the required facilities to finish my study and were always willing to offer what I needed.

Finally, my heartfelt appreciation goes to my lovely, caring, and supporting wife. Your words of support when things became tough were greatly appreciated and remembered. I owe you absolutely everything.

Table of contents

| | |
|--|------|
| Table of contents | I |
| Abstract | IV |
| Zusammenfassung | VI |
| List of figures | VIII |
| List of tables | XII |
| Abbreviations | XIII |
| Symbols | XIV |
| 1. Introduction | 1 |
| 1.1 Motivation and problem statement | 1 |
| 1.2. Previous studies on using membrane technology to separate LA | 2 |
| 1.3. Aim of work | 3 |
| 2. Basic of membrane separation process | 5 |
| 2.1 Types of membranes | 6 |
| 2.1.1 Membranes classification based on their nature | 6 |
| 2.1.1.1 Organic membranes | 6 |
| 2.1.1.2 Inorganic membranes | 8 |
| 2.1.2 Membranes classification based on their structure | 9 |
| 2.1.3 Membranes classification based on their geometry | 10 |
| 2.1.4 Membranes classification based on the transport mechanism | 12 |
| 2.1.5 Classification of membranes according to their average pore sizes | 13 |
| 2.2 Membrane separation fundamental concepts and terminology | 14 |
| 2.3 Characteristics of the membrane-separation process | 16 |
| 2.3.1 Microfiltration | 18 |
| 2.3.2 Ultrafiltration | 18 |
| 2.3.3 Reverse osmosis | 18 |
| 2.3.4 Nanofiltration | 19 |
| 2.3.4.1 Commercial NF membranes and their applications | 20 |
| 2.3.4.2 Mass transport and rejection mechanism in NF membranes | 21 |
| 2.3.4.2.1 Donnan exclusion | 24 |
| 3. Green biorefinery | 27 |
| 3.1. Grass silage | 27 |
| 3.1.1 Grass pretreatment | 28 |

| | |
|---|----|
| 3.1.2 Lactic acid (LA) | 33 |
| 3.1.2.1. Physical properties of LA | 34 |
| 3.1.2.2. Chemistry of LA | 35 |
| 3.1.2.3. Thermodynamic properties of LA | 36 |
| 3.1.2.3.1 Vapor pressures of LAs at different temperatures | 36 |
| 3.1.2.3.2 Temperature dependence of densities of LA | 37 |
| 3.1.2.3.3 Temperature dependence of viscosity of LA | 37 |
| 3.1.2.4 Production of LA | 37 |
| 3.1.2.4.1 Production of LA by chemical synthesis | 38 |
| 3.1.2.4.2 Production of LA by fermentation | 38 |
| 3.1.2.4.2.1 Lactic acid bacteria (LAB) | 40 |
| 3.1.2.4.2.2 Carbohydrates for LA production | 41 |
| 3.1.2.4.2.3 Downstream processing/purification of LA | 42 |
| 3.1.3. Production of LA from grass silage | 43 |
| 4. Experimental equipment and procedure | 44 |
| 4.1 Experimental setup | 44 |
| 4.2 The membranes | 46 |
| 4.3 Chemicals | 46 |
| 4.4 An overview of the conducted experiments | 47 |
| 4.4.1 Determination of the optimal operating temperature for the LA recovery experiments | 47 |
| 4.4.1.1 Water permeability | 47 |
| 4.4.1.2 Model solution filtration | 48 |
| 4.4.2. Determination of the optimal pH value for LA recovery Experiments | 48 |
| 4.4.2.1 Water permeability | 48 |
| 4.4.2.2 Model solution filtration | 48 |
| 4.4.3. Determination of the best membrane for LA recovery Experiments | 49 |
| 4.4.3.1 Water permeability | 49 |
| 4.4.3.2 Model solution filtration | 49 |
| 4.4.4. Experimental investigation on the effect of different minerals on LA recovery. | 50 |
| 4.4.4.1 Water permeability | 50 |
| 4.4.4.2 Model solution filtration | 50 |
| 5. Analytical methods | 54 |
| 5.1 pH and conductivity measurements | 54 |
| 5.2 Determination of anions and cations concentration | 54 |

| | |
|---|----|
| 5.3 Determination of the concentration of the organic solutes | 56 |
| 6. Results and discussion | 59 |
| 6.1 Determination of the optimal operating temperature for the LA recovery | 59 |
| 6.2. Determination of the optimal pH value for LA recovery | 61 |
| 6.3. Determination of the best membrane for LA recovery | 64 |
| 6.4. Investigation of the effect of different minerals on LA recovery | 65 |
| 6.4.1 LA separation performance from the model solution with and without a binary ionic system | 67 |
| 6.4.1.1 Ionic rejection of NaCl with and without organic solutes | 68 |
| 6.4.1.2 Ionic rejection of MgCl₂·6H₂O with and without organic solutes | 69 |
| 6.4.1.3 The ionic rejection of CaCl₂ with and without organic solutes | 69 |
| 6.4.1.4 The ionic rejection of Na₂SO₄ with and without organic solutes | 70 |
| 6.4.1.5 The ionic rejection of NH₄Cl with and without organic solutes | 70 |
| 6.4.1.6 The ionic rejection of KOH with and without organic solutes | 71 |
| 6.4.2 LA separation performance from the model solution with and without a ternary ionic system | 72 |
| 6.4.2.1 The ionic rejection of NaCl+ MgCl₂·6H₂O with and without organic solutes | 73 |
| 6.4.2.2 The ionic rejection of CaCl₂+MgCl₂·6H₂O with and without organic solutes | 74 |
| 6.4.2.3 The ionic rejection of NaCl+Na₂SO₄ with and without organic solutes | 74 |
| 6.4.3 LA separation performance from the model solution with and without a quaternary ionic system. | 75 |
| 6.4.3.1 The ionic rejection of NH₄Cl+KOH with and without organic solutes | 76 |
| 6.4.3.2 The ionic rejection of MgCl₂·6H₂O + Na₂SO₄ with and without organic solutes | 77 |
| 6.4.3.3 The ionic rejection of CaCl₂ + KOH with and without organic solutes | 78 |
| 6.4.4 LA separation performance from the model solution with and without an octonary ionic system | 79 |
| 6.4.4.1 The ionic rejection of NaCl + MgCl₂·6H₂O + CaCl₂ + Na₂SO₄ + NH₄Cl + KOH with and without organic solutes | 79 |
| 7. Summary and conclusions | 81 |
| 8. References | 84 |

Abstract

Lactic acid (LA) is an essential product due to its massive uses, particularly in the pharmaceutical, cosmetic, chemical, and food sectors. LA is manufactured either fermentatively or chemically; around 90 % of all LA produced globally is produced by bacterial fermentation. The LA industry, which uses a fermentation process, faces many challenges to be overcome, which are the process of separation and purification of the many accompanying by-products and the cost of recovery.

Membrane-based technology has gained prominence in recent years in the production of LA through the purification of a fermentation broth due to low energy consumption and high process efficiency, particularly Nanofiltration (NF).

NF membranes can retain components with a molecular weight cut off in the range 200-1000 Dalton. Additionally, most NF membranes develop a fixed electric charge in aqueous environments due to surface group ionization and/or adsorption of charged species from the solution onto the membrane surface. Consequently, NF membranes separate solutes by a complicated process that includes steric hindrance, Donnan exclusion, and dielectric exclusion (in the case of charged solutes).

In the present work, various experiments were conducted initially on four commercially available NF membranes (NF-Alfa Laval, NF Toray, NF270, and Selro MPF-36) using synthetic grass silage (model solution) to determine the best membrane, the optimal operating temperature, and pH value for LA recovery. After determining the optimal temperature, pH, and best membrane, additional experiments were conducted to investigate the effect of different minerals (NaCl, MgCl₂·6H₂O, CaCl₂, Na₂SO₄, NH₄Cl, and KOH) on the LA and acetic acid (AA) separation process.

NF-Alfa Laval achieves a high LA recovery at room temperature and pH value around 2.

The permeate flux and the LA rejection rate by an NF-Alfa Laval membrane were changed remarkably when minerals (NaCl, MgCl₂·6H₂O, CaCl₂, Na₂SO₄, NH₄Cl, and KOH) were added to the organic solution.

The rejection rate of LA and AA increased when a binary ionic system ((K⁺ + OH⁻) or (Na⁺ + SO₄²⁻)) were added to the solution, in opposition to; the rejection rate of LA and AA decreased when a binary ionic system ((Na⁺ + Cl⁻), (NH₄⁺ + Cl⁻), (Ca²⁺ + Cl⁻), or (Mg²⁺ + Cl⁻)) were added to the solution.

When ternary ionic system ((Mg²⁺ + Na⁺ + Cl⁻), or (Mg²⁺ + Ca²⁺ + Cl⁻)) were added to the solution, the rejection rate of LA and AA increased, in opposition to, the rejection rate of LA and AA decreased when the ternary ionic system (Na⁺ + Cl⁻ + SO₄²⁻) was added to the solution.

When quaternary ionic systems ((NH₄⁺ + Cl⁻ + K⁺ + OH⁻), (Na⁺ + Cl⁻ + Mg²⁺ + SO₄²⁻), or (Ca²⁺ + Cl⁻ + K⁺ + OH⁻)) were added to the solution, the rejection rate of LA and AA decreased.

When the octonary ionic system ($\text{Na}^+ + \text{K}^+ + \text{NH}_4^+ + \text{Mg}^{2+} + \text{Ca}^{2+} + \text{OH}^- + \text{Cl}^- + \text{SO}_4^{2-}$) was added to the solution, the rejection rate of LA and AA decreased.

The addition of an ionic system (binary, ternary, quaternary, or octonary ionic system) did not affect the rejection of glucose (Glu) and fructose (Fru). Since all membranes were compressed before the filtering operation, the rejection of Glu and Fru may be attributed to the steric hindrance effect.

On the other hand, our investigation confirmed that the membrane is positively charged when the feed solution's pH is less than 4.5 and negatively charged when the feed solution's pH is more than 4.5, as shown by the co-ions rejection behavior when they are subjected to the Donnan exclusion.

Because divalent co-ions are exposed to a stronger Donnan exclusion, they have a higher rejection rate, which may explain why salts containing divalent co-ions have a more significant impact on reducing LA and AA rejection.

The LA and AA rejections variation by adding minerals depending on the ionic strength as a result of Hofmeister's effects, pore swelling, the difference in the osmotic pressures of minerals, the electroviscous effect, the compression of the electrical double layer generated at the membrane surface, and the molecules' polarizability.

Zusammenfassung

Milchsäure ist aufgrund ihrer massiven Verwendungen insbesondere in der Pharma-, Kosmetik-, Chemie- und Lebensmittelbranche ein unverzichtbares Produkt. Milchsäure wird entweder fermentativ oder chemisch hergestellt. Etwa 90 % der weltweit produzierten Milchsäure wird durch bakterielle Fermentation hergestellt. Die Milchsäureindustrie, die einen Fermentationsprozess verwendet, steht vor vielen Herausforderungen, die es zu bewältigen gilt, wie der Prozess der Abtrennung und Reinigung der vielen Nebenprodukte und die Kosten der Rückgewinnung. Membranbasierte Technologie insbesondere der Nanofiltration (NF) hat sich in den letzten Jahren bei der Herstellung von Milchsäure durch die Reinigung einer Fermentationsbrühe, aufgrund des geringen Energieverbrauchs und der hohen Prozesseffizienz, durchgesetzt.

NF-Membranen können Komponenten mit einem Molekulargewichts-Cut-Off im Bereich von 200-1000 Dalton ausschließen. Darüber hinaus entwickeln die meisten NF-Membranen in wässrigen Umgebungen, aufgrund von Oberflächengruppenionisation und/oder Adsorption geladener Spezies aus der Lösung auf der Membranoberfläche, eine feste elektrische Ladung. Folglich trennen NF-Membranen gelöste Stoffe durch einen komplizierten Prozess, der sterische Hinderung, Donnan- und dielektrische Effekte (im Fall von geladenen gelösten Stoffen) umfasst.

In der vorliegenden Arbeit wurden zunächst verschiedene Experimente an vier kommerziell erhältlichen NF-Membranen (NF-Alfa Laval, NF Toray, NF270 und Selro MPF-36) mit synthetischer Grassilage durchgeführt, um die beste Membran, die optimale Betriebstemperatur und den pH-Wert für die Rückgewinnung von Milchsäure zu bestimmen.

Nach der Bestimmung der optimalen Temperatur des pH-Wertes und der besten Membran wurden zusätzliche Experimente durchgeführt, um den Einfluss verschiedener Mineralien (NaCl, $MgCl_2 \cdot 6H_2O$, $CaCl_2$, Na_2SO_4 , NH_4Cl und KOH) auf den Milchsäuretrennprozess zu untersuchen.

NF-Alfa Laval Membran erreicht bei Raumtemperatur und einem pH-Wert von etwa 2 eine hohe Milchsäurerückgewinnung.

Durch Zugabe von Salzen (NaCl, $MgCl_2 \cdot 6H_2O$, $CaCl_2$, Na_2SO_4 , NH_4Cl und KOH) zur organischen Lösung änderten sich der Permeatfluss und Ausschlussrate der Milchsäure und der Essigsäure einer NF-Alfa-Laval-Membran deutlich.

Es konnte festgestellt werden, dass die Ausschlussrate von Milchsäure und Essigsäure zunimmt, wenn der Lösung ein binäres Ionensystem ($(K^+ + OH^-)$ oder $(Na^+ + SO_4^{2-})$) zugesetzt wurde. Im Gegensatz dazu wurde gefunden, dass die Ausschlussrate von Milchsäure und Essigsäure abnimmt, wenn die binäre Ionensysteme ($(Na^+ + Cl^-)$, $(NH_4^+ + Cl^-)$, $(Ca^{2+} + Cl^-)$ oder $(Mg^{2+} + Cl^-)$) der Lösung zugesetzt wurden.

Wenn der Lösung ein ternäres Ionensystem ($(\text{Mg}^{2+} + \text{Na}^+ + \text{Cl}^-)$, oder $(\text{Mg}^{2+} + \text{Ca}^{2+} + \text{Cl}^-)$) zugesetzt wurde, erhöhte sich die Ausschlussrate von Milchsäure und Essigsäure, während die Ausschlussrate von Milchsäure und Essigsäure abnahm, wenn $(\text{Na}^+ + \text{Cl}^- + \text{SO}_4^{2-})$ der Lösung zugesetzt wurde.

Wenn der Lösung ein quartäres ionisches System ($(\text{NH}_4^+ + \text{Cl}^- + \text{K}^+ + \text{OH}^-)$, $(\text{Na}^+ + \text{Cl}^- + \text{Mg}^{2+} + \text{SO}_4^{2-})$, oder $(\text{Ca}^{2+} + \text{Cl}^- + \text{K}^+ + \text{OH}^-)$) zugesetzt wurde, verringerte sich die Ausschlussrate von Milchsäure und Essigsäure.

Wenn der Lösung ein oktonisches Ionensystem $(\text{Na}^+ + \text{K}^+ + \text{NH}_4^+ + \text{Mg}^{2+} + \text{Ca}^{2+} + \text{OH}^- + \text{Cl}^- + \text{SO}_4^{2-})$ zugesetzt wurde, verringerte sich die Ausschlussrate von Milchsäure und Essigsäure.

Die Zugabe eines ionischen Systems (binäres, ternäres, quaternäres oder oktonäres Ionensystem) hatte keinen Einfluss auf die Ausschlussrate von Glucose und Fructose. Da alle Membranen vor dem Filtrvorgang komprimiert wurden, kann die Zurückweisung von Glucose und Fructose auf den sterischen Hinderungseffekt zurückgeführt werden.

Andererseits bestätigte unsere Untersuchung, dass die Membran positiv geladen ist, wenn der pH-Wert der Beschickungslösung weniger als 4,5 beträgt. Er ist negativ geladen, wenn der pH-Wert der Beschickungslösung mehr als 4,5 beträgt. Dies wurde durch das Co-Ionen-Abstoßungsverhalten gezeigt, wenn die Co-Ionen dem Donnan-Ausschluss ausgesetzt werden.

Da zweiwertige Co-Ionen einem stärkeren Donnan-Ausschluss ausgesetzt sind, haben sie eine höhere Abstoßungsrate, was erklären könnte, warum Salze, die zweiwertige Co-Ionen enthalten, einen signifikanteren Einfluss auf die Verringerung des Milchsäureausschlusses haben, indem sie die, durch die erhöhte Abstoßung im Inneren Poren verursachte Schwellung, erhöhen.

Die Milchsäure- und Essigsäure-Ausschlussraten ändern sich durch Zugabe von Salzen in Abhängigkeit von der Ionenstärke des zugegebenen Salzes infolge der Hofmeister-Effekte, der Porenquellung, der Differenz der osmotischen Drücke der Salze, des elektroviskosen Effekts, der Kompression der elektrisch erzeugten Doppelschicht an der Membranoberfläche und die Polarisierbarkeit der Moleküle.

List of figures

| | |
|--|----|
| Figure 1. Graphical representation of the aim of the work..... | 4 |
| Figure 2. The two main types of membrane filtration: dead-end filtration (A), and cross-flow (Nagy 2019b)..... | 5 |
| Figure 3. The classification of membranes, adopted from (Dai et al. 2016)..... | 6 |
| Figure 4. Schematic representation of the asymmetric inorganic membrane (Tan and Li 2015). | 8 |
| Figure 5. Schematic diagrams of the membrane types based on their structure: (a) symmetric porous membrane; (b) symmetric nonporous/dense membrane; (c) immobilized liquid membrane; (d) asymmetric membrane with porous selective layer; (e) asymmetric membrane with dense selective layer (Tan and Li 2015). | 10 |
| Figure 6. Schematic figure of the tubular membrane module (Nagy 2019b). | 10 |
| Figure 7. Schematic figure of the plate-and-frame module (Nagy 2019b). | 11 |
| Figure 8. Schematic figure of the spiral-wound module (Nagy 2019b). | 11 |
| Figure 9. Diagram of the hollow-fiber membranes (Synder-filtration 2021). | 12 |
| Figure 10. Diagram of the submerged membrane modules (Nagy 2019b). | 12 |
| Figure 11. Schematic diagram of the permeation in porous and dense membranes (Tan and Li 2015). | 13 |
| Figure 12. Mechanisms of component transport depend on the pore size inside the membrane matrix (Nagy 2019b)..... | 13 |
| Figure 13. Approximate pore size ranges of different types of membranes, compared to dimensions of some components separated by membrane processes (Mikhaylin and Bazinet 2016). | 14 |
| Figure 14. Transmembrane pressure in a cross-flow membrane module (Charcosset 2012). | 16 |
| Figure 15. Osmotic phenomena. At osmotic equilibrium, the osmotic pressure ($\Delta\pi$) across the membrane is counterbalanced by the hydrostatic pressure (ΔP) applied to the concentrated solution (Basile et al. 2015). | 19 |
| Figure 16. NF classification based on operating pressure and separation limit (Melin and Rautenbach 2007)..... | 20 |
| Figure 17. The mechanisms by which solutes are transported across a membrane in NF, adapted from (Roy et al. 2017)..... | 22 |
| Figure 18. Schematic representation of solute exclusion mechanisms in NF, adapted from (Roy et al. 2017)..... | 23 |
| Figure 19. Concentration gradients (single salt, 1 cation: 1 anion) beside the membrane caused by concentration polarization, partition at the pore entrance, concentration gradients inside the | |

| | |
|---|----|
| membrane pores, and partition at the pores outlet are shown in simplified form. (-) anion and (+) cation subscripts, adapted from (Roy et al. 2017). | 23 |
| Figure 20. Retention of Na^+ and Cl^- in the presence of SO_4^{2-} (Sirkar 1992)..... | 25 |
| Figure 21. The Donnan equilibrium in the existence of an ion-selective membrane (Melin and Rautenbach 2007). | 26 |
| Figure 22. The electric double layer In a pore with negatively charged walls (Melin and Rautenbach 2007)..... | 26 |
| Figure 23. A diagrammatic representation of the processes and products generated in green biorefineries, adapted from (Zhang et al. 2015)..... | 27 |
| Figure 24. Grass silage bale (Goeweil 2021). | 28 |
| Figure 25. The structural breakdown of lignocellulosic biomass, adapted from (Muley and Boldor 2017)..... | 29 |
| Figure 26. LA industrial applications, adapted from (Alves de Oliveira et al. 2018). | 34 |
| Figure 27. Two enantiomeric forms of LA (Compounds Identification 2021)..... | 34 |
| Figure 28. LA condensation reactions, adapted from (Auras 2010)..... | 36 |
| Figure 29. The chemical synthesis of LA, adapted from (Kern 2020). | 38 |
| Figure 30. The production of LA by fermentation, adapted from (Kern 2020)..... | 39 |
| Figure 31. When glucose is converted to pyruvate, chemical energy (ATP) and reducing equivalents (NADH) are produced, adapted from (Auras 2010). | 39 |
| Figure 32. LA formation from pyruvate: NADH and NAD are reoxidized; NAD may then be employed in the procedure shown in Figure 31, adapted from (Auras 2010)..... | 40 |
| Figure 33. Schematic diagram of the traditional LA production process includes fermentation (Big Chemical Encyclopedia 2021). | 42 |
| Figure 34. Production of carboxylates from solid biomass (Agler et al. 2011). | 43 |
| Figure 35. Experimental equipment..... | 44 |
| Figure 36. The PolyScience Ultra-low refrigerating/heating circulator. | 45 |
| Figure 37. Block flow diagram of the filtration process unit. | 45 |
| Figure 38. Ultrapure water system. | 46 |
| Figure 39. WTW, model pH/Cond 3320 pH and conductivity meter..... | 54 |
| Figure 40. Dionex ICS-5000+ ion chromatography system..... | 55 |
| Figure 41. Chromatogram for Cl^- and SO_4^{2-} ions. | 56 |
| Figure 42. Chromatogram for Na^+ , Mg^{2+} , Ca^{2+} , K^+ and NH_4^+ ions. | 56 |
| Figure 43. Shimadzu Prominence 20 HPLC System. | 57 |
| Figure 44. The chromatogram for LA, AA, Glu, and Fru. | 58 |

Figure 45. The flux variation with time for LA solution and deionized water before and after filtration for four commercially available NF membranes $T = 25\text{ }^{\circ}\text{C}$, $p = 32\text{ bar}$, $\text{pH} = 2.67$ 59

Figure 46. The flux variation with time for LA solution and deionized water before and after filtration for four commercially available NF membranes $T = 40\text{ }^{\circ}\text{C}$, $p = 32\text{ bar}$, $\text{pH} = 2.67$ 60

Figure 47. The effect of applied temperature on the LA solution permeate flux for four commercially available NF membranes at $p = 32\text{ bar}$, $\text{pH} = 2.67$ 60

Figure 48. The effect of applied temperature on the LA solution rejection for four commercially available NF membranes at $p = 32\text{ bar}$, $\text{pH} = 2.67$ 61

Figure 49. The flux variation with time for LA solution and deionized water before and after filtration for four commercially available NF membranes at $T = 25\text{ }^{\circ}\text{C}$, $p = 32\text{ bar}$, $\text{pH} = 3.8$ 62

Figure 50. The flux variation with time for LA solution and deionized water before and after filtration for four commercially available NF membranes at $T = 25\text{ }^{\circ}\text{C}$, $p = 32\text{ bar}$, $\text{pH} = 6$ 62

Figure 51. The effect of pH on the LA solution permeate flux for four commercially available NF membranes at $p = 32\text{ bar}$, $T = 25\text{ }^{\circ}\text{C}$ 63

Figure 52. The effect of pH on the LA solution rejection for four commercially available NF membranes at $p = 32\text{ bar}$, $T = 25\text{ }^{\circ}\text{C}$ 63

Figure 53. The separation performance of four commercially available NF membranes for LA, AA, Glu, and Fru at $p = 32\text{ bar}$, $T = 25\text{ }^{\circ}\text{C}$, and $\text{pH} = 2.67$ 64

Figure 54. The Hofmeister series of cations, anions, and the relative effect of some salts on promoting hydrophobic interactions, adapted from (Liu et al. 2017) 66

Figure 55. The permeate flux and the rejection of LA, AA, Glu, and Fru with and without a binary ionic system using NF-Alfa Laval Membrane at $p = 32\text{ bar}$, $T = 25\text{ }^{\circ}\text{C}$ 67

Figure 56. Ionic rejection of NaCl with and without organic solutes..... 68

Figure 57. Ionic rejection of $\text{MgCl}_2 \cdot 6\text{H}_2\text{O}$ with and without organic solutes..... 69

Figure 58. The ionic rejection of CaCl_2 with and without organic solutes. 70

Figure 59. The ionic rejection of Na_2SO_4 with and without organic solutes. 70

Figure 60. The ionic rejection of NH_4Cl with and without organic solutes..... 71

Figure 61. The ionic rejection of KOH with and without organic solutes. 72

Figure 62. The permeate flux and the rejection of LA, AA, Glu, and Fru with and without a ternary ionic system using NF-Alfa Laval Membrane at $p = 32\text{ bar}$, $T = 25\text{ }^{\circ}\text{C}$ 72

Figure 63. The ionic rejection of $\text{NaCl} + \text{MgCl}_2 \cdot 6\text{H}_2\text{O}$ with and without organic solutes. 73

Figure 64. The ionic rejection of $\text{CaCl}_2 + \text{MgCl}_2 \cdot 6\text{H}_2\text{O}$ with and without organic solutes..... 74

Figure 65. The ionic rejection of $\text{NaCl} + \text{Na}_2\text{SO}_4$ with and without organic solutes. 75

Figure 66. The permeate flux and the rejection of LA, AA, Glu, and Fru with and without a quaternary ionic system using NF-Alfa Laval Membrane at $p = 32$ bar, $T = 25$ °C..... 75

Figure 67. The ionic rejection of $\text{NH}_4\text{Cl} + \text{KOH}$ with and without organic solutes. 77

Figure 68. The ionic rejection of $\text{MgCl}_2 \cdot 6\text{H}_2\text{O} + \text{Na}_2\text{SO}_4$ with and without organic solutes. 77

Figure 69. The ionic rejection of $\text{CaCl}_2 + \text{KOH}$ with and without organic solutes. 78

Figure 70. The permeate flux and the rejection of LA, AA, Glu, and Fru with and without an octonary ionic system using NF-Alfa Laval Membrane at $p = 32$ bar, $T = 25$ °C. 79

Figure 71. The ionic rejection of $\text{NaCl} + \text{MgCl}_2 \cdot 6\text{H}_2\text{O} + \text{CaCl}_2 + \text{Na}_2\text{SO}_4 + \text{NH}_4\text{Cl} + \text{KOH}$ with and without organic solutes. 80

Figure 72. A graphic summary of the investigation of the presence of minerals on the LA recovery using NF membrane technology. 83

List of tables

| | |
|--|----|
| Table 1. The typical composition of grass silage juice (Ecker et al. 2012)..... | 3 |
| Table 2. Chemical structure of organic polymers used for membrane separation (Nagy 2019b)..... | 7 |
| Table 3. Types of inorganic membranes (Tan and Li 2015). | 9 |
| Table 4. Membrane separation processes (Nagy 2019b). | 17 |
| Table 5. Osmotic pressures at 25 °C (Ooi et al. 2019)..... | 19 |
| Table 6. Commercial NF membranes (Melin and Rautenbach 2007). | 21 |
| Table 7. Overview of pretreatment technology (Way Cern Khor 2017) | 30 |
| Table 8. Physical properties of LA, adapted from (Auras 2010). | 35 |
| Table 9. The density of aqueous solution of various concentrations of LAs at various temperatures (Auras 2010)..... | 37 |
| Table 10. The viscosity of an aqueous solution of various concentrations of LAs at various temperatures (Auras 2010). | 37 |
| Table 11. The properties of the NF membranes. | 46 |
| Table 12. Optimal operating temperature for LA recovery experiments. | 48 |
| Table 13. Optimal pH value for LA recovery experiments. | 49 |
| Table 14. The best membrane for LA recovery experiments. | 50 |
| Table 15. Investigate the effect of different minerals on LA recovery with NF-Alfa Laval membrane at 25 °C and 32 bar experiments. | 51 |
| Table 16. Dionex ICS-5000+ ion chromatography maximum ions concentrations detection limits. | 55 |
| Table 17. Shimadzu Prominence 20 HPLC System's maximum concentration detection limits..... | 58 |

Abbreviations

| | |
|------------------|--|
| AA | Acetic acid |
| AA (sum) | Amino acids |
| ADP | Adenosindiphosphat |
| ATP | Adenosinetriphosphate |
| CA..... | Cellulose acetate |
| CAS number | Chemical Abstracts Service Registry Number |
| CAGR | Compound annual growth rate |
| Fru..... | Fructose |
| Glu | Glucose |
| HPLC | High-performance Liquid Chromatography |
| IC | Ion Chromatography |
| IEX | Ion exchange |
| LA..... | Lactic acid |
| LAB..... | Lactic acid bacteria |
| LIM | Liquid immobilized membrane |
| MF..... | Microfiltration |
| MWCO..... | Molecular weight cut-off |
| NAD..... | Nicotinamide Adenine Dinucleotide |
| NADH | Reduced Nicotinamide Adenine Dinucleotide |
| NF | Nanofiltration |
| OS..... | Organic solutes |
| PPA..... | Polypiperazinamide |
| PES..... | Polyethersulfone |
| PLA..... | Polylactic acid |
| RO..... | Reverse osmosis |
| PVDF | Polyvinylidene fluoride |
| SEDE..... | The Steric, Electric, and Dielectric Exclusion model |
| TF..... | Thin-film |
| UPLC | Ultra-performance liquid chromatography |
| UF..... | Ultrafiltration |
| VFA..... | Volatile fatty acid |
| ZSM-5 | Zeolite Socony Mobil-5 |

Symbols

| Symbol | Meaning | Unit |
|-------------------|---|--|
| α | Activity | [-] |
| $\alpha_{A/B}$ | The separation factor (selectivity) | [-] |
| $C_{i,m}$ | The feed concentration of the species i at the membrane-feed solution interface | [mole .m ⁻³] |
| $C_{i, Feed}$ | The feed concentration of the species i | [mole .m ⁻³] |
| $C_{i, permeate}$ | The permeate concentration of the species i | [mole .m ⁻³] |
| $C_{i, pore}$ | The concentration of the species i inside the pore | [mole .m ⁻³] |
| $D_{i, pore}$ | The intra-pore diffusion coefficient of species i | [m ² .s ⁻¹] |
| D_A | the diffusion coefficient of component A across a membrane | [m ² .s ⁻¹] |
| dp | Average pore diameter | [m] |
| ds | Average molecule diameter | [m] |
| δ_m | The membrane thickness | [m] |
| $\Delta\pi$ | Osmotic pressure | [bar] |
| $\Delta\mu$ | Chemical potential gradient | [kJ .kmol ⁻¹] |
| $\Delta\phi$ | Electrical potential gradient | [V] |
| Δx | Membrane active layer thickness | [m] |
| ε | The membrane porosity | [-] |
| F | Faraday constant | 96485 [C.mol ⁻¹] |
| φ | The internal potential of the phase | [V] |
| γ_i | activity coefficient | [-] |
| J | The permeation flux | [m ³ .m ⁻² .s ⁻¹] |
| J_A | The permeation flux of component A | [m ³ .m ⁻² .s ⁻¹] |
| J_w | Pure water volume flux | [m ³ .m ⁻² .s ⁻¹] |
| $J_{i,pore}$ | The solute flux of the species i | [mol.m ⁻² .s ⁻¹] |
| $k_{i,c}$ | Hydrodynamic coefficient | [m.s ⁻¹] |
| L_p | The membrane's hydraulic permeability | [m ³ .m ⁻² .s ⁻¹ .bar ⁻¹] |
| λ | The free path of molecules | [m] |
| μ | The solvent viscosity | [pa.s] |
| μ_j | The chemical potential | [kJ .kmol ⁻¹] |
| η_j | The electrochemical potential | [V] |

List of abbreviations and symbols

| | | |
|---------------|---|---|
| ϕ_i |Fugacity coefficient | [-] |
| p |Pressure | [bar] |
| p_i^{sat} |Saturation pressure of component i | [bar] |
| P_{in} |The pressure of the bulk solution at the device's inlet | [bar] |
| P_{out} |The pressure of the bulk solution at the device's outlet | [bar] |
| P_f |The pressure on the filtrate side | [bar] |
| R |The retention | [%] |
| R | Ideal gas constant |8,314 [Jmol ⁻¹ .K ⁻¹] |
| r |The pore radius | [m] |
| T | Temperature | [K] |
| T.M.P |The transmembrane pressure | [bar] |
| \tilde{V}_j |Molar volume | [m ³ .kmo1 ⁻¹] |
| x |The coordinate | [m] |
| x_A |Mole fractions of components A in the feed |[-] |
| x_i |Liquid phase compositions | [-] |
| ψ |The local electrical potential inside the pore | [V] |
| y_A |Mole fractions of components A in the permeate | [-] |
| y_i |Vapor phase compositions | [-] |
| z_i |The valence of species i | [eq .mol ⁻¹] |
| z_j |The number of charges of the transported component |[-] |

1. Introduction

1.1 Motivation and problem statement

Production of economically valuable goods via microbial biotechnology has received enormous interest in the past decade. Initially, This topic is mainly related to current problems, such as increasing global energy demand and environmental concerns, which are the primary causes of creating new ways to manufacture virtually every product using green methods (Eş et al. 2018). In addition, because biorefinery uses renewable resources as feedstock, it may help to decrease the carbon footprint and achieve sustainable development.

In Austria, According to official estimates, the potential grassland-biomass may equal 500,000 to 1,000,000 tons of dry matter per year in the future. If the grassland pasture is not appropriately used in the future, the cultural landscape can suffer greatly (Factory of Tomorrow 2001). The fundamental idea is that, similar to petrochemistry, the raw material grassland biomass such as grass, clover, and alfalfa, is utilized in combination with the whole plant to create several more valuable product groups without producing waste. Since grassland biomass does not include a single principal component, such as sugar beet (sucrose) or maize (starch), establishing a multi-product system is appealing (Biorefinery system). An essential facet of the Austrian strategy is the use of silage rather than fresh biomass. Sugars are transformed into lactic acid (LA), and proteins are hydrolyzed to form free amino acids during fermentation. As a result, LA and amino acids are essential components of a Green Biorefinery based on grass silage (Kromus et al. 2004).

LA is an essential organic acid that has received significant attention due to its versatile applications, particularly as one of the essential building blocks for producing biodegradable and biocompatible poly-lactate polymers (PLA). However, it also has many applications in the food, cosmetic, agricultural, and pharmaceutical industries (Abedi and Hashemi 2020).

LA may be produced using fermentation or chemical synthesis methods. (Eş et al. 2018)It is widely known that chemical production results in racemic DL-lactic acid combinations (Alves de Oliveira et al. 2018). Because of this, it isn't easy to regulate the final product's chemical and physical characteristics. It is also inappropriate for usage in the food, pharmaceutical, and medical sectors. In addition, some businesses need LA with high enantiomeric purity for particular purposes. This feature also adds to the appeal of LA generation through fermentation over chemical manufacture.

Approximately 90 % of all LA manufactured globally is obtained from bacterial fermentation (Alves de Oliveira et al. 2018). However, the LA industry, which uses a fermentation process, faces many challenges to be overcome, which are the process of separation and purification of the many

accompanying by-products and the cost of recovery; along with these challenges come environmental issues, with increasingly stringent legislation regarding the use of solvents and waste generation.

As a result, various techniques for LA recovery have been devised to prevent the development of gypsum during the traditional recovery process. Electrodialysis (Heriban et al. 1993), distillation with simultaneous esterification (Choi and Hong 1999), ion exchange resin (Evangelista and Nikolov 1996), and extraction are a few of these techniques (Matsumoto et al. 2003).

Applying the methods mentioned above to grass silage juice seems to be pretty challenging; due to the heterogeneity of the silage microflora, the selective separation of LA needs deft unit procedures to provide an appropriate final product (Danner et al. 2000).

Due to low energy consumption and high process efficiency, innovative approaches using membrane separation processes are continuously developing to augment or entirely replace traditional separation methods (such as distillation, flocculation, sedimentation, and extraction). Membrane filtration is gaining popularity as a green technology owing to its little to no chemical usage and low maintenance requirements; the Membrane-based technology has gained prominence in recent years in the biotechnology sector, particularly the Nanofiltration (NF), owing to its unique separation concept of selective transport based on the molecular sieve effect and/or the charge effect depending on the membrane type employed and the feed characteristics. NF effectively separated monovalent salts and tiny organic molecules from divalent ions and bigger species such as glucose (Glu) and fructose (Fru) by changing the membrane's characteristics, including its surface electrical charges (zeta potential). Due to the unique properties of NF, it can be used to separate the LA present in artificial grass silage from the remaining by-products; this was the primary motivation for studying the effect of the various components such as minerals on the recovery of LA, which is present in synthetic grass silage, using NF membrane technology.

1.2. Previous studies on using membrane technology to separate LA

Various studies have been conducted to date on the separation of LA using membrane technology, such as using membrane technology to recover LA and minerals from acid whey (Talebi et al. 2020). This study showed the possibility of treating acid whey using membrane technology to generate high-quality whey powder at the pilot size. Three different process combinations were evaluated: 1) ultrafiltration and electrodialysis, 2) ultrafiltration, nanofiltration, and electrodialysis, and 3) ultrafiltration, diafiltration, and electrodialysis. All three combinations were effective in reducing the LA and mineral content of acid whey. Furthermore, other research (González et al. 2008), shows that LA can be recovered by NF from whey fermentation broths and artificial solutions. Herefore, the recovery of LA from clarified fermentation broths using NF was investigated in this study. Based on

the feed concentration, flow rate, transmembrane pressure, and pH, the impact of these variables on flux and rejection was determined. Furthermore, other research (Lee et al. 2017). This research describes an integrated membrane separation method using ultrafiltration (UF) and NF for the recovery of LA from the fermentation broth, in conjunction with ion exchange (IEX) and vacuum-assisted evaporation. The UF and NF procedures eliminated the majority of organic and inorganic components from the LA fermentation broth, including microorganisms, Glu, and inorganic salt ions. However, membrane fouling grew severe in the UF process owing to the high concentration of microorganisms and organic chemicals.

Diverse studies have been aimed at determining the effectiveness of recovering LA using membrane technology. However, to the present day, no research has been published in the public literature that investigates the effect of minerals on LA recovery from grass silage using NF membrane technology.

1.3. Aim of work

As mentioned before, this study aims to conduct an experimental investigation into the effect of various minerals on the recovery of LA from synthetic grass silage juice (Model solution) using NF membrane technology.

To accomplish this, synthetic grass silage (Model solution) was made that closely resembles the chemical composition of real grass silage juice. Table 1 shows the typical composition of grass silage juice. Various experiments were conducted initially on four different commercially available NF membranes (NF-Alfa Laval, NF Toray, NF270, and Selro MPF-36) using pure LA solution with change the operating Temperature and pH values to determine:

Table 1. The typical composition of grass silage juice (Ecker et al. 2012).

| Material | Concentration [g.L ⁻¹] |
|--|------------------------------------|
| Lactic acid | 20.4 |
| Acetic acid | 3.31 |
| AA(sum) | 19.3 |
| Arginine | 1.91 |
| Aspartic acid | 2.04 |
| Leucine | 1.84 |
| Glucose | 4.27 |
| Fructose | 6.53 |
| Ca ²⁺ , Mg ²⁺ (sum) | 1.09 |
| Cl ⁻ | 1.01 |
| SO ₄ ²⁻ | 0.23 |
| Other salt components (Na ⁺ , K ⁺ , NH ₄ ⁺) | 4.2 |
| Dry matter | 102 |

The optimal operating temperature and pH value for LA recovery. Furthermore, additional experiments were conducted on these four different commercially available NF membranes using the synthetic grass silage (Model solution) at the determined optimal operating temperature and pH value to determine the best membrane for LA recovery. After determining the optimal temperature, pH, and best membrane, additional experiments were conducted to investigate the effect of different minerals (NaCl, MgCl₂·6H₂O, CaCl₂, Na₂SO₄, NH₄Cl, and KOH) on the LA separation process. Complex mixtures composed entirely of minerals with and without Organic solutes were produced, and solutions containing octonary ionic, quaternary ionic, ternary ionic, or binary ionic systems were obtained.

In this research, the interaction of ions (Na⁺, K⁺, NH₄⁺, Ca²⁺, Mg²⁺, Cl⁻, OH⁻, SO₄²⁻) and organic solutes (Glu, Fru, AA, and LA) and the impact of ions on LA rejection and permeate flux were investigated. The details of these complex feed solutions will be discussed in detail in Chapter 4.

Fig .1 represents a graphical abstract of the aim of this work.

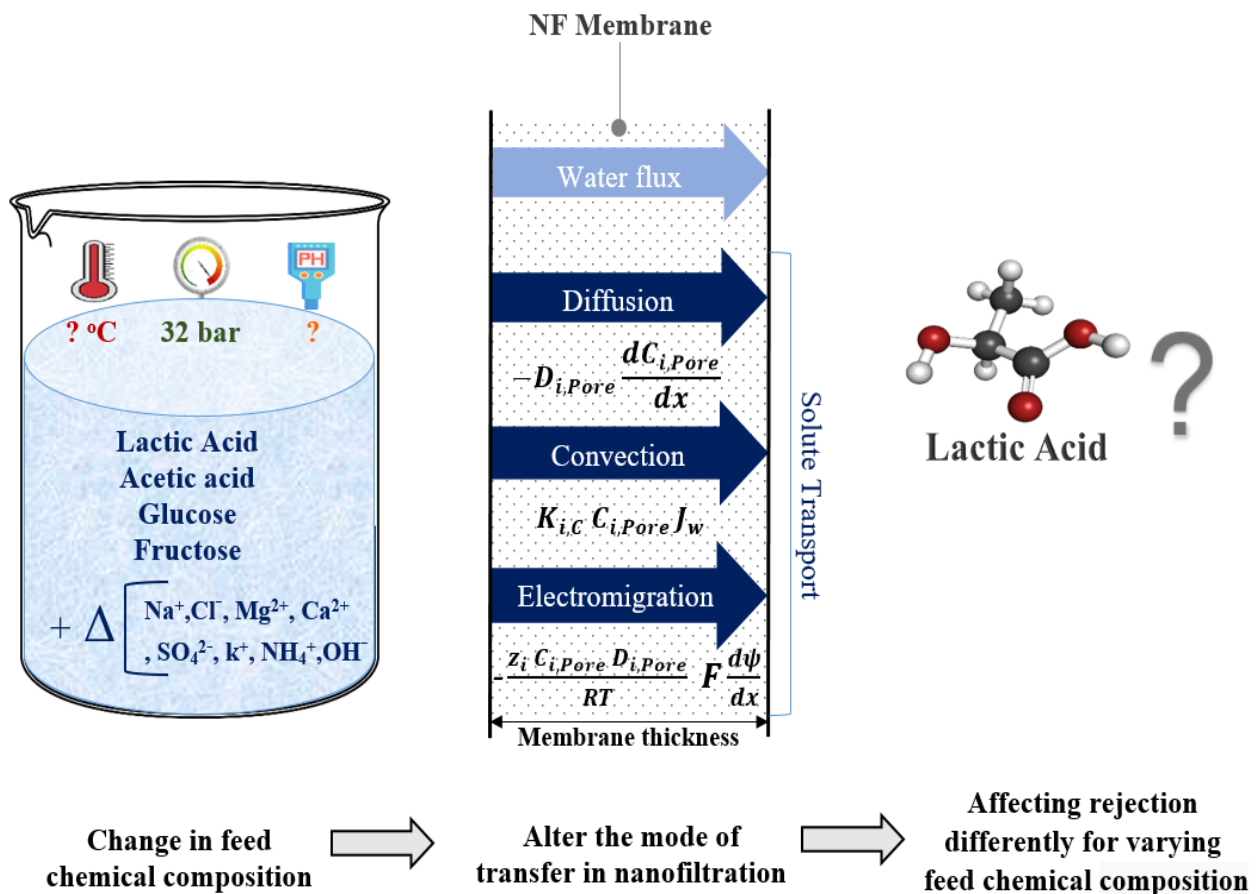


Figure 1. Graphical representation of the aim of the work.

2. Basic of membrane separation process

The membrane is a permeable or semipermeable layer of organic or inorganic materials with typically different structures that often result in very selective separation of some particles in a fluid phase. The concept of a membrane separation process is represented in Fig 2. The membrane divides the feed into two streams retentate and permeate, by adjusting the relative transport rates of distinct species.

Two primary characteristics ultimately determine the separation efficiency of a mixture's components. They are the physical (and eventually chemical) interactions between the transported components and the membrane material and the structure of the membrane matrix. Besides that membrane performance is characterized by flux, retention, and selectivity.

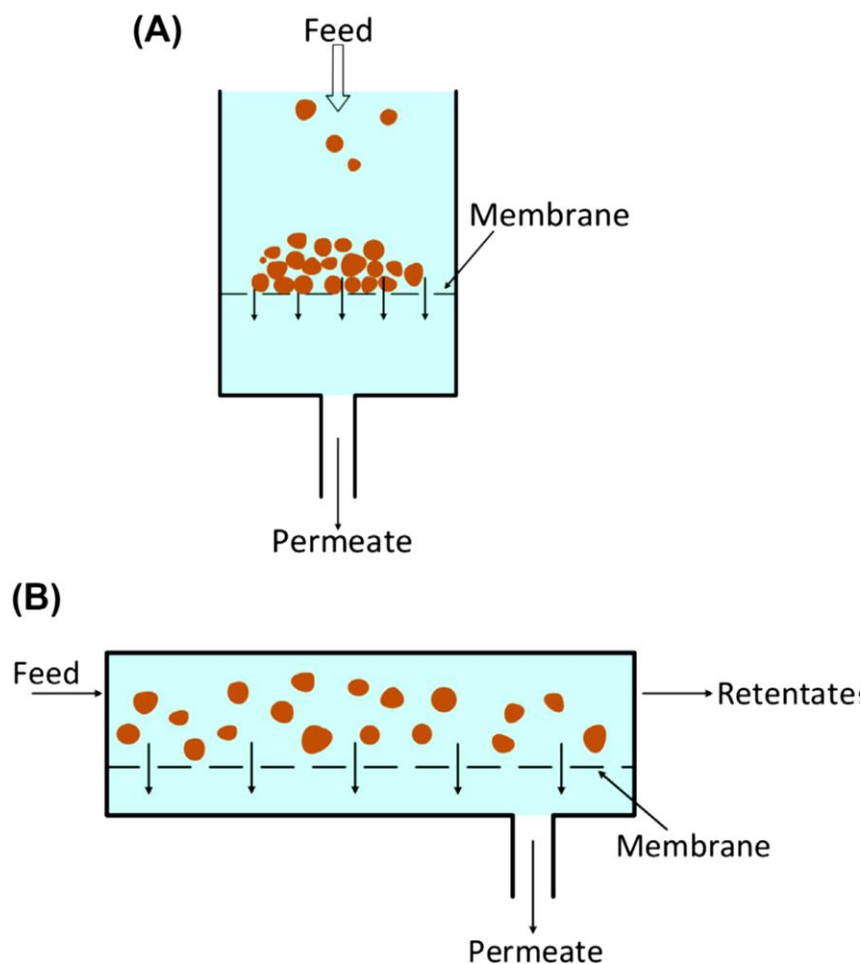


Figure 2. The two main types of membrane filtration: dead-end filtration (A), and cross-flow (Nagy 2019b).

2.1 Types of membranes

Many categorization schemes have been proposed to classify membranes into various classes (Dai et al. 2016), for example as illustrated in Fig 3. Membranes may be categorized based on various factors such as their nature, internal structure, geometry, or the transport mechanism through the membrane.

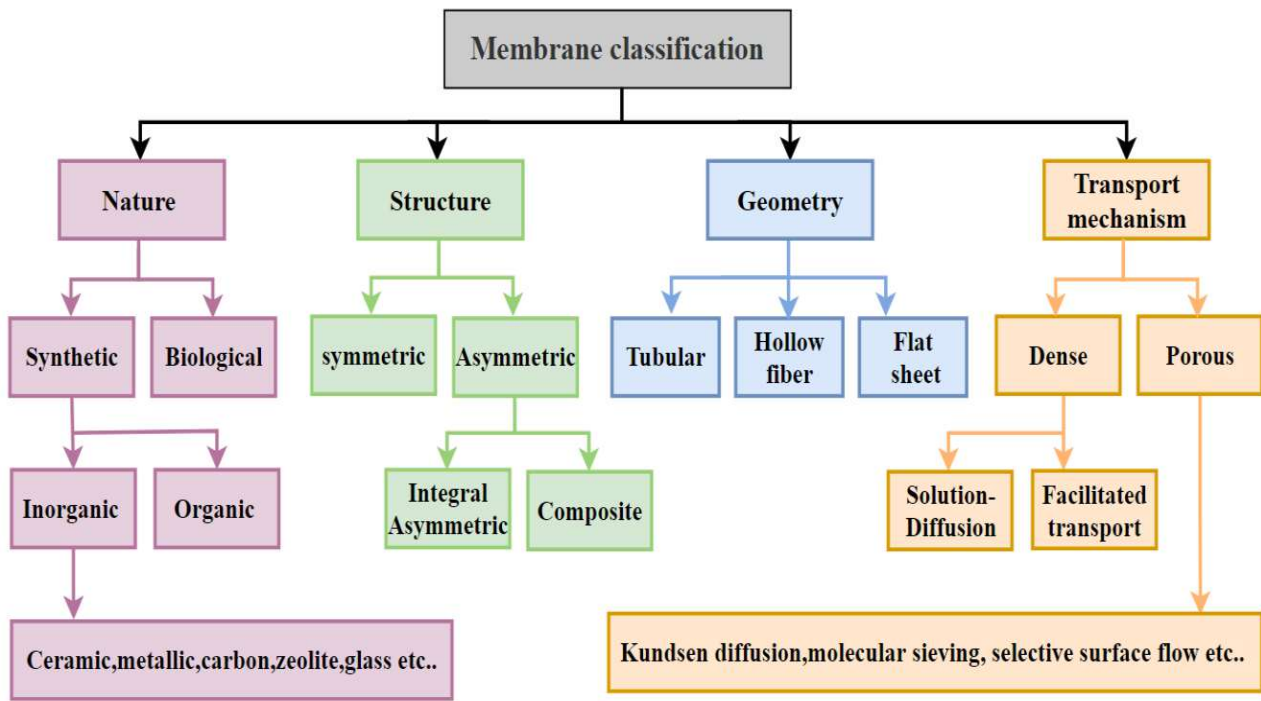


Figure 3. The classification of membranes, adopted from (Dai et al. 2016).

2.1.1 Membranes classification based on their nature

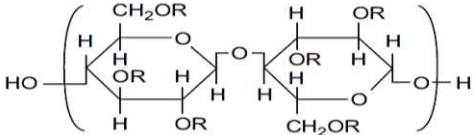
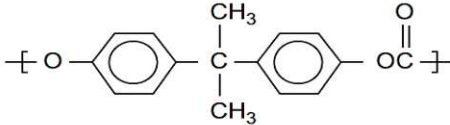
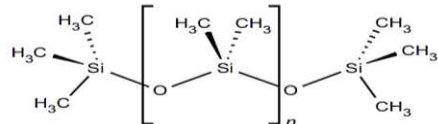
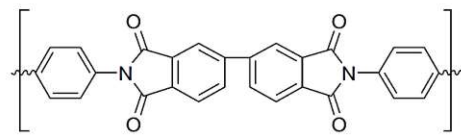
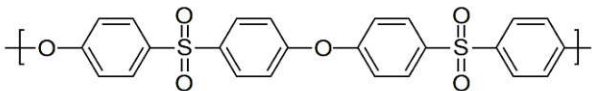
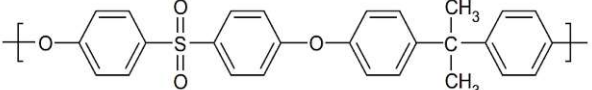
This first classification in Fig 3 distinguishes between naturally occurring biological membranes and synthetic membranes. Biological membranes comprise a self-organizing lipid bilayer 8 nm thick and contain numerous transmembrane proteins specialized in transport tasks. Biological membranes are necessary for all kinds of life on earth because they maintain the integrity of the cell while allowing for the vital, selective exchange of substances with the environment. Furthermore, biological membranes outperform technical membranes in terms of selectivity and flow and are thus sometimes used as a model for developing synthetic membranes (Melin and Rautenbach 2007). There are two types of synthetic membranes: liquid membranes and solid membranes. Organic or inorganic materials are used to create synthetic solid membranes.

2.1.1.1 Organic membranes

Organic membranes are primarily used in industry, such as ultrafiltration, microfiltration, nanofiltration, reverse osmosis, pervaporation, and gas separation. Organic membranes offer high selectivity and permeability, but the pH of the solution limits their stability in various solvent liquids.

However, at higher temperatures, their uses are similarly limited. Table 2 lists the chemical structures of the most commonly utilized organic membranes.

Table 2. Chemical structure of organic polymers used for membrane separation (Nagy 2019b).

| Polymer | Chemical Structure |
|-------------------------|--|
| Polyethylene | $\text{[-CH}_2\text{-CH}_2\text{-]}$ |
| Polypropylene | $\text{[-CH}_2\text{-CH(CH}_3\text{)-]}$ |
| Polyvinylalcohol | $\text{[-CH}_2\text{-CH(OH)-]}$ |
| Polyacrylonitrile | $\text{[-CH}_2\text{-CH(CN)-]}$ |
| Cellulose acetate |  |
| Polyvinylchloride | $\text{[-CH}_2\text{-CH(Cl)-]}$ |
| Polycarbonate |  |
| Polydimethylsiloxane |  |
| Polyimide |  |
| Polyethersulfone |  |
| Polyvinylidene fluoride | $\text{[-CH}_2\text{-CF}_2\text{-]}$ |
| Polysulfone |  |

Polysulfone (PS) and polyethersulfone (PES) are common materials used in ultrafiltration, nanofiltration, and reverse osmosis. Polypropylene (PP) and polyvinylidene fluoride (PVDF) is a common polymer used in microfiltration (Nagy 2019b). One significant disadvantage of these polymers is their intrinsic hydrophobicity, which causes undesirable fouling, leading to reduced separation performance, higher separation costs, and a narrower operating range. In addition, organics, inorganics, colloids, microbes attached to the surface, and other chemicals present in the solvent can all induce fouling.

It needs significant intensive work to enhance these membranes' chemical/thermal/pH stability to reduce their hydrophobicity and make them more hydrophilic by surface modification. Cellulose acetate (CA) is a hydrophilic membrane frequently combined with other hydrophobic polymers to create composite membranes like PES/CA and PVDF/CA. As a result, these composite membranes can have excellent antifouling characteristics.

2.1.1.2 Inorganic membranes

Metals, ceramics, zeolites, glasses, and other inorganic materials are used to make inorganic membranes. Inorganic membranes are often made up of several layers of one or more distinct inorganic materials. Inorganic membranes can be symmetric or asymmetric in structure. Symmetric membranes are frequently relatively thick; this is not ideal for achieving high fluxes, which requires thin separation layers. Most suitable inorganic membranes have a multi-layered asymmetric structure, as shown in Fig 4, to achieve high fluxes.

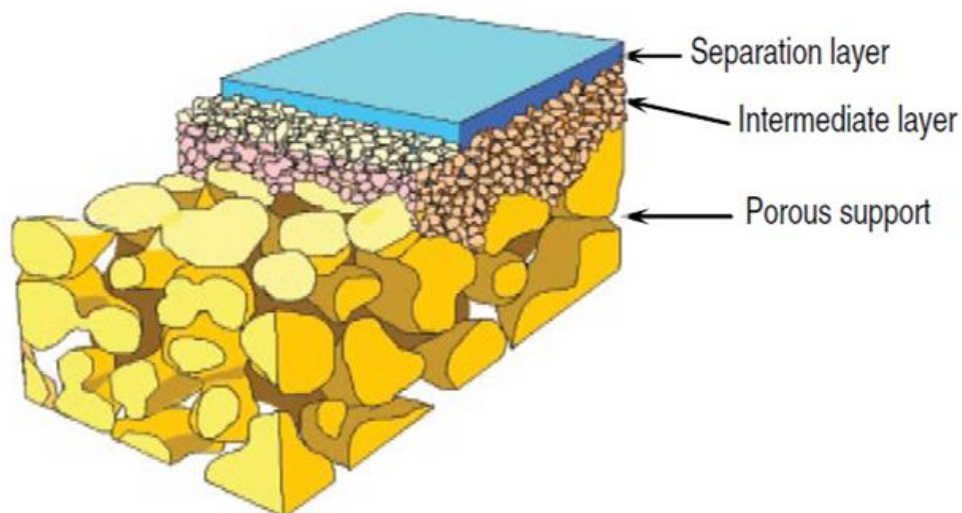


Figure 4. Schematic representation of the asymmetric inorganic membrane (Tan and Li 2015).

A variety of inorganic membranes are outlined in Table 3.

Table 3. Types of inorganic membranes (Tan and Li 2015).

| Material | Structure | | Configuration |
|---|--|------------------------|--|
| Metal or alloys (Pd, Ag, Ni) | Symmetric / composite | Dense | Tube; plate; hollow fiber |
| Stainless steel | Symmetric | Porous | Tube; hollow fiber |
| Metal oxides (Al ₂ O ₃ , ZrO ₂ , TiO ₂ , etc.) | Symmetric / Asymmetric | Porous / mesoporous | Tube; hollow fiber; monolith |
| Glass | Symmetric | Mesoporous | Hollow fiber; tube |
| Silica (SiO ₂) | Composite | Microporous | Plate; tube; hollow fiber; monolith |
| Zeolites (NaA, ZSM-5, etc.) | Composite | Microporous | Plate; tube; hollow fiber |
| Carbon | Symmetric/ asymmetric | Microporous | Tube; hollow fiber |
| Mixed ionic–electronic ceramic conductors | Symmetric/ asymmetric/ composite | Dense | Tube; disk; plate; hollow fiber |
| ZrO ₂ - or CeO ₂ -based ionic conductors | Symmetric/ asymmetric | Dense | Tube; disk; plate; hollow fiber |
| LIM (molten salt) | Symmetric | Dense | Tube; disk |

2.1.2 Membranes classification based on their structure

Membranes are categorized as symmetric or asymmetric based on their internal structure (Baker 2012). In cross-sections, symmetric membranes have consistent pore diameters. Asymmetric membrane pores are often smaller on the membrane surface. Composite membranes include two distinct structures into a single membrane. The several layers can be symmetric or asymmetric, with different pore size distributions, aspect ratios, and thicknesses. Multi-layer membranes are made up of multiple stacked membranes cast individually with the desired pore size and surface properties. The first layer is often employed as a pre-filter, while the application determines the pore size of the second layer. Fig 5 depicts schematic diagrams of the membrane types based on their structure.

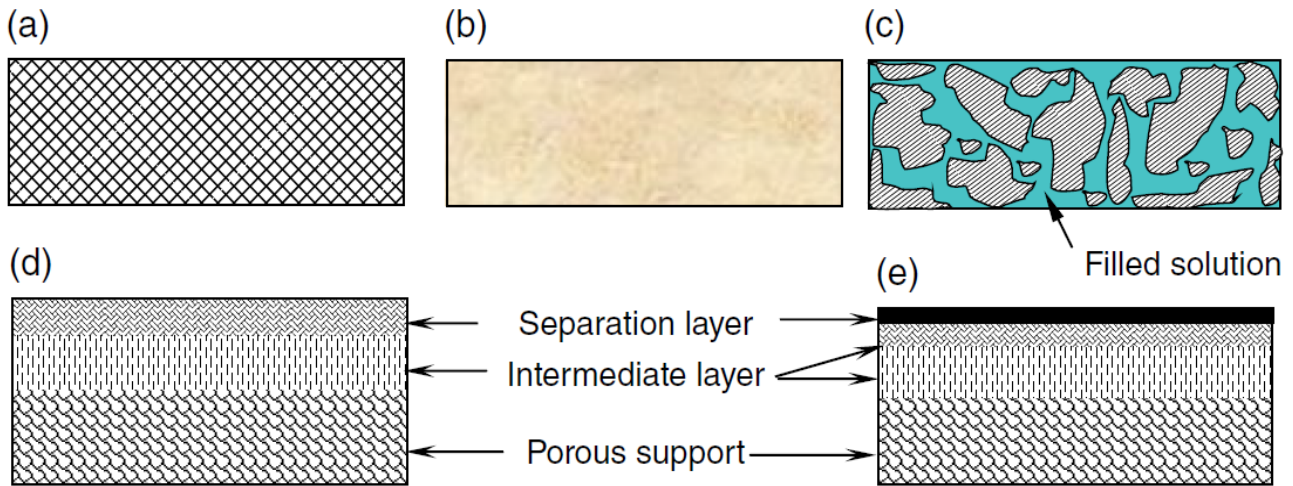


Figure 5. Schematic diagrams of the membrane types based on their structure: (a) symmetric porous membrane; (b) symmetric nonporous/dense membrane; (c) immobilized liquid membrane; (d) asymmetric membrane with porous selective layer; (e) asymmetric membrane with dense selective layer (Tan and Li 2015).

2.1.3 Membranes classification based on their geometry

Membranes are classified into five types based on their geometry (Nagy 2019b):

- Tubular.
- Plate-and-frame.
- Spiral wound
- Capillary hollow fiber.
- Submerged module.

Permselective tubes (typically ceramic) with fairly large inner diameters (about 1 cm) are placed parallel within a module housing in the tubular module. The solutes to be separated are supplied into the lumen of these tubes. In Fig 6, the tubular membrane module is depicted schematically.

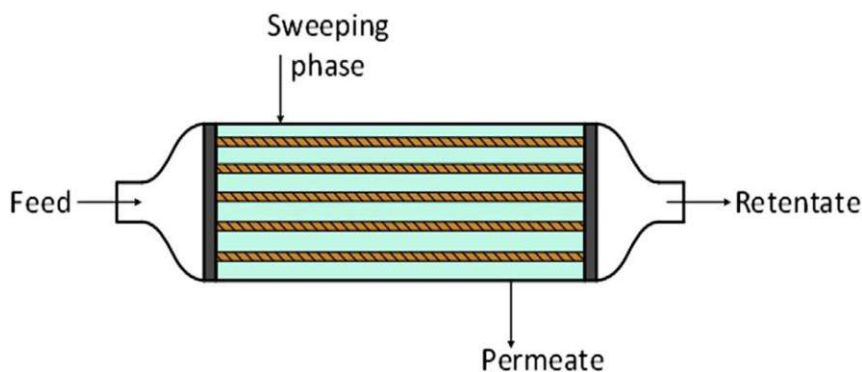


Figure 6. Schematic figure of the tubular membrane module (Nagy 2019b).

In the plate-and-frame module, the selective membrane layer is sandwiched between two support plates, which give flow channels to the fluid on both sides of the membrane; they are collected exiting the plane sheet membrane layers. In Fig 7, the plate-and-frame module is represented schematically.

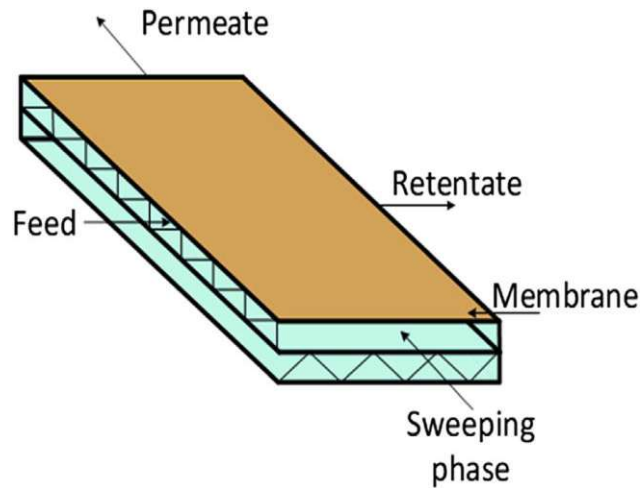


Figure 7. Schematic figure of the plate-and-frame module (Nagy 2019b).

The spiral-wound module forms the plane sheet membrane into a spiral, cylindrical form around a perforated center permeate tube. In Fig 8, the spiral-wound module is demonstrated schematically.

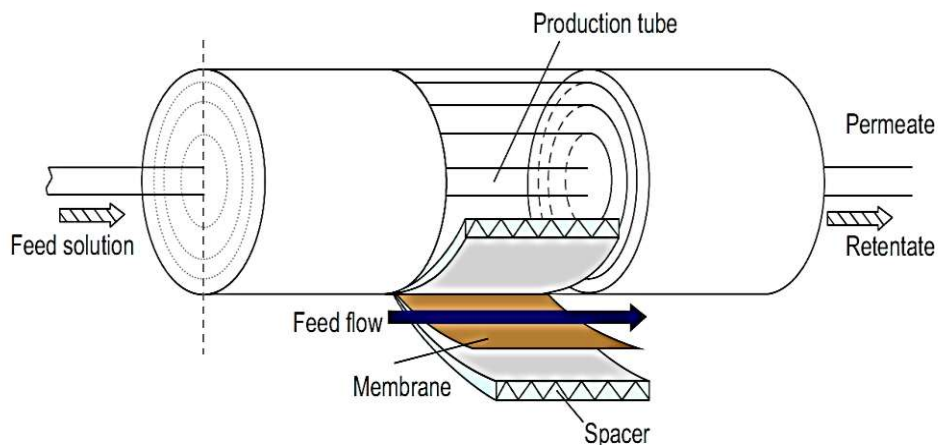


Figure 8. Schematic figure of the spiral-wound module (Nagy 2019b).

The hollow-fiber membranes have an inner diameter of no more than 3 mm. Because of the tiny diameter, this membrane module has a high packing density and a significant overall surface area. In addition, the capillary membrane's design enables a wide range of feeds, including those with high solids content. In Fig 9, the hollow-fiber membrane module is illustrated.

Submerged membrane modules, this module is shown in Fig 10. The low pressure provided in the lumen of the porous membrane pulls the treated water through the membrane, retaining the undesirable solutes and colloids.

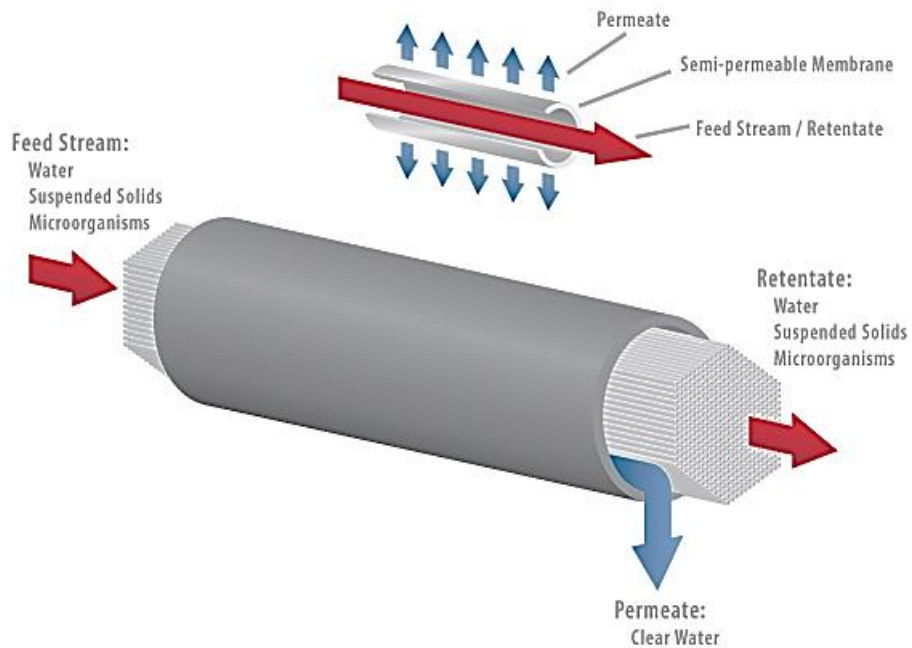


Figure 9. Diagram of the hollow-fiber membranes (Synder-filtration 2021).

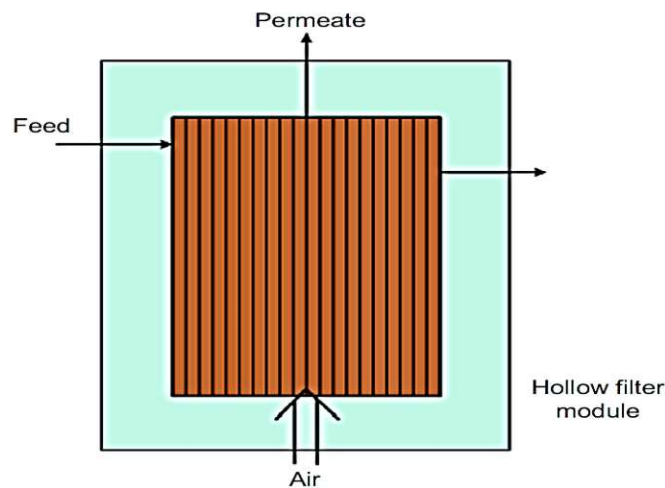


Figure 10. Diagram of the submerged membrane modules (Nagy 2019b).

2.1.4 Membranes classification based on the transport mechanism

Membranes are classified into two types based on their morphological state: dense and porous as shown in Fig 11. Membranes are assumed to be dense when component transport requires a dissolution and diffusion across the substance that forms the membrane.

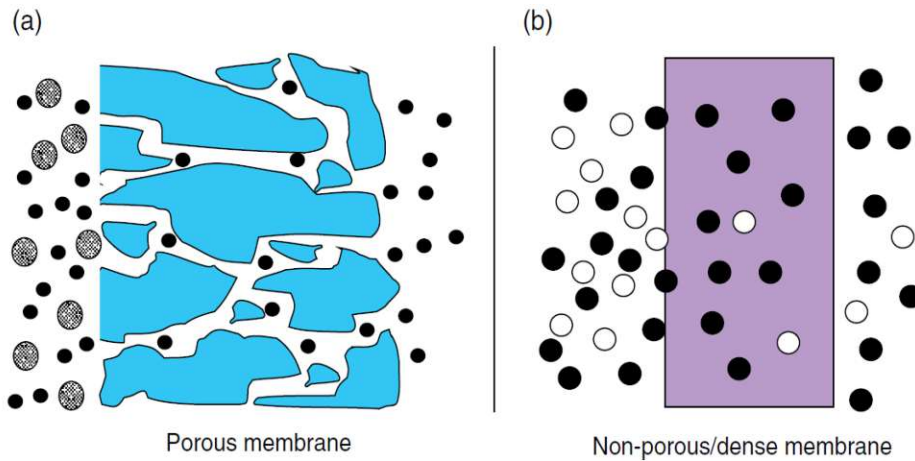


Figure 11. Schematic diagram of the permeation in porous and dense membranes (Tan and Li 2015).

Fig 12 shows the mechanisms of component transport depending on the pore size inside the membrane matrix; when permeate transport occurs predominantly in the continuous fluid phase that fills the membrane pores, the membrane is assumed to be porous (Charcosset 2012).

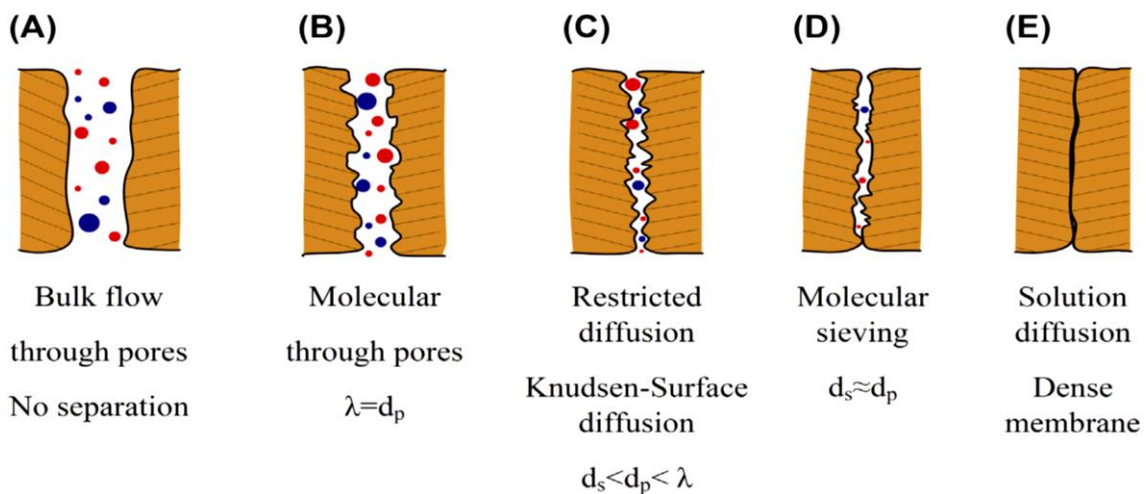


Figure 12. Mechanisms of component transport depend on the pore size inside the membrane matrix (Nagy 2019b).

Where λ denotes the free path of molecules, d_p is the average pore diameter, and d_s is the average molecule diameter.

2.1.5 Classification of membranes according to their average pore sizes

Membranes are typically categorized based on their average pore size as shown in Fig 13. Microfiltration (MF) membranes generally have pore diameters of 0.1 – 1.0 mm and filter particles, cellular materials, and bacteria. Ultrafiltration (UF) membranes have pore diameters of 0.001 – 0.1 mm and may retain species with molecular weights ranging from 300 – 10,000 Da; it can filter more significant biomolecules such as proteins and viruses. Reverse osmosis (RO) membranes retain

solutes with molar masses less than 1000 Da, such as salts and amino acids. Finally, nanofiltration (NF) membranes retain solutes in the molar mass range of 100 - 1000 Da like small polypeptides and divalent ions.

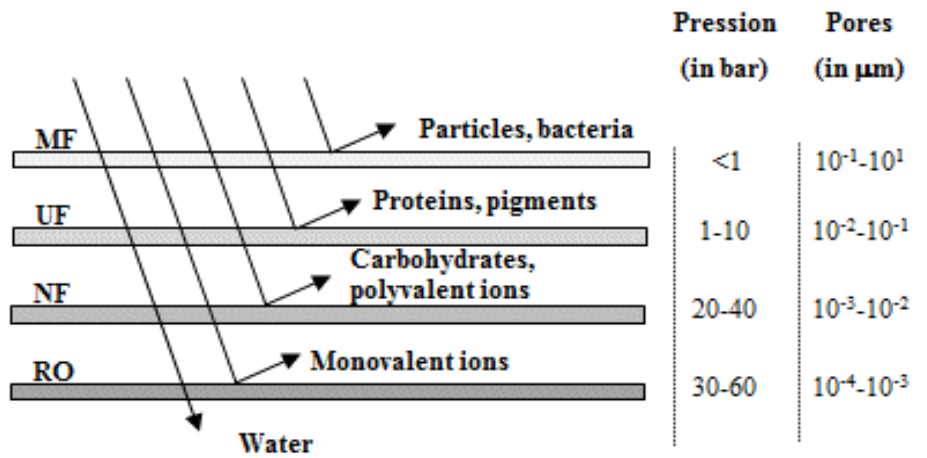


Figure 13. Approximate pore size ranges of different types of membranes, compared to dimensions of some components separated by membrane processes (Mikhaylin and Bazinet 2016).

2.2 Membrane separation fundamental concepts and terminology

The permeation flux [$\text{m}\cdot\text{s}^{-1}$] and membrane permselectivity may be used to characterize its separation performance. The permeation flux is often normalized per unit of pressure [$\text{m}\cdot\text{s}^{-1}\cdot\text{Pa}^{-1}$], referred to as the permeance, or per unit of a thickness [$\text{m}^2\cdot\text{s}^{-1}\cdot\text{Pa}^{-1}$], referred to as the permeability if the separation layer thickness is known.

The term "permeation flux" refers to the molar, volumetric or mass flow rate of the fluid penetrating the membrane per unit area of the membrane. It is defined by the driving force exerted on a specific component and the mechanism used to transport it. In general, the permeation flux (J) across a membrane is proportional to the driving force; the flux–force relationship may be represented by the following linear phenomenological equation Eq. (2.1) (Nagy 2019a):

$$J = -L \frac{dX}{dx} \quad (2.1)$$

Where L is the phenomenological coefficient and dX/dx denotes the driving force, defined as the X gradient (pressure, temperature, concentration, etc.) along the coordinate (x) perpendicular to the transport barrier.

A concentration, pressure, temperature gradient, or electric field may cause mass transfer across a membrane by convection or diffusion of an individual molecule.

Membrane permeation may be triggered by a chemical potential gradient ($\Delta\mu$), an electrical potential gradient ($\Delta\phi$), or the electrochemical potential. Fick's law Eq. (2.2) (Harasek 2018) may represent the transport equation when the concentration gradient is the driving force.

$$J_A = -D_A \frac{dC_A}{dx} \quad (2.2)$$

Where D_A [$m^2 \cdot s^{-1}$] is the diffusion coefficient of component A across a membrane. It is a measure for the mobility of individual molecules over a membrane, and its value is dependent on the species' characteristics, chemical compatibility, membrane material, and membrane structure. Efficient fluxes across the membrane may be achieved by using ultra-thin membranes with large concentration gradients across them in industrial applications.

Darcy's law Eq. (2.3) (Nagy 2019a) may explain the transport equation for pressure-driven convective flow, which is the most frequently used flow description in a capillary or porous medium.

$$J_A = -KC_A \frac{dp}{dx} \quad (2.3)$$

Where dp/dx denotes the pressure gradient present in the porous medium, C_A indicate the concentration of component A in the medium, and K represents a coefficient reflecting the nature of the medium. In general, convective-pressure-driven membrane fluxes are high compared with those obtained by simple diffusion.

A membrane's perm-selectivity toward a mixture is usually described as one of two parameters: the separation factor or retention. The separation factor is defined by Eq. (2.4) (Nagy 2019a):

$$\alpha_{A/B} = \frac{y_A/y_B}{x_A/x_B} \quad (2.4)$$

Where, y_A , y_B , x_A and x_B are the mole fractions of components A and B in the permeate and the retentate streams, respectively.

The retention is defined as the fraction of solute in the feed retained by the membrane, which is expressed by Eq. (2.5) (Harasek 2018):

$$R = \left(1 - \frac{C_p}{C_f}\right) \times 100\% \quad (2.5)$$

Where C_f and C_p denote the feed and permeate solute concentrations, respectively. For a selective membrane, the separation factors have values of 1 or greater, whereas the retention values are 1 or less.

The transmembrane pressure (TMP), Eq. (2.6) (Charcosset 2012) is the difference between the feed and permeate pressures. The transmembrane pressure is calculated for a cross-flow device as the mean of the pressures at the device's inlet and outlet Fig 14:

$$TMP = \frac{(P_{in} + P_{out})}{2} - P_f \quad (2.6)$$

Where P_{in} and P_{out} denote the pressure of the flowing bulk solution at the device's inlet and outlet, typically, the pressure on the permeate side, P_f is negligible.

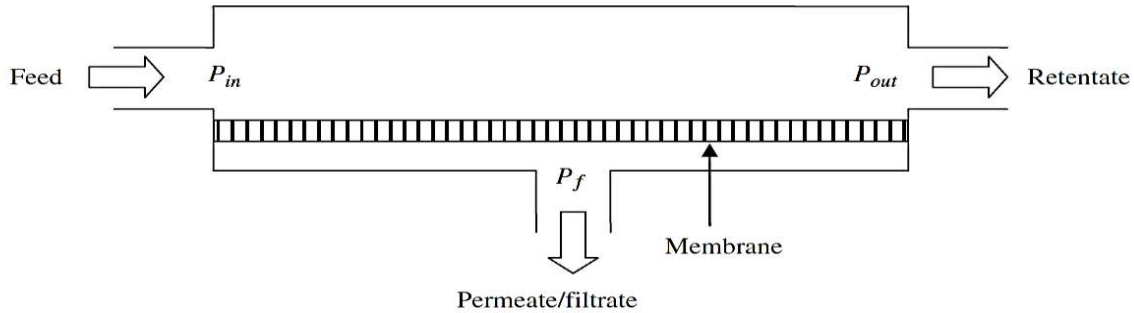


Figure 14. Transmembrane pressure in a cross-flow membrane module (Charcosset 2012).

By increasing the TMP, the permeate flux across the membrane is increased. Therefore, hydraulic permeability is a significant indication of membrane performance. J_A is proportional to the TMP as in Eq. (2.7).

$$J_A = L_p TMP \quad (2.7)$$

Where, L_p is the membrane's hydraulic permeability, other definitions for hydraulic permeability may be employed to consider the impacts of solution viscosity and membrane thickness.

For an idealized membrane consisting of a parallel array of uniform cylindrical pores, L_p is usually written as Eq. (2.8) (Charcosset 2012):

$$L_p = \frac{J_A}{TMP} = \frac{\epsilon r^2}{8\mu\delta_m} \quad (2.8)$$

Where ϵ is the membrane porosity, r is the pore radius, μ is the solvent viscosity, and δ_m is the membrane thickness. Equation (2.8) is only valid in the absence of osmotic pressure and/or solute rejection.

2.3 Characteristics of the membrane-separation process

Various membrane technologies, including microfiltration, ultrafiltration, nanofiltration, reverse osmosis, and even electrodialysis, are currently used in the industry for various applications.

Table 2.3 is divided into two sections: (1) membrane processes driven by pressure; and (2) mass transport properties defined by the membrane's separation efficiency. Membrane pressure-driven processes are based on the differential in pressure between the two sides of the membrane.

Table 4. Membrane separation processes (Nagy 2019b).

| Membrane operation | Driving force | Membrane | Permeant | Transport mechanism |
|---|---------------------------------------|-----------------|--------------------|----------------------------|
| Pressure-driven membrane processes | | | | |
| Reverse osmosis | Pressure difference | Nonporous | Solvent | Solution/diffusion |
| Microfiltration | Pressure difference | Porous | Solvent | Convection, sieve effect |
| Ultrafiltration | Pressure difference | Porous | Solvent | Convection, sieve effect |
| Nanofiltration | Pressure difference | Porous | Solvent | Convection, sieve effect |
| Mass transport-based membrane operations | | | | |
| Gas separation | Concentration gradient | Nonporous | Enriched penetrant | Solution/diffusion |
| Pervaporation | Vapor pressure difference | Nonporous | Enriched penetrant | Solution/diffusion |
| Vapor permeation | Vapor pressure difference | Nonporous | Enriched penetrant | Solution/diffusion |
| Membrane absorption | Concentration gradient | Porous | Solute | Solution/diffusion |
| Membrane desorption | Concentration gradient | Porous | Solute | Diffusion |
| Membrane extraction | Concentration gradient | Porous | Solute | Diffusion |
| Electrodialysis | Electrochemical potential difference | Porous | Solute | Diffusion |
| Gas separation | Concentration and pressure difference | Porous | Enriched penetrant | Diffusion |
| Membrane distillation | Temperature gradient | Porous | Solvent | Diffusion |
| Osmotic distillation | Osmotic pressure difference | Porous | Solvent | Diffusion |
| Pressure-retarded osmosis | Osmotic pressure difference | Nonporous | Solvent, solute | Diffusion |
| Forward osmosis | Osmotic pressure difference | Nonporous | Solvent, solute | Diffusion |
| Liquid membrane | Concentration gradient | Porous | Penetrant | Diffusion |

2.3.1 Microfiltration

Microfiltration (MF) is the oldest membrane process and historically operated in a dead-end mode in small volume applications, which remains an essential industrial application (Basile et al. 2015).

Microfiltration is a pressure-driven separation technique often used to concentrate, purify, or separate macromolecules, colloids, and suspended particles from the solution. The nominal pore diameters of MF membranes are usually in the range of 0.1–1.0 μm . In the food sector, MF processing is extensively utilized for wine, juice, beer clarity, wastewater treatment, and plasma separation for medicinal and commercial purposes. MF is operated at relatively low TMPs (4 bar). However, the feed stream is tangential to the membrane surface to avoid cake layer development and, therefore, membrane fouling.

As trapped particles collect on and inside the membrane, permeate flow diminishes with time. External fouling or cake formation of cells, cell debris, or other rejected particles on the membrane surface is typically reversible. In contrast, deposition and adsorption of small particles or macromolecules within the internal pore structure of the membrane is frequently irreversible (internal fouling).

2.3.2 Ultrafiltration

Ultrafiltration (UF) is a membrane technique that operates similarly to microfiltration but utilizes asymmetric membranes to provide 'tighter' filtrations (Basile et al. 2015). The pore size of the membrane top layer is in the range of 1 nm to 50 nm. The primary foundation for separation is molecule size, although other factors like molecule structure and charge may also play a role.

UF membranes are often operated in a cross-flow mode, in which the feed stream sweeps tangentially over the membrane's surface during filtration, which optimizes the flux rate and membrane life. The applied pressure, typically between 1 and 7 bar, is used mainly to overcome the viscous resistance of liquid penetration through the membrane's porous network.

2.3.3 Reverse osmosis

A process in which a solvent passes through a semipermeable membrane in the direction opposite to that for natural osmosis when subjected to a hydrostatic pressure higher than the osmotic pressure (Ooi et al. 2019). The procedure is shown schematically in Fig 15. The most typical use of reverse osmosis is for salt water and brackish water desalination, the purpose of this procedure is to remove dissolved salts and organic material from water. Due to the high osmotic pressure of seawater 23 bar, reverse osmosis facilities must often run at extremely high pressures up to 70 bar, and its components must be much more durable than those used in other membrane-based technologies.

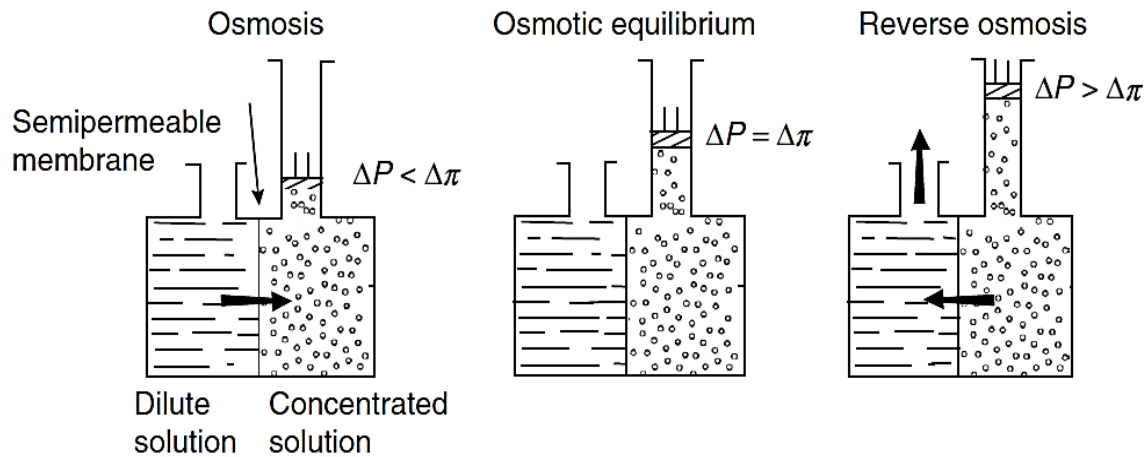


Figure 15. Osmotic phenomena. At osmotic equilibrium, the osmotic pressure ($\Delta\pi$) across the membrane is counterbalanced by the hydrostatic pressure (ΔP) applied to the concentrated solution (Basile et al. 2015).

The osmotic pressure of sodium chloride, seawater, and sucrose solutions as a function of concentration is shown in Table 5

Table 5. Osmotic pressures at 25 °C (Ooi et al. 2019).

| Species | Concentration [mg.L ⁻¹] | Osmotic pressure [Mpa] |
|----------|-------------------------------------|------------------------|
| NaCl | 35,000 | 2.79 |
| | 5,000 | 0.39 |
| | 1,000 | 0.12 |
| | 500 | 0.09 |
| Seawater | 44,000 | 3.23 |
| | 32,000 | 2.31 |
| Sucrose | 34,000 | 0.26 |
| | 340,000 | 2.60 |
| Glucose | 18,000 | 0.24 |
| | 90,000 | 1.21 |

2.3.4 Nanofiltration

Nanofiltration (NF) falls between RO and UF in terms of its ability to reject molecular or ionic species as shown in Fig 16. However, while RO retains organic components with a molar mass of $M = 150$ [kg.Kmol⁻¹] almost entirely, NF membranes achieve significant retention capacities only above a molar mass of $M = 200$ [kg.Kmol⁻¹], which corresponds to a molecular size of approximately 1 nm. In addition, the transmembrane pressure differential required for nanofiltration is 3 to 30 bar less than

the values required for reverse osmosis membranes to produce the same fluxes. Therefore, nanofiltration is sometimes referred to as "loose reverse osmosis" due to its characteristics.

A unique property of NF membranes is their ion selectivity. Whereas salts with monovalent anions may flow through the membrane relatively easily (if not completely), salts with polyvalent anions (e.g., sulfates and carbonates) are retained to a considerably higher degree. Thus, the permeability of salt is mainly influenced by the anion's valence. According to series experiments on various NF membranes, the retention of anions rises in the following order: NO_3^- , Cl^- , OH^- , SO_4^{2-} , and CO_3^{2-} . The retention of cations rises in the following order: H^+ , Na^+ , K^+ , Ca^{2+} , Mg^{2+} , and Cu^{2+} . Nanofiltration's ion selectivity is based on negative charge groups on or in the membrane, which inhibit the penetration of multivalent anions through electrostatic interactions. Charge densities of between 0.5 and 2 meq.g⁻¹ have been reported in the literature (Melin 2004). However, the precise magnitude of this number is a trade secret of the commercial membrane producer. For membranes containing charged groups (such as COO^- , SO_3^- , etc.), the MWCO of ionized molecules could be considerably smaller (Koros 2001)

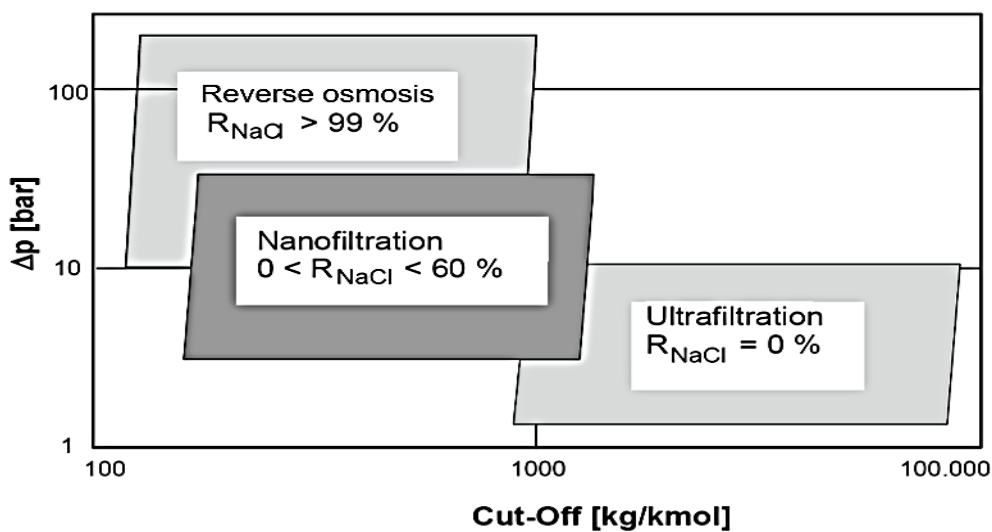


Figure 16. NF classification based on operating pressure and separation limit (Melin and Rautenbach 2007).

2.3.4.1 Commercial NF membranes and their applications

In the early 1960s, the first membranes with nanofiltration characteristics were developed as asymmetrical RO and UF membranes composed of cellulose acetate. Initially, these membranes were referred to as "loose" RO or "tight" UF membranes. Table 6 provides a summary of the presently available NF membranes (status 04/2006).

The membrane characteristics result in the following common areas of use for NF:

- Retention of polyvalent anions during monovalent ion penetration,

- Retention of organic molecules during monovalent salt penetration,
- Retention of organic molecules during monovalent and divalent salt permeation,
- Separation of low and high molecular weight components in aqueous solutions.

Table 6. Commercial NF membranes (Melin and Rautenbach 2007).

| Manufacture | membrane | Active layer / Support layer | pH [-] | P _{max} [bar] | T _{max} [°C] | R [%] | Flux [L.m ⁻² .h ⁻¹] |
|----------------|----------|------------------------------|---------|------------------------|-----------------------|--------------------|--|
| Aquious | AFC40 | N/A | 1.5-9.5 | 60 | 60 | 60 | N/A |
| Dow Filmtec | NF 90 | PA /N/A | 3-10 | 41 | 45 | 85-95 | 32 |
| Dow Filmtec | NF 270 | PA / N/A | 3-10 | 41 | 45 | 40-60 ^a | 63 ^a |
| Ge Osmonics | GE PES | PES / N/A | N/A | N/A | 130 | N/A | N/A |
| Koch | MPS-34 | N/A | 0-14 | 35 | 70 | 35 | 60 ^b |
| Koch | MPS-36 | N/A | 1-13 | 35 | 70 | 10 | 200 ^b |
| Microdyn-Nadir | NP010 | PES / N/A | 1-14 | N/A | 9 | 10 | >200 ^b |
| Microdyn-Nadir | NP030 | PES /N/A | 1-14 | N/A | 95 | 30 | >40 ^b |
| Nitto Denko | ES15-D | N/A | 6-8 | 41 | 40 | 99.5 | 42 |
| Norit | NF50 M10 | PA /PES | 4-10 | 7 | 40 | 35 | N/A |
| Toray | SU-610 | PA / N/A | 3-8 | 41 | 45 | 55 | 27 |

^a for CaCl₂, ^b pure water flow

2.3.4.2 Mass transport and rejection mechanism in NF membranes

(Szymczyk et al. 2003) developed the Steric, Electric, and Dielectric Exclusion (SEDE) model for NF, based on the extended Nernst–Planck equation to represent mass transport across the membrane and accounts for ion distribution at the pore inlet and outlet through equilibrium partitioning relations (Cavaco Morão et al. 2008). This model has been demonstrated to fit the experimental data reasonably well for symmetric and asymmetric single salts. The solute flux through the membrane is governed by the Steric, Electric, and Dielectric Exclusion equation (SEDE). For each solute *i*, the (SEDE) equation is given by Eq. (2.9)

$$J_{i, \text{pore}} = -D_{i, \text{pore}} \frac{dC_{i, \text{pore}}}{dx} - \frac{z_i C_{i, \text{pore}} D_{i, \text{pore}}}{RT} F \frac{d\psi}{dx} + k_{i,c} C_{i, \text{pore}} J_w \quad (2.9)$$

Where, $J_{i, \text{pore}}$ is the solute flux of the species *i*, consisting of the diffusive, electromigration, and convective terms, respectively, in the order shown in the Eq. (2.9). $D_{i, \text{pore}}$, $C_{i, \text{pore}}$ and z_i are the intra-pore diffusion coefficient, concentration, and valence respectively of species *i*, F Faraday constant, R ideal gas constant, T temperature, J_w pure water volume flux, ψ local electrical potential inside the

pore, $k_{i,c}$ hydrodynamic coefficient accounting for the effect of pore walls on convective transport, Δx the effective thickness of the membrane active layer.

The transport and rejection mechanisms of NF membranes are determined by the membrane structure and the interactions between the membrane and the molecules being transported. This results in the existence of three different modes of solute transport through the membrane. As shown in Fig 17

- Diffusion (molecule movement produced by concentration gradients),
- Convection (molecule movement induced by flow),
- Electromigration (When charged molecules are transported, the electrical field plays an essential role in their transport) (Handojo et al. 2019).

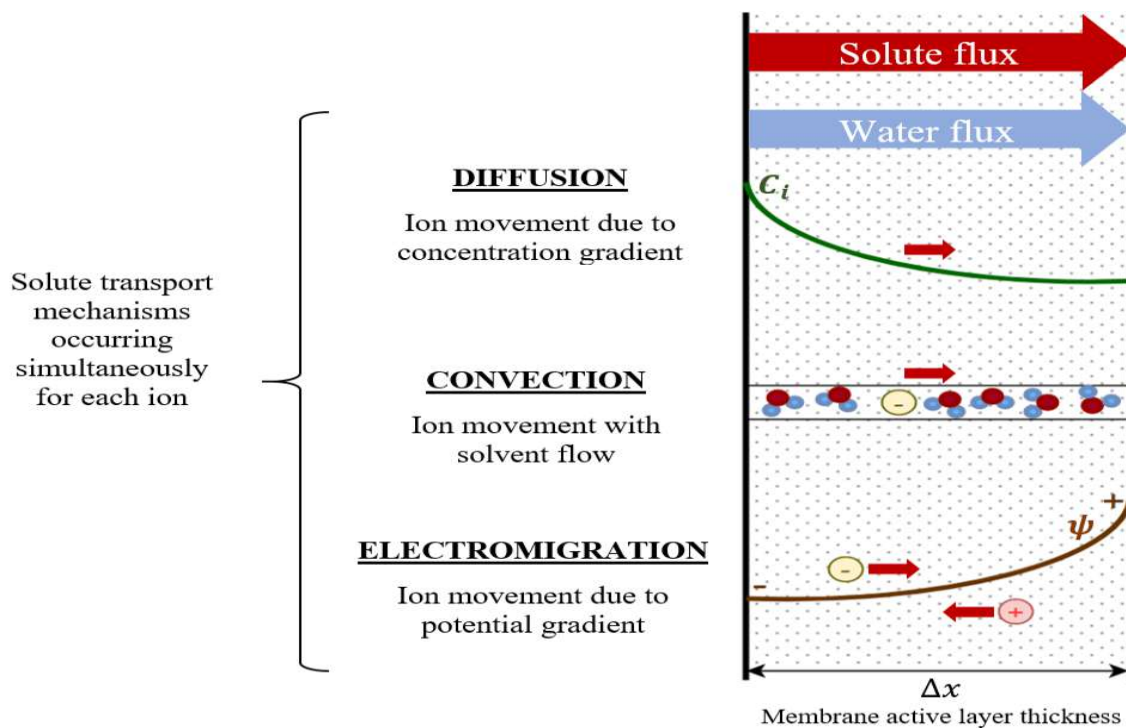


Figure 17. The mechanisms by which solutes are transported across a membrane in NF, adapted from (Roy et al. 2017).

In addition to size (steric) exclusion, which is the fundamental rejection mechanism for most filtration systems, there are significant impacts in NF such as surface charge and hydration (solvation shell). Therefore, the term "dielectric exclusion" refers to the exclusion caused by hydration. In addition, this term refers to the dielectric constants (energy) associated with a particle's presence in solution versus within a membrane substrate. As a result, NF has three exclusion mechanisms: steric exclusion, dielectric exclusion, and Donnan exclusion. These processes are schematically shown in Fig 18.

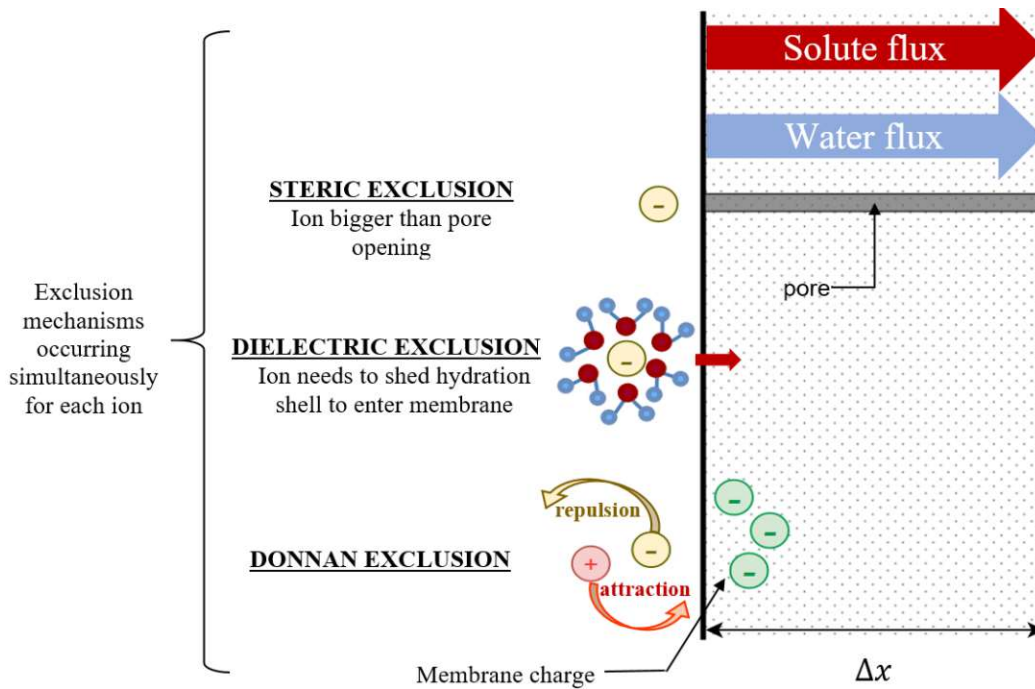


Figure 18. Schematic representation of solute exclusion mechanisms in NF, adapted from (Roy et al. 2017)

The Steric, Electric, and Dielectric Exclusion (SEDE) model for NF shown in Fig 19 takes into consideration the following: (1) Concentration polarization at the feed side; (2) species partitioning

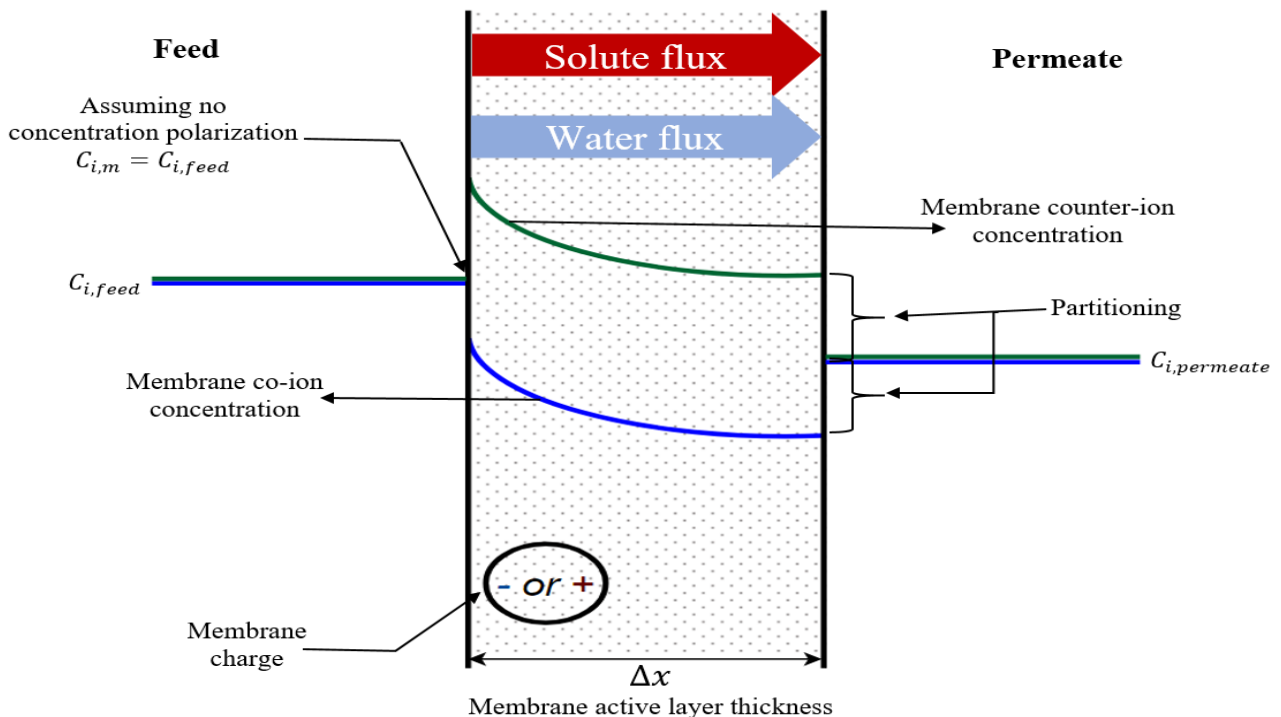


Figure 19. Concentration gradients (single salt, 1 cation: 1 anion) beside the membrane caused by concentration polarization, partition at the pore entrance, concentration gradients inside the membrane pores, and partition at the pores outlet are shown in simplified form. (-) anion and (+) cation subscripts, adapted from (Roy et al. 2017).

equilibrium at the feed/membrane interface, (3) convection, diffusion, and electromigration cause the movement of solutes through the pores (for charged solutes only), and (4) species partitioning on an equilibrium basis at the membrane/permeate contact. When exposed to an aqueous solution, most NF membranes develop an electric charge. This charge may be generated in several ways, including dissociating functional groups (Labbez et al. 2002) or the adsorption of charged species from the solution onto the pore walls (Schaep and Vandecasteele 2001).

Thus, electrostatic interactions between the membrane material and ions in solution play a significant role in the rejection mechanism in the tiny pores such as those found in NF (Szymczyk et al. 2003). SEDE model for NF Membranes describes mass transport at interfaces between the membrane and external solution by considering three well-known rejection mechanisms: steric hindrance, Donnan exclusion, and dielectric exclusion (Vezzani and Bandini 2002).

2.3.4.2.1 Donnan exclusion

The Donnan effect occurs when NF membranes are employed to desalinate solutions containing monovalent and polyvalent anions, as shown in Fig 20. The figure illustrates the retention of chloride and sodium when sodium sulfate is progressively added to a 0.05 M sodium chloride solution, thus forming a three-ion system. The retention curve shown was obtained at a temperature of 25 °C and a feed pressure of 20 bar.

As the divalent sulfate anion concentration increases, the retention for the monovalent chloride anion falls and even reaches negative values. Negative retention indicates that the chloride anion concentration in the permeate is greater than its concentration in the feed. This effect is beneficial in processes requiring monovalent anions' permeation, such as water softening or solution desalination. As a result, the anions' permeation is accelerated, and the osmotic pressure difference is reduced. To understand this effect, consider the equilibrium across a membrane impermeable to divalent anions but permeable to monovalent anions and cations.

As in the previous experiment, NaCl is weighed in phase I, and once equilibrium is achieved, Na₂SO₄ is progressively added to this phase. The electrochemical potential η_j is required to describe the Donnan equilibrium as in Eq (2.10) (Lawson and Lloyd 1997):

$$\eta_j = \mu_j + z_j F \varphi \quad (2.10)$$

The electrochemical potential differs from the known chemical potential through the additive term $z_j F \varphi$, which reflects the influence of an electric field on the permeating ions. z_j is the number of charges of the transported component, Faraday constant (F) is the amount of charge per mole of a singly charged component. φ is called the internal potential of the phase and has the dimension of an

electrical voltage. For neutral components, $z_j = 0$, the electrochemical potential corresponds to the known chemical potential.

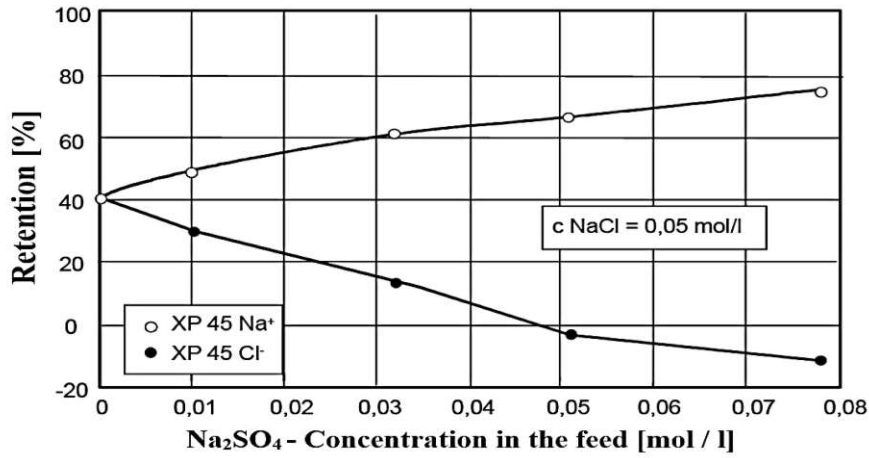


Figure 20. Retention of Na^+ and Cl^- in the presence of SO_4^{2-} (Sirkar 1992).

When both phases are in equilibrium, their electrochemical potentials are equal Eq (2.11):

$$\eta_j^I = \eta_j^{II} \quad (2.11)$$

The permeating Na^+ and Cl^- ions fulfill the equilibrium requirement according to Eq. (2.12) and Eq. (2.13):

$$\mu_{\text{Na}}^I - \mu_{\text{Na}}^{II} = z_{\text{Na}} F \Delta \varphi \quad (2.12)$$

$$\mu_{\text{Cl}}^I - \mu_{\text{Cl}}^{II} = z_{\text{Cl}} F \Delta \varphi \quad (2.13)$$

Using the chemical potential equation Eq. (2.14):

$$\mu_j(T, p, x) = \mu_{j,0}(T, p_0) + RT \ln a_j(T, p_0, x) + \tilde{V}_j(p - p_0) \quad (2.14)$$

If the pressure term is ignored, the Eq. (2.15) is obtained by subtracting (2.12) and (2.13):

$$RT \ln \left(\frac{a_{\text{Na}}^I}{a_{\text{Na}}^{II}} \right)^{z_{\text{Na}}} - RT \ln \left(\frac{a_{\text{Cl}}^I}{a_{\text{Cl}}^{II}} \right)^{z_{\text{Cl}}} = 0 \quad (2.15)$$

For dissolved components, the ideal dilution of the component serves as the reference state for the electrochemical potential. At low concentrations, the condition of ideal dilution is attained Eq. (2.16)

$$x_j \rightarrow 0 : y_j \rightarrow 1 \quad \text{and} \quad a_j = y_j x_j \rightarrow x_j \quad (2.16)$$

When molar proportions are small, the molar fraction x_j and the concentration C_j are proportional. Thus, for example, if one replaces the activity of the various ions in Eq. (2.15) with their concentrations in the case of ideal dilution and takes into consideration that $z_{\text{Na}} = +1$ and $z_{\text{Cl}} = -1$ in the provided example, the concentration ratio in equilibrium is as Eq. (2.17):

$$\frac{a_{\text{Na}}^I}{a_{\text{Na}}^{II}} = \frac{a_{\text{Cl}}^{II}}{a_{\text{Cl}}^I} \quad (2.17)$$

The concentrations of the permeating sodium and chloride ions are inversely correlated in the example given. Eq. (2.17) does not include the sulfate concentration because the sulfate ions do not permeate or participate in the equilibrium. The concentration dependence of the retention is a result of the Donnan equilibrium, among other things.

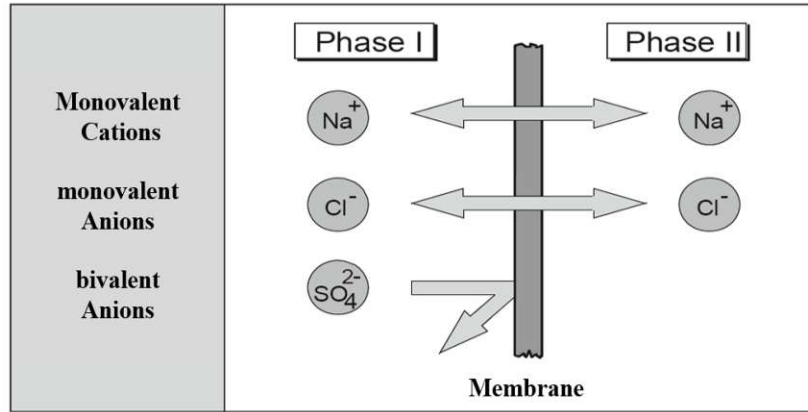


Figure 21. The Donnan equilibrium in the existence of an ion-selective membrane (Melin and Rautenbach 2007).

The higher ion concentration in the feed solution, the higher concentration in the pore and therefore in the permeate, since the membrane retention decreases with increasing concentration. Another factor contributing to the retention being concentration-dependent is the shielding of the fixed ions by the mobile ions. The negatively charged pore wall results in an electrical double layer inside the pore, as shown schematically in Fig 22.

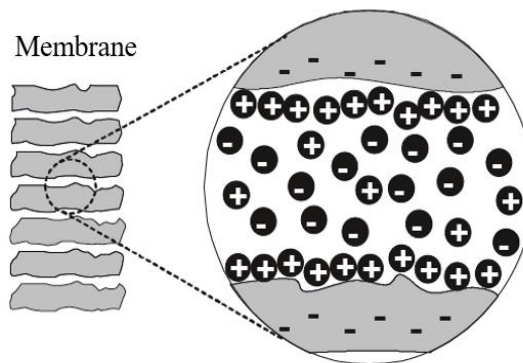


Figure 22. The electric double layer In a pore with negatively charged walls (Melin and Rautenbach 2007).

Near the wall, positively charged ions are concentrated. Electrical forces and the thermal self-motion of the ions combine to form an ion distribution that protects the negative solid ions' charge from the interior of the pores. The greater the number of mobile ions, the more the charge shielding, i.e., the fixed ions' effect diminishes. Consequently, as the feed concentration increases, more anions may enter the membrane, and the membrane's retention diminishes.

3. Green biorefinery

Scientists and industries have long been interested in using various kinds of biomass to create various products. However, the world has grown more worried about the usage of fossil fuels, which has been linked to the increase in the concentration of atmospheric greenhouse gases, resulting in environmental problems such as global warming, ocean acidification, and Arctic sea ice loss. And since then, biomass use in these domains has grown (Corona et al. 2018).

Crops and plants are often the first targets in the hunt for new sources of chemicals and fuels, owing to their abundance and human capacity to grow them. The green biorefinery idea is derived from the concept that uses grassland biomass solely to produce various products such as lactic acid, proteins, and biogas. Fig 23 illustrates the many processes and products that may be generated in a green biorefinery:

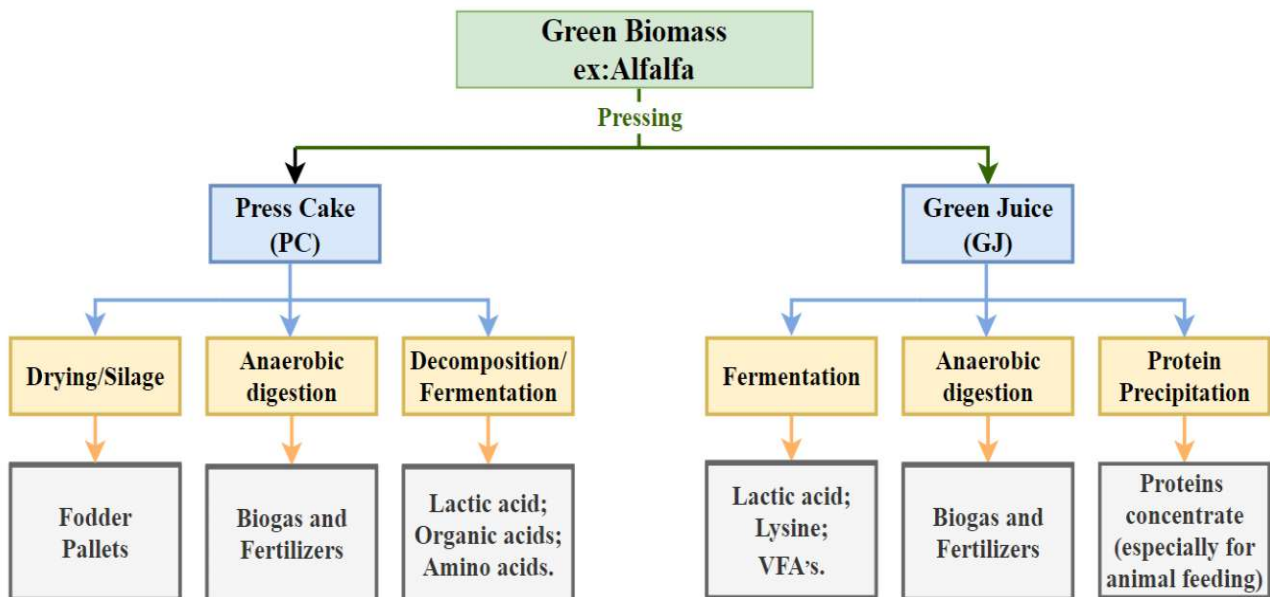


Figure 23. A diagrammatic representation of the processes and products generated in green biorefineries, adapted from (Zhang et al. 2015).

3.1. Grass silage

The grass may have existed for about 55 to 70 million years (Kellogg 2001). Nowadays, it is mainly utilized for grazing and as animal feed, either fresh or preserved (e.g., Grass silage bale) as shown in Fig 24. In addition, the grass may be used as a renewable carbon source in industrial operations, and it is regarded as a valuable feedstock for biorefineries (Sharma et al. 2012)

Given the vast quantity of grass accessible on a global scale, this substrate has tremendous promise. However, although grass's structural and chemical characteristics have been studied in the past for biofuel generation (Anderson and Akin 2008), the potential of grass remains primarily untapped.



Figure 24. Grass silage bale (Goeweil 2021).

Among the primary obstacles are the scarcity and supply of biomass. While the area is covered densely with grass, it is dispersed over a wide surface area. Additionally, although most grass species grow rapidly, grass supply is not consistent throughout the year. In tropical zones with year-round temperatures of 30 °C or more, grass may proliferate, and supply can be more consistent, but availability is restricted by the quantity of rain received. The grass is accessible exclusively during specific seasons in temperate zones such as the Mediterranean and subtropics. As a result, a storage system is often required to guarantee a consistent supply of grass. An ideal storage system protects biomass's (organic) content and 'prepares' it for future use without adding undue expense, process complexity, safety, or environmental concerns.

Ensiling is a very efficient technique of storing grass, which involves compressing it to a density of between 106 to 434 [kg.m⁻³] (Richard E. Muck and Brian J. Holmes 2000), wrapping or covering it to prevent oxygen infiltration. This stimulates the formation of LA by lactic acid bacteria (LAB, mostly *Lactobacillus* spp.), lowering the pH of the silage to below 4. Due to the low pH, other microbes cannot thrive, leading to the preservation of grass silage. Other storage techniques include adding sulphuric acid and calcium hydroxide to produce pH values less than 3 or more than 11 to prevent bacterial development. To use grass, it must be collected, transported to a processing facility, and stored, with each step being very efficient to ensure that the process is viable.

3.1.1 Grass pretreatment

Plant biomass is often resistant to biodegradation due to the refractory nature of lignin and its structural carbohydrates. Lignin, along with phenolic compounds and ferulic acid, is a component of the aromatic components of biomass that contribute to the structure's strength. Hemicellulose and

cellulose are strong natural polymers found in plants that provide structural support and are also the target components for conversion processes.

Because lignin protects the hemicellulose and cellulose fractions, pretreatment methods are often required to degrade or remove lignin and hydrolyze the cellulose and hemicellulose into simple monomer sugars such as glucose and xylose as shown in Fig 25 Removing lignin can avoid inhibiting chemicals that may be harmful to microorganisms during the biological conversion.

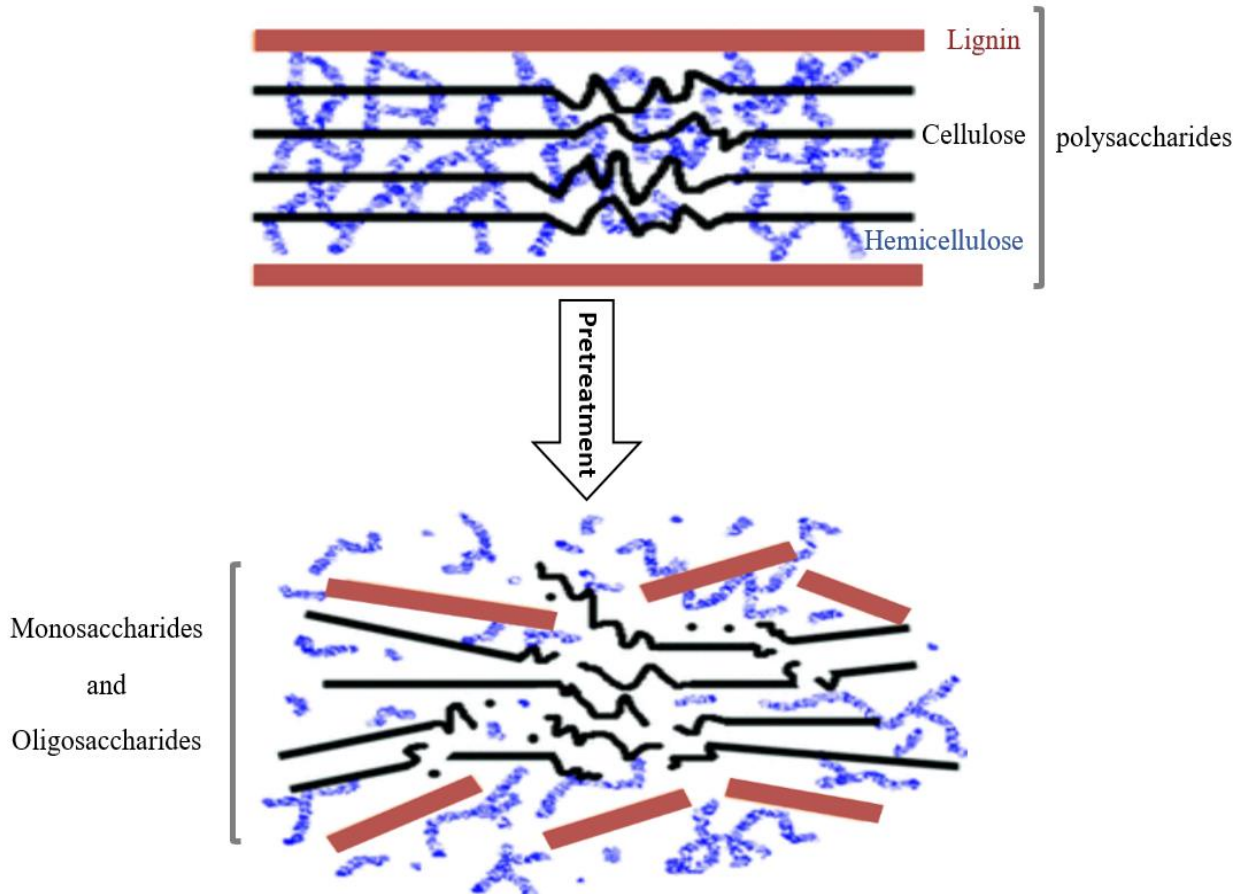


Figure 25. The structural breakdown of lignocellulosic biomass, adapted from (Muley and Boldor 2017).

Biomass is often shredded before it is stored to enhance bacteria's biological activity. Numerous pretreatment techniques have been investigated until now; a quasi overview is given in Table 7. While cost is the primary factor when selecting a pretreatment technique, biocompatibility (the eligibility of biomass for biological conversion after pretreatment) and environmental sustainability are often considered.

Table 7. Overview of pretreatment technology (Way Cern Khor 2017) .

| Category | Method | Types | Advantages | Disadvantages |
|----------|----------------------|--|--|--|
| | Grinding/ Milling | Hammer Ball Two-roll Colloid | - Reduces particle size and cellulose crystallinity | - High power consumption |
| | | Vibro (electroporation) | | |
| | Irradiation | Gamma-ray Electron beam Microwave | - Reduces the crystallinity and the molecular weight of cell wall polymers | - High energy input - Difficult to scale up - Possible environmental and safety issues |
| | | Hydrothermal / Hot liquid water / Autohydrolysis | - Low solvent cost (water) - Moderate temperature is Used[< 200°C], minimizing degradation/inhibitory products for biological conversion - Hydrolysis of hemicellulose | - High energy demand on downstream processing due to extensive water volume |
| | | High pressure steaming | - No chemicals are required - Scale-up can be done relatively easily - Continuous operation can be achieved | - High energy input |
| Physical | Others | Extrusion | - Lower energy consumption as compared to milling | - High maintenance cost of equipment |
| | | Pyrolysis | - Rapid conversion to gas and liquid products | - High temperature |
| | | Torrefaction | - Ash produced is a valuable side product | |
| | | Freezing / Thaw | - No chemicals are required - Does not produce Inhibitory compounds for biological conversion | - High operating cost |
| | | Ionic liquid | - Effective solubilization of lignin and hemicellulose | - High cost (at present) |

Table 7. (Continued)

| Category | Method | Types | Advantages | Disadvantages |
|-------------------------------|--------------------------|--|---|---|
| Physical | Others | Pulsed electrical field | <ul style="list-style-type: none"> - Can be performed at ambient conditions - Disrupts plant cells | <ul style="list-style-type: none"> - More research is needed |
| Chemical/ Physico-chemical | Alkali/ Thermo-alkali | Sodium hydroxide | <ul style="list-style-type: none"> - Low requirement on equipment - Moderate temperature | <ul style="list-style-type: none"> - Irrecoverable salts formed and incorporated into biomass - Not effective for high lignin biomass (for some alkali) |
| | | Potassium hydroxide | <ul style="list-style-type: none"> - Cost can be reduced depending on choice and combination of chemicals | |
| | | Magnesium hydroxide | <ul style="list-style-type: none"> - Removal of lignin - Less inhibitory compounds are formed compared to acid pretreatment | |
| | | Calcium hydroxide | | |
| | | Ammonia recycle percolation (ARP) | <ul style="list-style-type: none"> - Produce sulphur and sodium-free lignin | <ul style="list-style-type: none"> - Need to clean hydrolysate or remove ammonia |
| | Acid | Sulphuric acid Hydrochloric acid Phosphoric acid | <ul style="list-style-type: none"> - High reaction rate - Significant hydrolysis of (Hemi)cellulose and breakdown of lignin | <ul style="list-style-type: none"> - Equipment corrosion - Hydrochloric acid - Formation of inhibitory compounds |
| | Supercritical | Carbon dioxide Water | <ul style="list-style-type: none"> - Significant hydrolysis or dissolution of biomass | <ul style="list-style-type: none"> - High equipment cost - Discontinuity of process - Difficulty in upscaling - Safety issues |
| | Explosion | Steam explosion | <ul style="list-style-type: none"> - No recycling or environmental costs - Limited use of chemicals - Avoids excessive dilution of sugars - Relatively low energy input compared to physical pretreatment - Hydrolyses hemicellulose | <ul style="list-style-type: none"> - Partial destruction of xylan fraction - Incomplete disruption of the lignin carbohydrate matrix - Produces compounds inhibitory to microorganisms |

Table 7. (Continued)

| Category | Method | Types | Advantages | Disadvantages | |
|----------------------------------|--------------------|---------------------------|--|--|--|
| Chemical/ Physico chemical | Explosion | Ammonia fibre explosion | <ul style="list-style-type: none"> - Short residence time - High selectivity for reaction with lignin - Does not produce inhibitors for downstream processes - Moderate temperature - Ability to recycle ammonia - Removal of lignin | <ul style="list-style-type: none"> - Not efficient for biomass with high lignin content - Environmental concerns | |
| | | CO ₂ explosion | <ul style="list-style-type: none"> - Increases accessible surface area - Relatively cost-effective in terms of pretreatment efficiency | <ul style="list-style-type: none"> - High equipment cost | |
| | | SO ₂ explosion | <ul style="list-style-type: none"> - Does not cause formation of inhibitory compounds | | |
| | | SO ₃ explosion | <ul style="list-style-type: none"> - Ambient pressure | <ul style="list-style-type: none"> - Handling of corrosive chemicals | |
| | Oxidizing agents | Hydrogen peroxide | | <ul style="list-style-type: none"> - Fractionation of biomass at ambient pressure and low temperature | <ul style="list-style-type: none"> - Produce inhibitory compounds - High oxidants cost |
| | | | Wet oxidation | <ul style="list-style-type: none"> - Removal of lignin - Hydrolyses hemicellulose | <ul style="list-style-type: none"> - Production of inhibitory compounds is possible |
| | | Ozonolysis | | <ul style="list-style-type: none"> - Effectively removes lignin - Does not produce toxic residues | <ul style="list-style-type: none"> - Large amount of ozone is required |
| | | | | <ul style="list-style-type: none"> - Reactions are performed at Ambient temperature and pressure - High-quality lignin | <ul style="list-style-type: none"> - High cost |
| | Solvent extraction | | Ethanol-water | | |
| | | | Benzene-water | | |
| Butanol-water | | | <ul style="list-style-type: none"> - Hydrolyses lignin and hemicelluloses | <ul style="list-style-type: none"> - Solvents need to be drained from the the reactor, evaporated, condensed, and recycled | |
| Ethylene-water | | | | | |
| Swelling agents | | | | <ul style="list-style-type: none"> - High cost | |

Table 7. (continued)

| Category | Method | Types | Advantages | Disadvantages |
|------------|-----------------|--|--|---------------------------|
| Biological | Aerobic fungi | White/Brown rot fungi | - Degrades lignin and hemicelluloses - Low energy requirements | - Long retention time |
| | Anaerobic fungi | Manure/Rumen fungi | - Available and can be obtained in nature | - Long retention time |
| | Bacteria | Genetically modified E. coli, cyanobacteria, rhodobacter, etc. | - Genetic modification of bacteria can be performed relatively easily to improve pretreatment efficiency | - More research is needed |
| | Enzymes | | - Short retention time | - High cost |

3.1.2 Lactic acid (LA)

LA, as one of the essential products, is of particular interest because of its widespread applications, mainly in the pharmaceutical, cosmetic, chemical, and Food industries. Fig 26 shows a summarised LA industrial applications.

About 70% of the LA produced is utilized in the food production sector due to its crucial role in manufacturing yogurt and cheese (Castillo Martinez et al. 2013) Moreover, due to the hygroscopic and emulsifying properties of some LA derivatives, such as lactate esters, they can be applied as emulsifiers and improve agents in food products (Gao et al. 2011) Additionally, the great potential for producing green, biodegradable, and biocompatible polylactic acid polymers (PLA) is widely used as raw material in packaging and fibers and foams. However, at an industrial scale, while the PLA is compared with petrochemical raw materials, it can be considered as a relatively immature technology, mainly due to the high production cost of LA, as starting raw material for PLA.

The LA price varies by application and the cost of the feedstocks used in fermentation. The global LA market was worth USD 2.7 billion in 2020 and is projected to increase at an 8.0 percent compound annual growth rate (CAGR) between 2021 and 2028. (Market Analysis Report 2021)

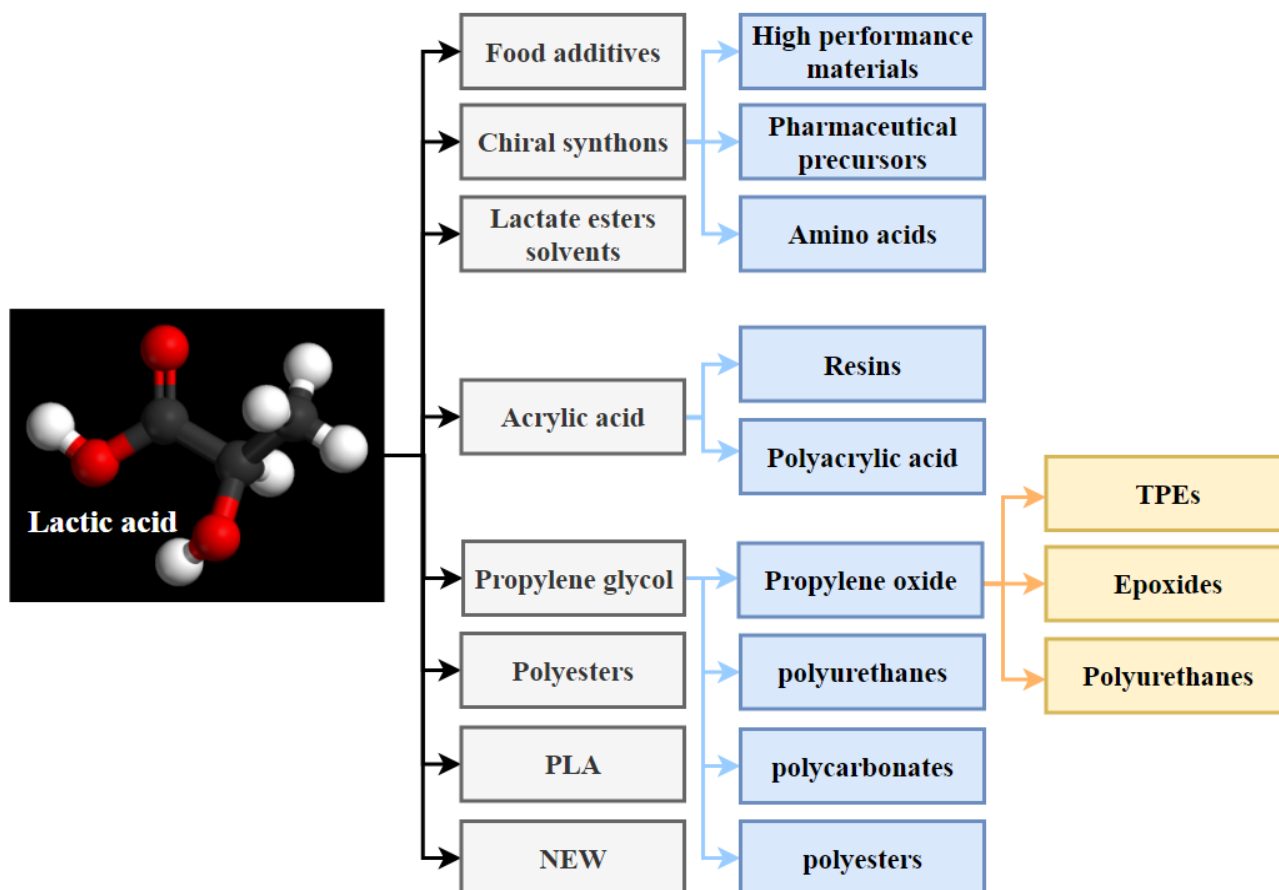


Figure 26. LA industrial applications, adapted from (Alves de Oliveira et al. 2018).

3.1.2.1. Physical properties of LA

LA is the simplest 2-hydroxycarboxylic acid with a chiral carbon atom and is found in two enantiomeric forms as shown in Fig 27.

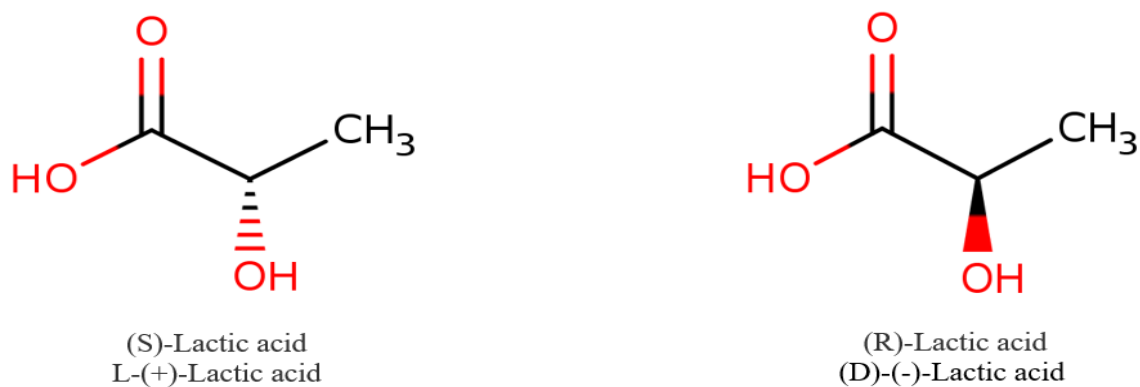


Figure 27. Two enantiomeric forms of LA (Compounds Identification 2021).

LA's chirality often causes nomenclatural difficulty. In the literature, a variety of distinct names are employed. This confusion arises from conflating the molecular structure with a physical characteristic (optical rotation). Table 8 outlines LA's physical properties.

Table 8. Physical properties of LA, adapted from (Auras 2010).

| Property | Value |
|--|---|
| CAS number | General: 50-21-5 (S)-Lactic acid: 79-33-4 (R)-Lactic acid: 10326-41-7 |
| Molecular weight [g.mol ⁻¹] | 90.08 |
| Formula | C ₃ H ₆ O ₃ |
| Melting point [°C] | 18 (racemic) 53 (chiral pure) |
| Crystal structure | (S)-Lactic acid: orthorhombic, space group P2 ₁ 2 ₁ 2 ₁ |
| Solid density [g.mL ⁻¹] | 1.33 (solid, 20 °C) |
| Solubility in water [wt %] | 86 (20 °C, monomeric(S)-lactic acid) |
| The heat of fusion [kJ.mol ⁻¹] | (S)-Lactic acid: 16.8 |
| Boiling point [°C] | 122 (at 14 mmHg) |
| Liquid density [g.mL ⁻¹ , 20 °C] | 1.224 (100% under cooled liquid) 1.186 (80.8% solution in water) |
| Viscosity [m.Pa.s] | 28.5 (85.3% solution in water, 25 °C) |
| pKa | 3.86 |
| Specific heat [J.g ⁻¹ .K ⁻¹ at 25 °C] | Crystalline (S)-lactic acid: 1.41 Liquid lactic acid: 2.34 |

3.1.2.2. Chemistry of LA

LA has both a hydroxyl and an acid functional group, which allows for intermolecular and intramolecular esterification processes. The first step is to construct a linear dimer (lactoyl lactic acid). Condensation may progress to higher oligomers when water is removed. Additionally, a cyclic dimer called lactide is generated in trace quantities. Lactide is generated when lactoyl lactic acid is esterified intramolecularly or when higher oligomers are degraded. All reactions are in equilibrium as shown in Fig 28.

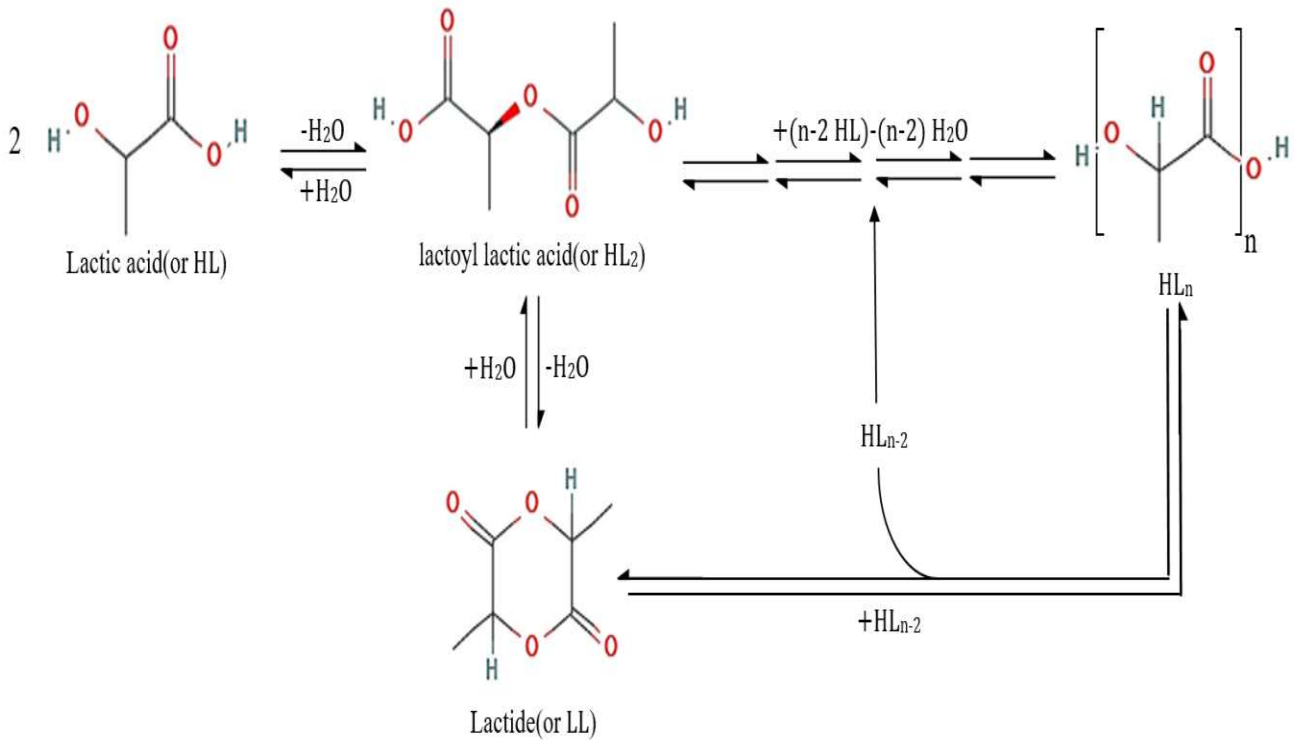


Figure 28. LA condensation reactions, adapted from (Auras 2010).

At equilibrium, LA solutions contain monomeric LA, dimeric LA or lactoyl Lactic acid, higher oligomers of LA, and lactide. All ratios are proportional to the quantity of water present; for example, a 90.1 percent LA solution (total acidity) includes around 59.3 percent monomeric LA and 27.3 percent lactoyl Lactic acid, and higher oligomers. (Auras 2010).

3.1.2.3. Thermodynamic properties of LA

3.1.2.3.1 Vapor pressures of LAs at different temperatures

The following equation Eq.3.1 typically describes vapor-liquid equilibrium at constant pressure P and temperature T for a particular mixture:

$$\phi_i y_i p_i = \gamma_i x_i p_i^{\text{sat}} \phi_i^{\text{sat}} \quad (3.1)$$

Where γ_i is the activity coefficient of component i , ϕ_i denotes the fugacity coefficient, and x_i and y_i Denote the liquid and vapor phase compositions, respectively. At temperature T , p_i^{sat} is the vapor pressure, and ϕ_i^{sat} is the fugacity coefficient of pure saturated vapor i at temperature T and pressure p_i^{sat} .

3.1.2.3.2 Temperature dependence of densities of LA

Previously, data on the acid density of aqueous LA solutions were published as shown in Table 9. These density statistics demonstrate that density rises roughly linearly as concentration increases and temperature decreases.

Table 9. The density of aqueous solution of various concentrations of LAs at various temperatures (Auras 2010).

| Temperature [°C] | Densities of LA solutions [g.mL ⁻¹] | | | | | |
|------------------|---|---------|---------|---------|---------|--------|
| | 9.16% | 24.35% | 45.48% | 64.89% | 75.33% | 85.32% |
| 20 | 1.01955 | 1.05678 | 1.10980 | 1.15526 | 1.17860 | 1.1989 |
| 25 | 1.01811 | 1.05446 | 1.10536 | 1.15181 | 1.17182 | 1.1918 |
| 30 | 1.01585 | 1.05183 | 1.10182 | 1.14723 | 1.17013 | 1.1901 |
| 40 | 1.01138 | 1.04715 | 1.09427 | 1.13987 | 1.16132 | 1.1813 |
| 50 | 1.00674 | 1.04146 | 1.08703 | 1.13205 | 1.15262 | 1.1718 |
| 60 | 1.00076 | 1.03513 | 1.07925 | 1.12357 | 1.14250 | 1.1631 |
| 70 | 0.99504 | 1.02958 | 1.07219 | 1.11532 | 1.13407 | 1.1536 |
| 80 | 0.98899 | 1.02260 | 1.06399 | 1.10762 | 1.12511 | 1.1443 |

3.1.2.3.3 Temperature dependence of viscosity of LA

As shown in Table 10, the viscosity of LA solutions increases as the concentration increases but it decreases as the temperature increases.

Table 10. The viscosity of an aqueous solution of various concentrations of LAs at various temperatures (Auras 2010).

| Temperature [°C] | Viscosity [10 ⁻³ Pa.s] | | | | |
|------------------|-----------------------------------|--------|--------|--------|--------|
| | 9.16% | 24.35% | 45.48% | 64.89% | 75.33% |
| 25 | 1.15 | 1.67 | 3.09 | 6.96 | 13.03 |
| 30 | 1.03 | 1.46 | 2.74 | 6.01 | 10.55 |
| 40 | 0.809 | 1.13 | 2.03 | 4.22 | 7.08 |
| 50 | 0.671 | 0.918 | 1.59 | 3.12 | 4.98 |
| 60 | 0.572 | 0.746 | 1.26 | 2.38 | 3.57 |
| 70 | 0.473 | 0.632 | 1.02 | 1.85 | 2.73 |
| 80 | 0.416 | 0.532 | 0.843 | 1.47 | 2.08 |

3.1.2.4 Production of LA

LA may be produced using fermentative (LA fermentation) or chemical synthesis methods (Eş et al. 2018). It is widely known that chemical production results in racemic DL-LA combinations (Alves de Oliveira et al. 2018). Because of this, it isn't easy to regulate the final product's chemical and

physical characteristics. It is also inappropriate for usage in the Food, pharmaceutical, and medical sectors. In addition, some businesses need LA with high enantiomeric purity for particular purposes. This feature also adds to the appeal of LA generation through fermentation over chemical manufacture. Approximately 90% of all lactic acid manufactured globally is obtained from bacterial fermentation (Alves de Oliveira et al. 2018).

3.1.2.4.1 Production of LA by chemical synthesis

To produce LA chemically, acetaldehyde reacts with hydrogen cyanide in the liquid phase and in the presence of a base under a high pressure to form lactonitrile, which is recovered by distillation. Next, hydrochloric or sulfuric acid is added to convert lactonitrile to LA, which is then esterified with methanol to form methyl lactate, then recovered and purified using distillation. Finally, the purified methyl lactate is hydrolyzed in an acidic aqueous solution to form LA and methanol, the latter being recycled in the same process (Castillo Martinez et al. 2013). The chemical production of LA is shown in Fig 29.



Figure 29. The chemical synthesis of LA, adapted from (Kern 2020).

3.1.2.4.2 Production of LA by fermentation

Microorganisms convert an appropriate carbohydrate to LA during fermentation. While some of the microorganisms utilized, such as the mold *Rhizopus*, need oxygen to grow, the actual conversion of carbohydrates to LA occurs in the absence of oxygen. Indeed, since complete oxidation of sugar to carbon dioxide and water is energetically much more favorable, LA is produced chiefly under anaerobic circumstances. The production of LA by fermentation is shown in Fig 30. Indeed when

oxygen is consistently present in high concentrations, most LA-producing microbes become inactive (Auras 2010). However, when sugar enters the cell, it is initially transformed into pyruvate through a series of enzymatic processes.

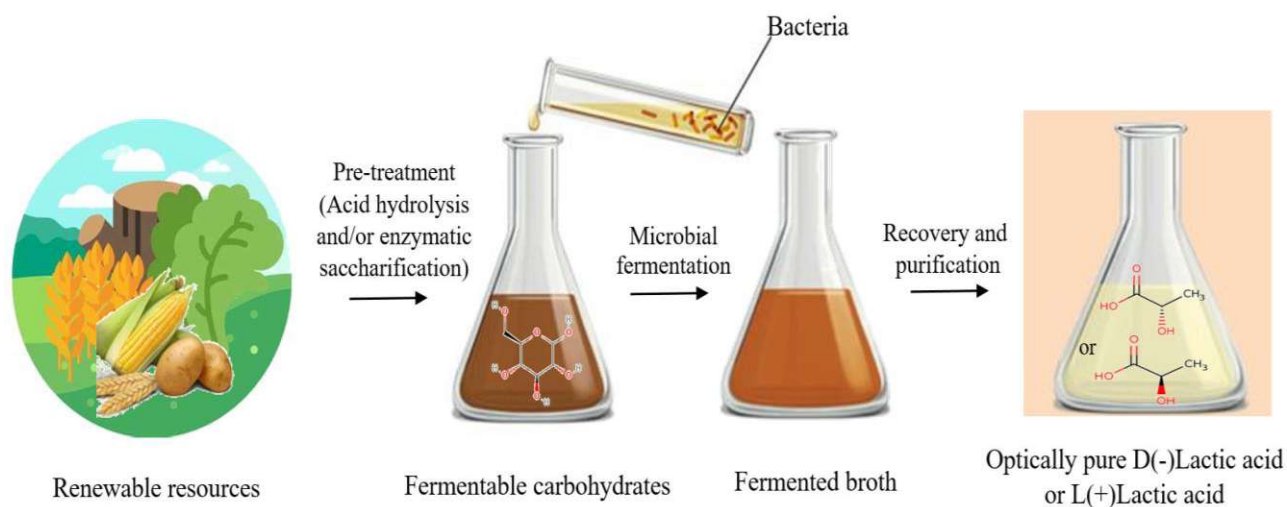


Figure 30. The production of LA by fermentation, adapted from (Kern 2020).

This conversion results in the generation of chemical energy in the form of ATP (adenosine triphosphate) and reducing equivalents (NADH) Fig 31 shows this reaction. Then, microorganisms recycle these reducing equivalents by converting pyruvate to more reduced lactic acid, Fig 32 shows this reaction. In other words, LA is mainly created to maintain essential cellular functions.

The chemical energy generated is employed in various functions throughout the cell, including cell growth, maintenance, and sometimes even motility.

The reaction seen in Fig 31 occurs in the so-called homofermentative lactic acid bacteria (LAB). In contrast to heterofermentative bacteria, which produce a combination of LA, acetate, CO₂, and acetate or ethanol as a fermentation product, homofermentative bacteria produce almost exclusively LA (Auras 2010).

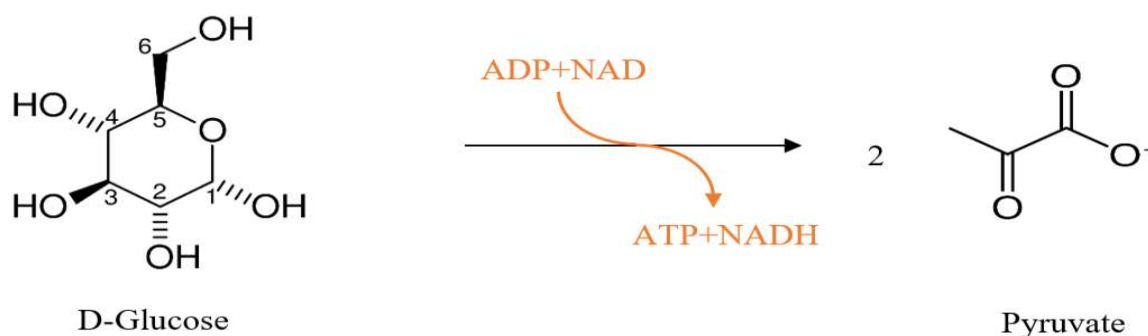


Figure 31. When glucose is converted to pyruvate, chemical energy (ATP) and reducing equivalents (NADH) are produced, adapted from (Auras 2010).

unable to continue fermentation due to the environment being too acidic. Numerous bases may be employed to neutralize the acidity produced during fermentation, and the base used will dictate the downstream processing method. Most industrial LA plants use calcium hydroxide or calcium carbonate, which creates a significant quantity of gypsum as a by-product. A significant issue in manufacturing LA is identifying or developing an efficient microbe capable of producing at such a low pH that the fermentation does not need neutralization.

3.1.2.4.2 Carbohydrates for LA production

In principle, any carbohydrate source containing pentoses (C₅ sugars) or hexoses (C₆ sugars) may be utilized to produce lactic acid; however, it is challenging for any microorganism to use all conceivable and available C₅ and C₆ sugars. On the other hand, sucrose from sugarcane or sugar beets and glucose from starch are abundant and readily fermentable. Polysaccharides such as cellulose or starch are more complex and need additional pretreatment. Usually, starch is a combination of two glucose homopolymers, amylopectin, and amylose. Corn, wheat, potato, or tapioca starch are all starch sources (BeMiller and Whistler 2009). While certain microbes can degrade and ferment starch directly to LA, most LA-producing microorganisms cannot hydrolyze starch. However, the starch may be hydrolyzed to glucose before fermentation using commercially available enzymes α -amylase and glucoamylase. Thus, the production of economically valuable goods via microbial biotechnology has received enormous interest in the past decade. Initially, This topic is mainly related to current problems, such as increasing global energy demand and environmental concerns, which are the primary causes of creating new ways to manufacture virtually every product using green methods (Eş et al. 2018). In addition, because biorefinery uses renewable resources as feedstock, it may help to decrease the carbon footprint and achieve sustainable development. This feedstock is abundantly available around the globe, such as lignocellulose is available in the grass.

Lignocellulose is made up of glucose homopolymer cellulose, heteropolymer hemicellulose, and lignin. Hemicellulose consists of hexoses and pentoses. Lignocellulose comprises around 80% fermentable sugars, although this varies significantly depending on the source (Auras 2010). The rest, lignin, is a phenolic polymer that is difficult to degrade and cannot be used directly in LA production. However, it may be utilized to generate energy, returning to the LA factory. Numerous pretreatments and separations are necessary to get monosaccharides from the raw material. After mechanical treatment, the lignocellulosic material is delignified (pulped) using a strong alkali or acid solution. Simultaneously, the (hemi) cellulose part becomes more accessible to enzymes. Following enzymatic treatment, glucose, xylose, and some arabinose are produced. Finally, the carbohydrate

source's price and availability in the local market dictate the raw material of choice for industrial fermentation.

3.1.2.4.2.3 Downstream processing/purification of LA

When Scheele discovered LA, he extracted and purified it from sour whey by saturation with lime, filtering out the crude calcium lactate, acidifying the crystal mass with oxalic acid, filtering out the calcium oxalate, and evaporating to obtain a crude viscous LA.

Essentially, this technique utilizes calcium-based neutralized fermentation and sulfuric acid instead of oxalic acid is identical to the one utilized in the industry today to produce crude LA. The disadvantages include the constant increase in the expense of lime/chalk, sulfuric acid, and other chemicals and the disposal of enormous amounts of gypsum ($\text{CaSO}_4 \cdot 2\text{H}_2\text{O}$), an inevitable by-product of this process. Fig 33 is a block diagram of the traditional lactic acid production process, which includes fermentation.

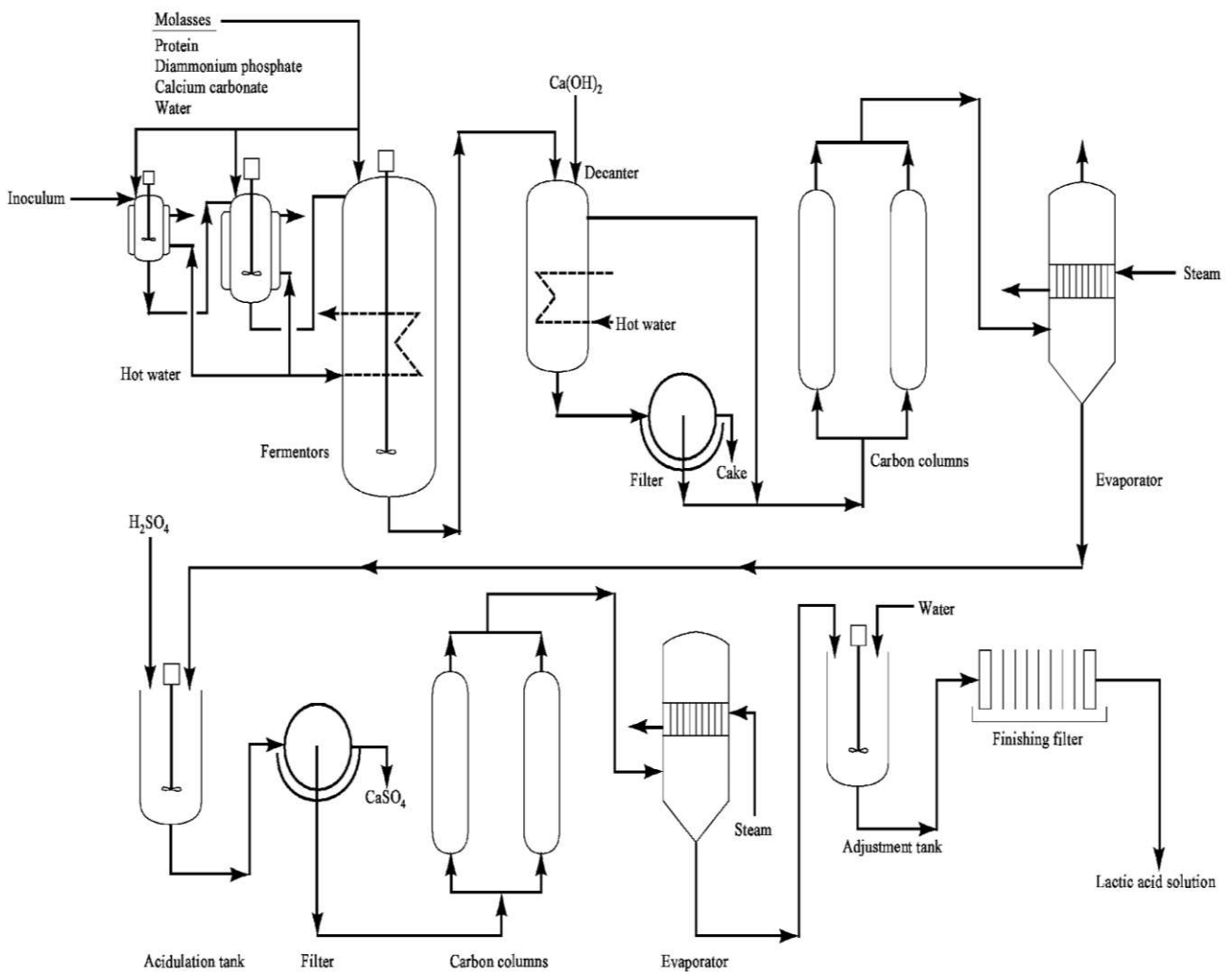


Figure 33. Schematic diagram of the traditional LA production process includes fermentation (Big Chemical Encyclopedia 2021).

4. Experimental equipment and procedure

4.1 Experimental setup

The filtration experiments were conducted using a lab-scale cross-flow unit OS-MAC-01 from Osmota, it can operate up to a maximum of 60 bar feed pressure and maximum flow capacity of 3.7 L.min⁻¹ with an active membrane area of 0.008 m². The feed solution was supplied to the recirculation loop through a 2-liter feed tank using a high-pressure piston pump Type: three plunger rods, positive displacement, reciprocating plunger pump, Model: 231. (CAT Pumps). The unit is composed of the components depicted in Fig 35.

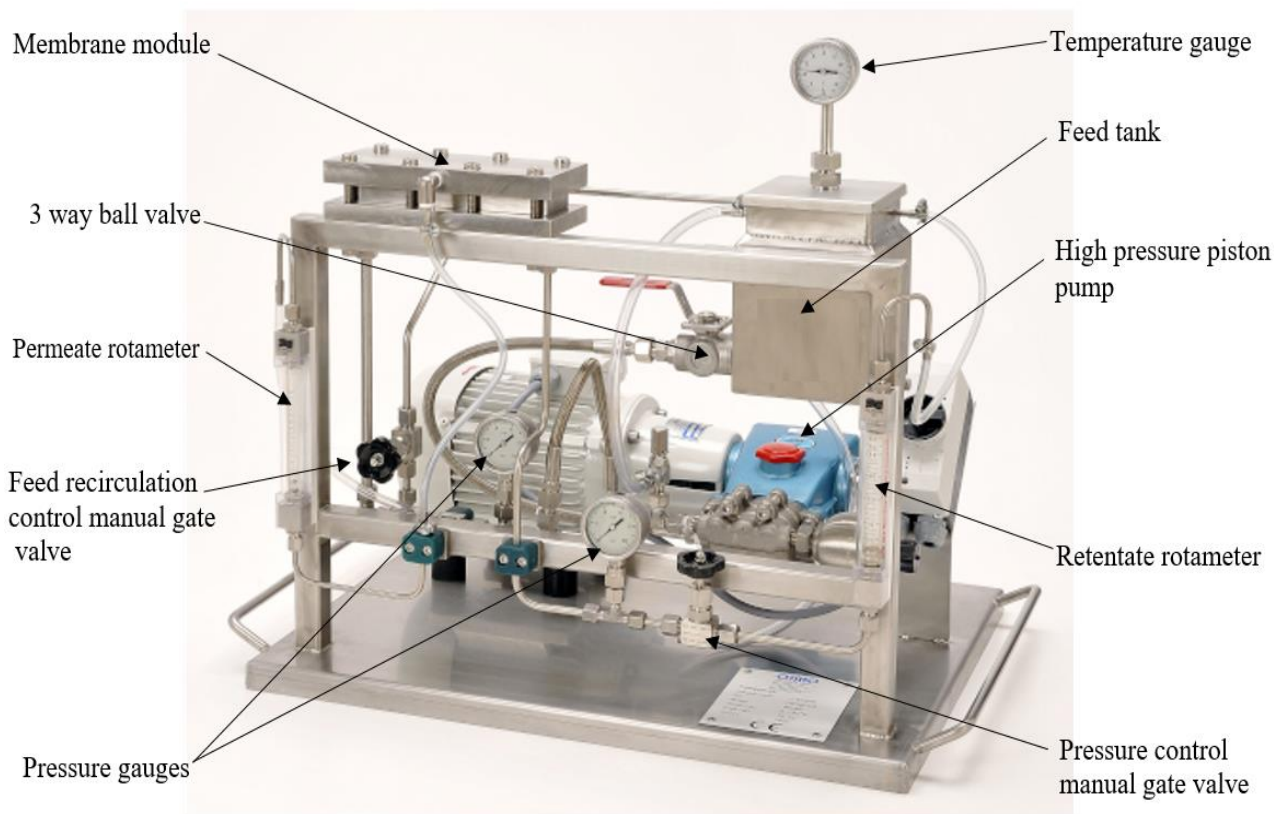


Figure 35. Experimental equipment.

Although the permeate flow rate can be determined using a rotameter, the mass flow rate of permeate during the experiments was determined using a digital electric balance at regular intervals. A manual gate valve on the feed recirculation line before the membrane module may be used to adjust and control the feed flow rate. A rotameter is used to determine the retentate flow rate. Two pressure

gauges across the membrane cell are used to measure the pressure. A temperature gauge and a digital thermometer are used to show and measure the temperature of the feed.

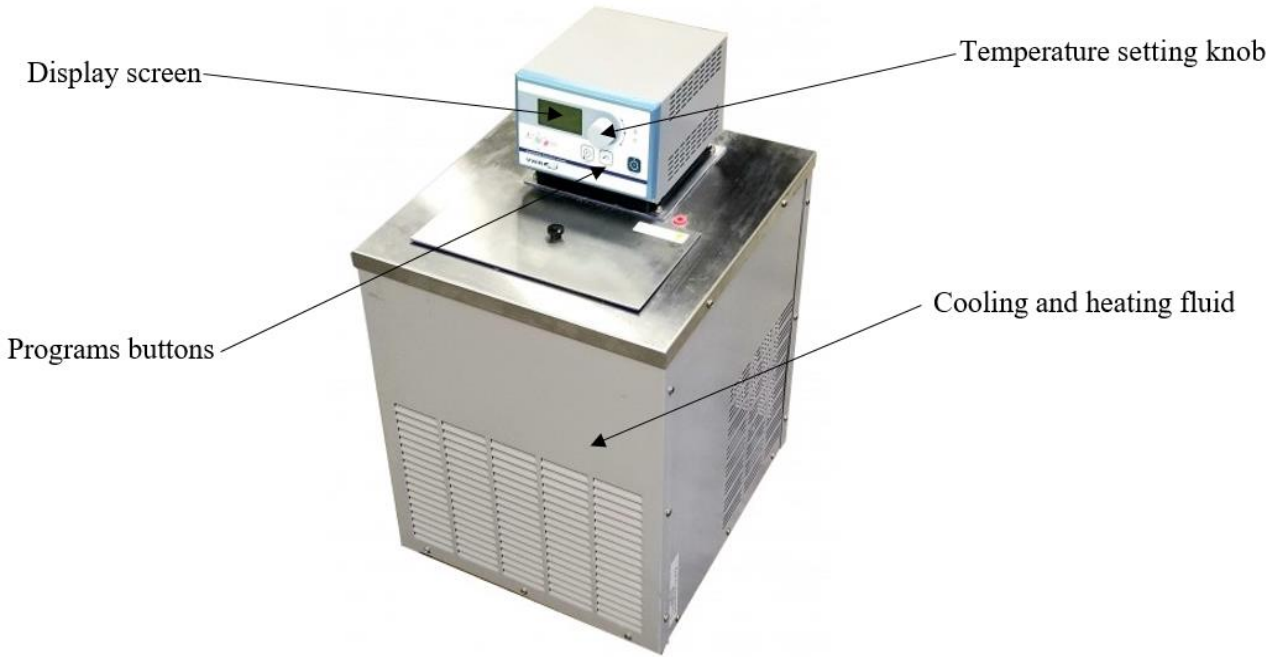


Figure 36. The PolyScience Ultra-low refrigerating/heating circulator.

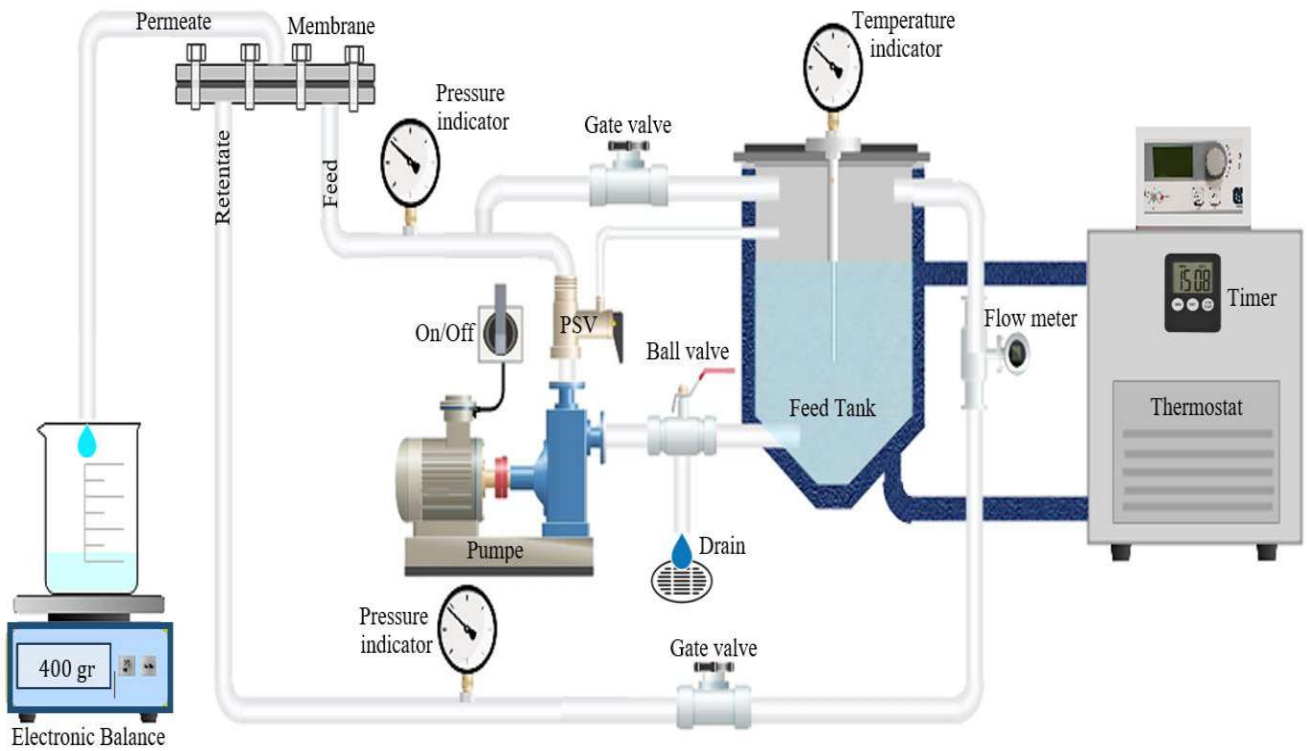


Figure 37. Block flow diagram of the filtration process unit.

The temperature of the feed is kept constant by flowing hot/cold water through the feed tank's jacket from a coupled Programmable PolyScience Ultra-low Refrigerating/Heating Circulator Model 9712. With Temperature range: -45 to 200 °C as shown in Fig 36. A block flow diagram of the filtration process is depicted in Fig 37.

4.2 The membranes

Four commercially available NF membranes (NF-Alfa Laval, NF Toray, NF270, and Selro MPF-36) were screened in this study. Their properties are shown in Table 11

Table 11. The properties of the NF membranes.

| Membrane | Manufacture | Chemical composition | MWCO [Dalton] | P _{max} [bar] | T _{max} [°C] | pH |
|---------------|-------------|--|---------------|------------------------|-----------------------|----------|
| NF-Alfa Laval | Alfa Laval | Polypiperazinamide Thin-Film Composite | 300 | 50 | 60 | 1-12.5 |
| NF -Toray | Toray | Polypiperazinamide Thin-Film Composite | 200 | 55.2 | 50 | 1.8-11.5 |
| NF270 | FilmTec | Polyamide Thin-Film Composite | 200 | 41 | 45 | 2-11 |
| Selro MPF-36 | koch | Polysulfone Thin-Film Composite | 1,000 | 45 | 70 | 0-14 |

4.3 Chemicals

In all the experiments, deionized water from the Ultrapure water system, arium® pro (Fig 38), with a conductivity of 0.055 µS.cm⁻¹ [18.2 MΩ.cm⁻¹ at 25 °C) was used.



Figure 38. Ultrapure water system.

Many chemicals were used to prepare the model solutions, including organic solutes such as Lactic acid $\text{CH}_3\text{CH}(\text{OH})\text{COOH}$ natural $\geq 85\%$, Acetic acid $\text{CH}_3\text{COOH} \geq 99.8\%$, D-(+)-Glucose $\text{C}_6\text{H}_{12}\text{O}_6 \geq 99.5\%$, D-(-)-Fructose $\text{C}_6\text{H}_{12}\text{O}_6 \geq 99\%$ from Sigma-Aldrich company. In addition, the inorganic solutes (salts) such as Sodium chloride $\text{NaCl} \geq 99.5\%$ from fluka, Sodium sulfate $\text{Na}_2\text{SO}_4 \geq 99\%$ from Roth, Magnesium chloride hexahydrate $\text{MgCl}_2 \cdot 6\text{H}_2\text{O}$ from Sigma-Aldrich, Calcium chloride CaCl_2 from Reagenzein Merck, Potassium hydroxide KOH , and Ammonium chloride NH_4Cl of analytical grade were used.

4.4 An overview of the conducted experiments

Experiments are classified as follows:

1. Determination of the optimal operating temperature for LA recovery,
2. Determination of the optimal pH value for LA recovery,
3. Determination of the best membrane for LA recovery,
4. Experimental investigation on the effect of different minerals on LA recovery.

4.4.1 Determination of the optimal operating temperature for the LA recovery experiments

The purpose of these experiments was to determine the optimal operating temperature for LA recovery, or, in other words, what temperature results in the lowest lactic acid retention. Two operating temperatures 25 and 40 °C were investigated.

4.4.1.1 Water permeability

Compaction of the fresh membrane is always required, the membrane was compacted for 20 mins at 32 bar using deionized water.

Water permeability before and after each filtration process was determined: The feed tank was filled with deionized water. At the beginning of the experiment the pump was turned on; the applied pressure was zero, at room temperature. This prevented the feed water to permeate the membrane and kept the membrane's surface moist and clean. For 10 min, the unit was maintained running. The device was then cleaned twice with deionized water at ambient pressure, room temperature, and a constant flow rate to eliminate any remaining contaminants. Following that, the thermostat was adjusted to 25 °C. The flow rate was adjusted to $3.6 \text{ L}\cdot\text{min}^{-1}$. The pressure was increased gradually to 32 bar from a low value to avoid damaging the membrane. Permeate recirculation was performed. After achieving and stabilizing the appropriate operating conditions and establishing a steady state, the permeate mass flow rate was measured every 5 min. To determine the average mass flow rate, it was measured three times.

4.4.1.2 Model solution filtration

After removing the water from the feed tank, the second step was the solution filtration process. 2 liters of the model solution containing LA, natural $\geq 85\%$ with a concentration of 25 g.L^{-1} in deionized water was prepared. Then the solution was added to the feed tank. The pump was started, the thermostat was adjusted to $25 \text{ }^\circ\text{C}$. The flow rate was adjusted to 3.6 L.min^{-1} . The pressure was increased to 32 bar once again gradually to avoid damage to the membrane. After that, permeate recirculation was performed. Once the required operating conditions were maintained and stabilized, the mass flow rate of permeate was recorded, and samples of permeate and retentate were collected. The conductivity and pH of the samples were determined every 10 min.

The procedure was carried out similarly for temperature $40 \text{ }^\circ\text{C}$, and each commercially available NF membrane (NF-Alfa Laval, NF Toray, NF270, and Selro MPF-36).

The experiments and their associated operating conditions are listed in Table 12 below.

Table 12. Optimal operating temperature for LA recovery experiments.

| Membrane | Solution | Concentration [g.L^{-1}] | pH | Pressure [bar] | Temperature [$^\circ\text{C}$] |
|---------------|----------|--|------|-------------------|-------------------------------------|
| NF-Alfa Laval | LA | 25 | 2,67 | 32 | 25-40 |
| NF -Toray | LA | 25 | 2,67 | 32 | 25-40 |
| NF270 | LA | 25 | 2,67 | 32 | 25-40 |
| Selro MPF-36 | LA | 25 | 2,67 | 32 | 25-40 |

4.4.2. Determination of the optimal pH value for LA recovery Experiments

The purpose of these experiments was to determine the optimal operating pH value for LA recovery, or, in other words, what pH value results in the lowest LA retention. Three operating pH values 2.67, 3.8, and 6 were investigated.

4.4.2.1 Water permeability

In the same way, as mentioned in Section 4.4.1.1

4.4.2.2 Model solution filtration

After removing the water from the feed tank, the second step was the solution filtration process. 2 liters of the model solution containing LA, natural $\geq 85\%$ with a concentration of 25 g.L^{-1} in deionized water was prepared. To adjust the pH, 7 g NaOH was added until a solution with a pH of 3.8 was obtained. Then the solution was added to the feed tank. The pump was started, the thermostat was adjusted to $25 \text{ }^\circ\text{C}$. The flow rate was adjusted to 3.6 L.min^{-1} . The pressure was increased to 32 bar

once again gradually to avoid damage to the membrane. After that, permeate recirculation was performed. Once the required operating conditions were maintained and stabilized, the mass flow rate of permeate was recorded, and samples of permeate and retentate were collected. The conductivity and pH of the samples were determined every 10 min.

The procedure was carried out similarly for the solution with a pH equal to 6; this time, 15 g NaOH was added until a solution with a pH equal to 6 was obtained. And for the four commercially available NF membranes (NF-Alfa Laval, NF Toray, NF270, and Selro MPF-36).

The experiments and their associated operating conditions are listed in Table 13 below.

Table 13. Optimal pH value for LA recovery experiments.

| Membrane | Solution | Concentration [g.L ⁻¹] | pH | Pressure [bar] | Temperature [°C] |
|---|----------|------------------------------------|------|----------------|------------------|
| NF-Alfa Laval NF -Toray NF270 Selro MPF-36 | LA | 25 | 2.67 | 32 | 25 |
| | LA | 25 | 3.8 | | |
| | NaOH | 7 | | | |
| | LA | 25 | 6 | | |
| | NaOH | 15 | | | |

4.4.3. Determination of the best membrane for LA recovery Experiments

The purpose of these experiments was to determine the best membrane for LA recovery from our four commercially available NF membranes (Alfa Laval, NF Toray, NF270, and Selro MPF-36) or, in other words, which membrane retains the least amount of LA. Simultaneously, it may retain the maximum quantity possible of the accompanying products from the model solution.

These measurements were conducted at feed temperatures of 25 °C at a feed pressure of 32 bar.

4.4.3.1 Water permeability

In the same way, as mentioned in Section 4.4.1.1

4.4.3.2 Model solution filtration

After removing the water from the feed tank, the second step was the solution filtration process. 2 liters of the model solution containing LA, AA, Glu, Fru, NaCl, MgCl₂·6H₂O, CaCl₂, Na₂SO₄, KOH, and NH₄Cl with concentration as mentioned in Table 14 in deionized water was prepared. Then the solution was added to the feed tank. The pump was started, the thermostat was adjusted to 25 °C. The flow rate was adjusted to 3.6 L.min⁻¹. The pressure was increased to 32 bar once again gradually to avoid damage to the membrane. After that, permeate recirculation was performed. Once the required operating conditions were maintained and stabilized, the mass flow rate of permeate was recorded, and samples of permeate and retentate were collected. The conductivity and pH of the samples were

determined every 10 min. The experiments and their associated operating conditions are listed in Table 14 below.

Table 14. The best membrane for LA recovery experiments.

| Membrane | Solution | Concentration [g.L ⁻¹] | pH | Pressure [bar] | Temperature [°C] |
|---|--------------------------------------|---------------------------------------|------|-------------------|---------------------|
| NF-Alfa Laval NF -Toray NF270 SELRO MPF-36 | LA | 20 | | | |
| | AA | 3.31 | | | |
| | Glu | 4.27 | | | |
| | Fru | 6.53 | | | |
| | NaCl | 1.2 | | | |
| | MgCl ₂ ·6H ₂ O | 1.2 | 2.31 | 32 | 25 |
| | CaCl ₂ | 0.5 | | | |
| | Na ₂ SO ₄ | 0.23 | | | |
| | KOH | 1 | | | |
| | NH ₄ Cl | 1 | | | |

4.4.4. Experimental investigation on the effect of different minerals on LA recovery.

The purpose of these experiments was to investigate the effect of different minerals (monovalent and divalent ions) on the LA recovery using a membrane selected from the four commercially available NF membranes. These measurements were conducted at feed temperatures of 25 °C at a feed pressure of 32 bar using the NF-Alfa Laval membrane.

4.4.4.1 Water permeability

In the same way, as mentioned in Section 4.4.1.1

4.4.4.2 Model solution filtration

After removing the water from the feed tank, the second step was the solution filtration process. 2 liters of complex mixtures solutions composed entirely of minerals with and without Organic solutes were produced, and solutions containing octonary ionic, quaternary ionic, ternary ionic, or binary ionic systems were obtained, as listed in Table 15.

Then the solution was added to the feed tank. The pump was started, the thermostat was adjusted to 25 °C. The flow rate was adjusted to 3.6 L.min⁻¹. The pressure was increased to 32 bar once again gradually to avoid damage to the membrane. After that, permeate recirculation was performed. Once the required operating conditions were maintained and stabilized, the mass flow rate of permeate was recorded, and samples of permeate and retentate were collected. The conductivity and pH of the samples were determined every 10 min.

The experiments and their associated operating conditions are listed in Table 15 below.

Table 15. Investigate the effect of different minerals on LA recovery with NF-Alfa Laval membrane at 25 °C and 32 bar experiments.

| Nr. solution | System | Solution | Concentration [g.L ⁻¹] | pH |
|--------------|--|--------------------------------------|------------------------------------|------|
| 1 | Organic solute + octonary ionic system | LA | 25 | 2.31 |
| | | AA | 3.31 | |
| | | Glu | 4.27 | |
| | | Fru | 6.53 | |
| | | NaCl | 1.2 | |
| | | MgCl ₂ ·6H ₂ O | 1.2 | |
| | | CaCl ₂ | 0.5 | |
| | | Na ₂ SO ₄ | 0.23 | |
| 2 | Organic solute + binary ionic system | LA | 25 | 2.04 |
| | | AA | 3.31 | |
| | | Glu | 4.27 | |
| | | Fru | 6.53 | |
| | | NaCl | 1.2 | |
| 3 | Organic solute + binary ionic system | LA | 25 | 2.06 |
| | | AA | 3.31 | |
| | | Glu | 4.27 | |
| | | Fru | 6.53 | |
| | | MgCl ₂ ·6H ₂ O | 1.2 | |
| 4 | Organic solute + binary ionic system | LA | 25 | 2.09 |
| | | AA | 3.31 | |
| | | Glu | 4.27 | |
| | | Fru | 6.53 | |
| | | CaCl ₂ | 0.5 | |
| 5 | Organic solute + binary ionic system | LA | 25 | 2.1 |
| | | AA | 3.31 | |
| | | Glu | 4.27 | |
| | | Fru | 6.53 | |
| | | Na ₂ SO ₄ | 0.23 | |
| 6 | Organic solute + binary ionic system | LA | 25 | 2.44 |
| | | AA | 3.31 | |
| | | Glu | 4.27 | |
| | | Fru | 6.53 | |
| | | KOH | 1 | |
| 7 | Organic solute + binary ionic system | LA | 25 | 2.1 |
| | | AA | 3.31 | |
| | | Glu | 4.27 | |
| | | Fru | 6.53 | |
| | | NH ₄ Cl | 1 | |

Table 15. (Continued)

| Nr. solution | System | Solution | Concentration [g.L ⁻¹] | pH |
|--------------|--|--------------------------------------|------------------------------------|------|
| 8 | Organic solute + ternary ionic system | LA | 25 | 2.08 |
| | | AA | 3.31 | |
| | | Glu | 4.27 | |
| | | Fru | 6.53 | |
| | | NaCl | 1.2 | |
| | | MgCl ₂ ·6H ₂ O | 1.2 | |
| 9 | Organic solute + ternary ionic system | LA | 25 | 2.08 |
| | | AA | 3.31 | |
| | | Glu | 4.27 | |
| | | Fru | 6.53 | |
| | | CaCl ₂ | 0.5 | |
| | | MgCl ₂ ·6H ₂ O | 1.2 | |
| 10 | Organic solute + ternary ionic system | LA | 25 | 2.08 |
| | | AA | 3.31 | |
| | | Glu | 4.27 | |
| | | Fru | 6.53 | |
| | | NaCl | 1.2 | |
| | | Na ₂ SO ₄ | 0.23 | |
| 11 | Organic solute + quaternary ionic system | LA | 25 | 2.45 |
| | | AA | 3.31 | |
| | | Glu | 4.27 | |
| | | Fru | 6.53 | |
| | | KOH | 1 | |
| | | NH ₄ Cl | 1 | |
| 12 | Organic solute + quaternary ionic system | LA | 25 | 2.08 |
| | | AA | 3.31 | |
| | | Glu | 4.27 | |
| | | Fru | 6.53 | |
| | | MgCl ₂ ·6H ₂ O | 1.2 | |
| | | Na ₂ SO ₄ | 0.23 | |
| 13 | Organic solute + quaternary ionic system | LA | 25 | 2.43 |
| | | AA | 3.31 | |
| | | Glu | 4.27 | |
| | | Fru | 6.53 | |
| | | CaCl ₂ | 0.5 | |
| | | KOH | 1 | |
| 14 | Organic solute without ions | LA | 25 | 2.13 |
| | | AA | 3.31 | |
| | | Glu | 4.27 | |
| | | Fru | 6.53 | |

Table 15. (Continued)

| Nr. solution | System | Solution | Concentration [g.L ⁻¹] | pH |
|--------------|-------------------------|--------------------------------------|------------------------------------|-------|
| 15 | Octonary ionic system | NaCl | 1.2 | 9.91 |
| | | MgCl ₂ ·6H ₂ O | 1.2 | |
| | | CaCl ₂ | 0.5 | |
| | | Na ₂ SO ₄ | 0.23 | |
| | | KOH | 1 | |
| | | NH ₄ Cl | 1 | |
| 16 | Binary ionic system | NaCl | 1.2 | 6.27 |
| 17 | Binary ionic system | MgCl ₂ ·6H ₂ O | 1.2 | 6.23 |
| 18 | Binary ionic system | CaCl ₂ | 0.5 | 6.7 |
| 19 | Binary ionic system | Na ₂ SO ₄ | 0.23 | 6.25 |
| 20 | Binary ionic system | NH ₄ Cl | 1 | 6.84 |
| 21 | Binary ionic system | KOH | 1 | 11.97 |
| 22 | Ternary ionic system | NaCl | 1.2 | 6.88 |
| | | MgCl ₂ ·6H ₂ O | 1.2 | |
| 23 | Ternary ionic system | CaCl ₂ | 0.5 | 6.3 |
| | | MgCl ₂ ·6H ₂ O | 1.2 | |
| 24 | Ternary ionic system | NaCl | 1.2 | 6.7 |
| | | Na ₂ SO ₄ | 0.23 | |
| 25 | Quaternary ionic system | KOH | 1 | 9.8 |
| | | NH ₄ Cl | 1 | |
| 26 | Quaternary ionic system | MgCl ₂ ·6H ₂ O | 1.2 | 7 |
| | | Na ₂ SO ₄ | 0.23 | |
| 27 | Quaternary ionic system | CaCl ₂ | 0.5 | 12.06 |
| | | KOH | 1 | |

5. Analytical methods

5.1 pH and conductivity measurements

pH and conductivity meter from WTW, model multi 3430 were used to determine these properties for feed, retentate, and permeate. The limit for pH ranges was from 0 to 14 and conductivity ranges were from 0 to 1000 $\text{mS}\cdot\text{cm}^{-1}$, as illustrated in Fig 39.

Conductivity is a numerical representation of an aqueous solution's capacity to conduct an electric current. This capability is dependent on the temperature and the presence of ions regarding their total concentration, mobility, valence, and relative concentrations. Most of the inorganic acids, bases, and salts are generally strong conductors of electricity. On the other hand, molecules of organic polar compounds do not dissociate in an aqueous solution and conduct weak currents.



Figure 39. WTW, model pH/Cond 3320 pH and conductivity meter.

5.2 Determination of anions and cations concentration

The concentrations of anions (Cl^- , and SO_4^{2-}) and cations (Na^+ , Mg^{2+} , Ca^{2+} , K^+ , and NH_4^+) were measured using Thermo Fisher Scientific's Dionex ICS-5000 + ion chromatography system, as illustrated in Fig 40. This system is equipped with:

- The dual pump system (DP) is equipped with two pumps.
- The Eluent organizer (EO) holds reservoirs of effluent.
- The Detector/chromatography compartment (DC) provides a temperature-controlled environment for Dionex ICS-5000+ chromatography components.
- The Autosampler (AS-AP) provides high-performance, automated sample processing for ion chromatography applications.

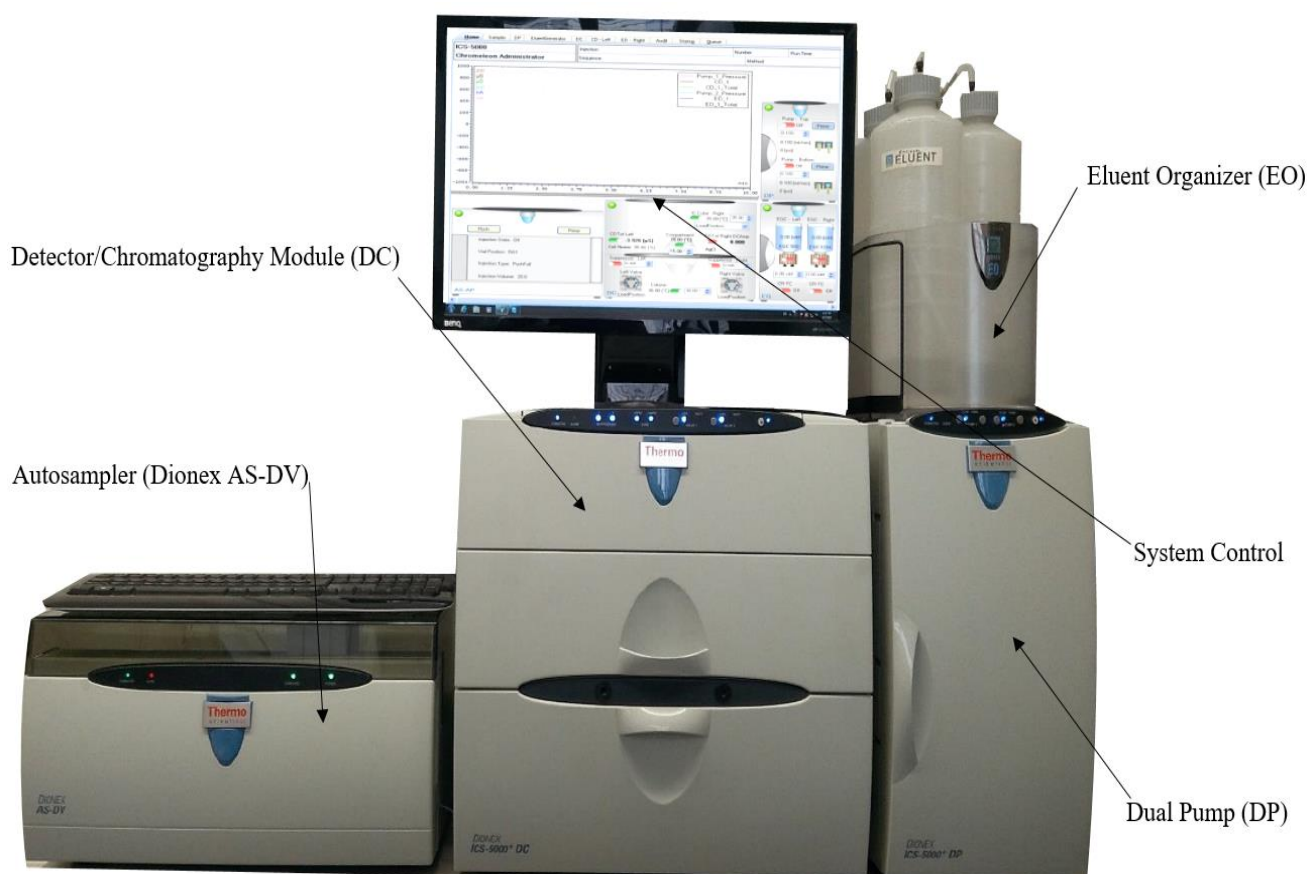


Figure 40. Dionex ICS-5000+ ion chromatography system.

The retentate and permeate samples were diluted with deionized water by a dilution factor of 150. Due to that Dionex ICS-5000+, ion chromatography system has maximum ions concentrations detection limits as shown in Table 16.

Table 16. Dionex ICS-5000+ ion chromatography maximum ions concentrations detection limits.

| Ion | maximum concentrations [mg.L ⁻¹] |
|-------------------------------|--|
| Cl ⁻ | 20 |
| SO ₄ ²⁻ | 20 |
| Na ⁺ | 20 |
| Mg ²⁺ | 20 |
| Ca ²⁺ | 20 |
| k ⁺ | 10 |
| NH ₄ ⁺ | 2 |

Fig 41 shows a typical chromatogram for Cl⁻ and SO₄²⁻ ions and Fig 42 shows a typical chromatogram for Na⁺, Mg²⁺, Ca²⁺, K⁺, and NH₄⁺ ions, where the conductivity (μS) is on Y-axis and time (min) is on X-axis.

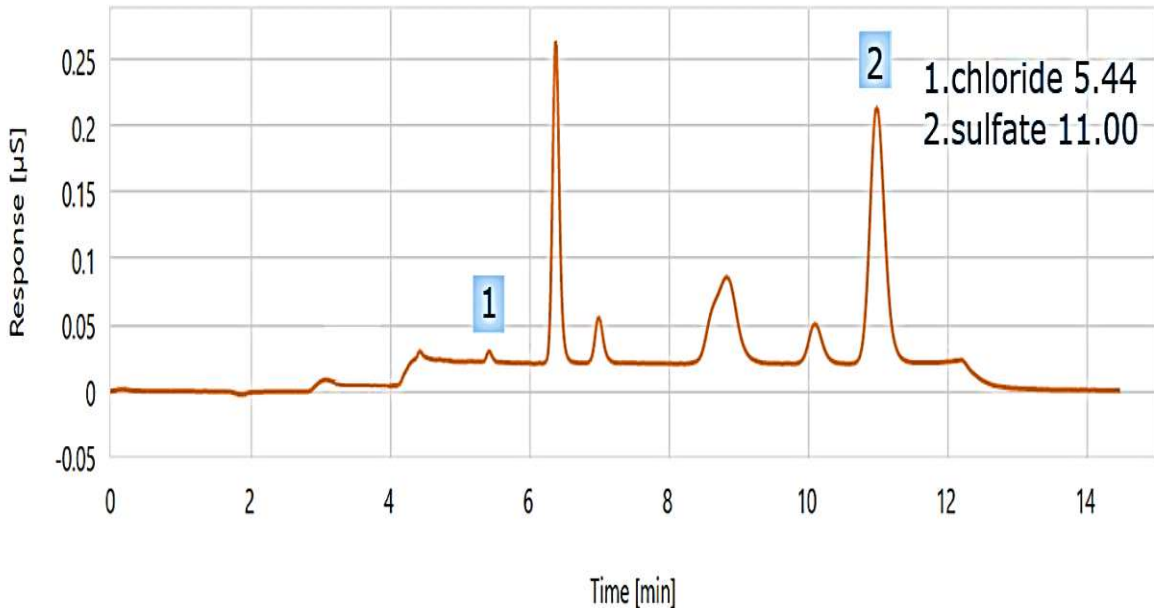


Figure 41. Chromatogram for Cl⁻ and SO₄²⁻ ions.

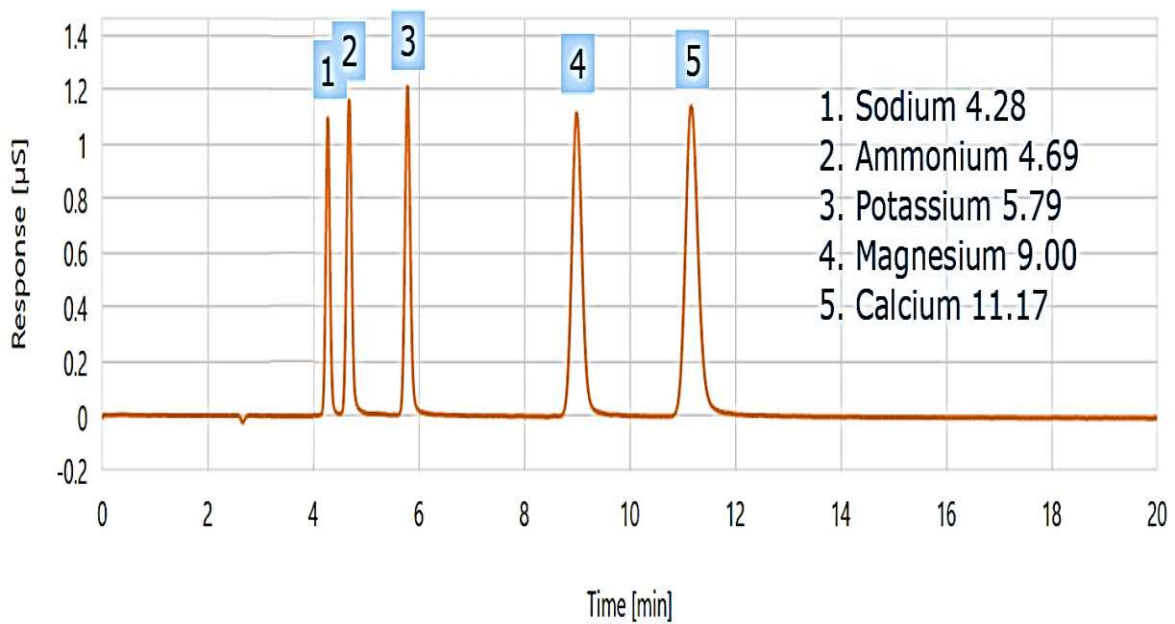


Figure 42. Chromatogram for Na⁺, Mg²⁺, Ca²⁺, K⁺ and NH₄⁺ ions.

5.3 Determination of the concentration of the organic solutes

The concentrations of organic solutes (LA, AA, Glu, and Fru) were measured using Shimadzu Prominence 20 HPLC UFLC System, as illustrated in Fig 43. This system includes the following components:

- The DGU-20A is used for degassing microbubbles formed by mixing liquids with differing gas solubilities. These microbubbles may affect the system, ranging from reduced check valve function to a noisy baseline to trapped bubbles in the detector flow cell.
- The LC-20AD pumps flow rates from 100 nL.min⁻¹ and achieve LC's highly stable flow-rate performance.
- The SIL-20A Series autosamplers achieve unparalleled speed, with a sample injection movement of just 10 seconds.
- The CTO-20AC has a temperature range of 10 °C below room temperature to 85 °C, allowing for improved separation performance.

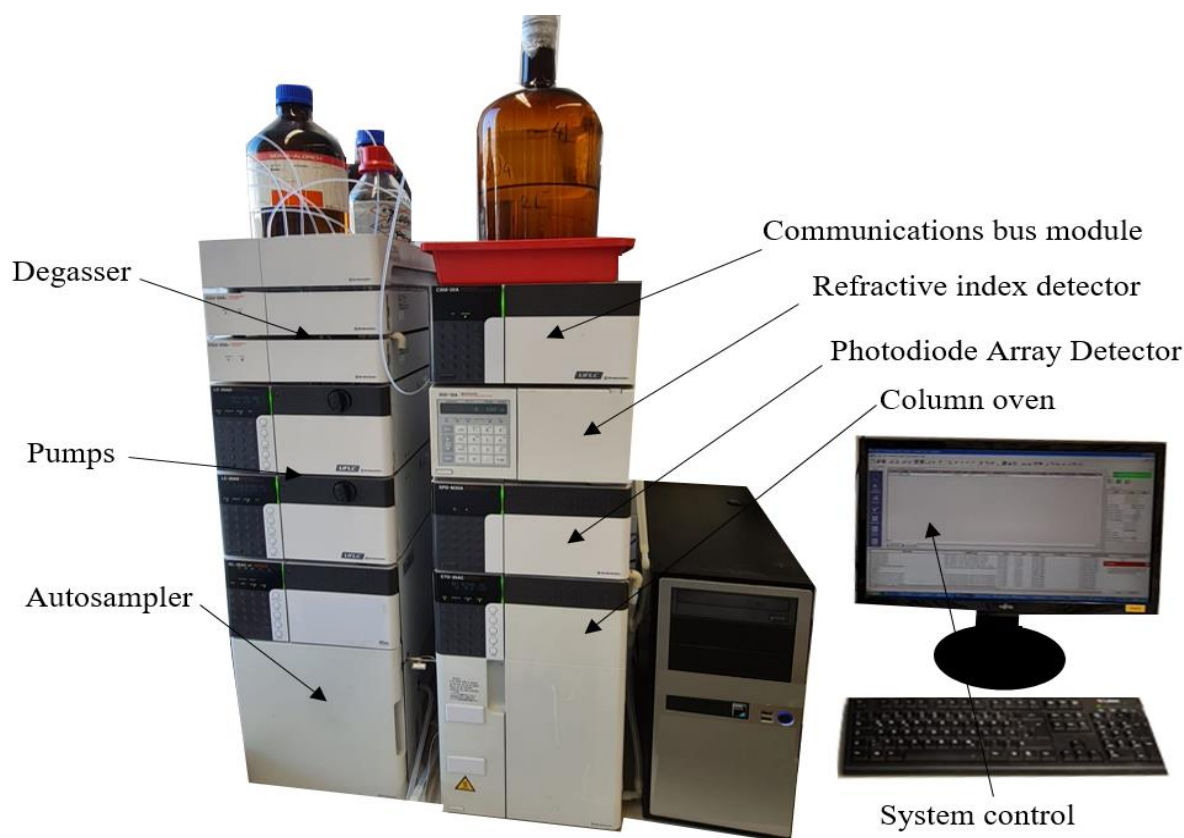


Figure 43. Shimadzu Prominence 20 HPLC System.

- The SPD-M20A is suitable for any UV measurements between 190 and 800 nm.
- The RID-10A differential refractive index detector has dual temperature control and a high level of stability.
- The CBM-20A communications bus module serves as a bridge enabling instruments to be connected to LC workstations or network-client PCs.
- The LC workstation

The retentate and permeate samples were diluted with deionized water by 2 different dilution factors of 8 and 2. Because LA is present in high concentrations, a dilution factor of 8 was used. In contrast, AA, Glu, and Fru are present at lower concentrations. Therefore, a dilution factor of 2 was used. That's because the Shimadzu Prominence 20 HPLC System's maximum concentration detection limits were as shown in Table 17.

Table 17. Shimadzu Prominence 20 HPLC System's maximum concentration detection limits.

| Material | Maximum concentration [g.L ⁻¹] |
|----------|--|
| LA | 5 |
| AA | 5 |
| Glu | 5 |
| Fru | 5 |

Fig 44 shows the chromatogram for LA, AA, Glu, and Fru, where the spectral sign (mV) is on Y-axis and time (min) is on X-axis.

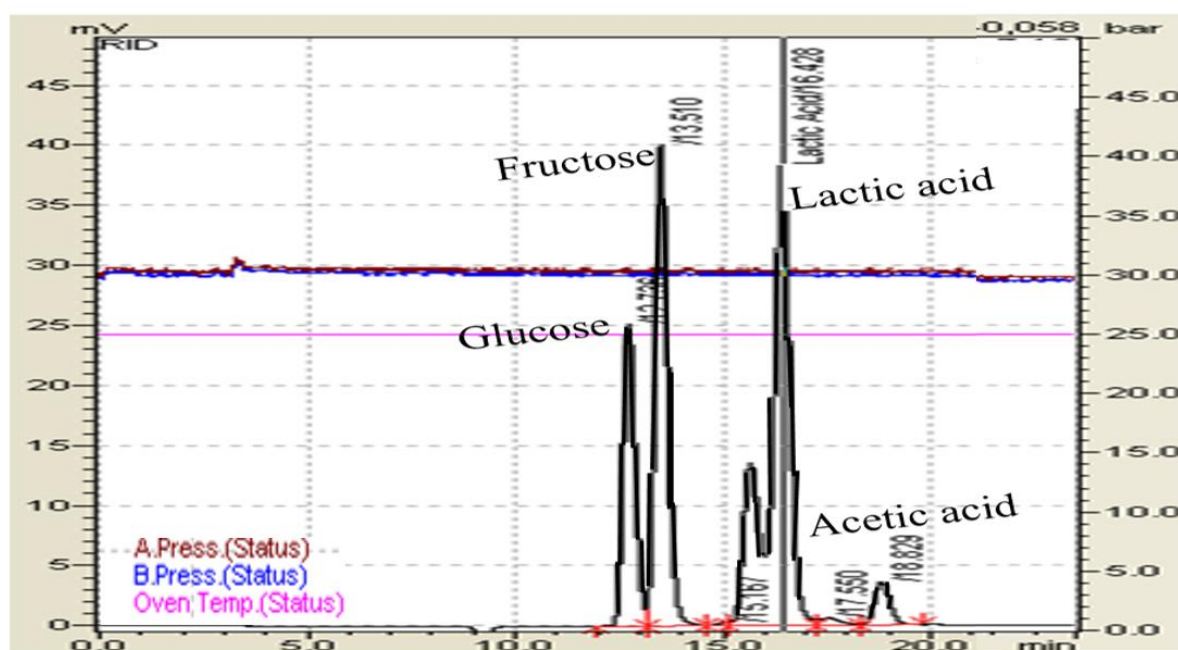


Figure 44. The chromatogram for LA, AA, Glu, and Fru.

In most of the measurements, two and sometimes three peaks were obtained at the area of lactic acid appearance. The reason for this may be that in the state of equilibrium, lactic acid solutions contain monomeric lactic acid, dimeric lactic acid or lactoyl lactic acid, higher oligomers of lactic acid, and lactide. All ratios are proportional to the quantity of water present.

6. Results and discussion

The results of extensive investigations of the performance of membranes will be presented in this section. First, we will investigate the effects of operation temperature, pH, and membrane structure. Finally, the membrane's separation behavior will be investigated using a variety of organic solutes solutions (LA, AA, Glu, and Fru) with and without a variety of salts (NaCl, $MgCl_2 \cdot 6H_2O$, $CaCl_2$, Na_2SO_4 , KOH, and NH_4Cl) combinations to determine the effect of various minerals on Lactic Acid recovery.

6.1 Determination of the optimal operating temperature for the LA recovery

Since adjusting the operation conditions enhance process performance, it is essential to investigate the effect of operating parameters such as temperature on membrane permeate flux and rejection to determine the optimal operating temperature for the LA recovery.

Fig 45 shows the flux variation with time for LA solution and deionized water before and after solution filtration process using four commercially available NF membranes (Alfa Laval, NF Toray, NF270, and Selro MPF-36) at 25 °C and 32 bar, pH around 2.67.

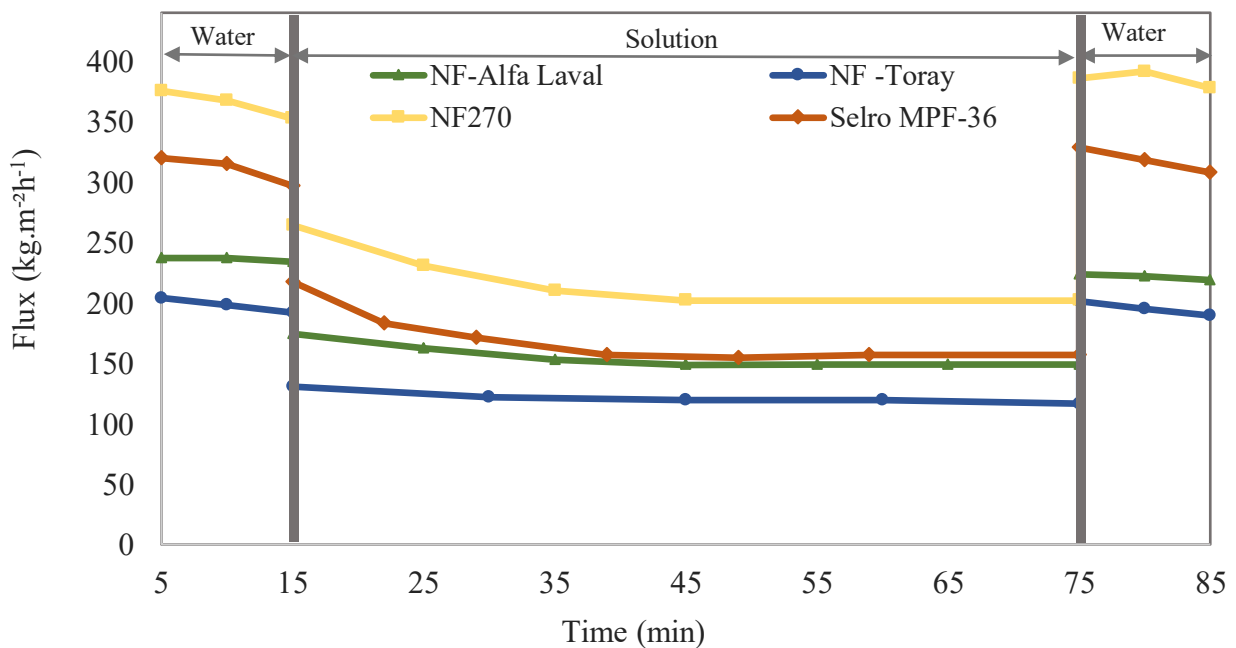


Figure 45. The flux variation with time for LA solution and deionized water before and after filtration for four commercially available NF membranes $T = 25$ °C, $p = 32$ bar, $pH = 2.67$.

The flux variation with time for LA solution and deionized water before and after solution filtration using four commercially available NF membranes (Alfa Laval, NF Toray, NF270, and Selro MPF-36) at 40 °C and 32 bar, pH around 2.67 is presented in Fig 46.

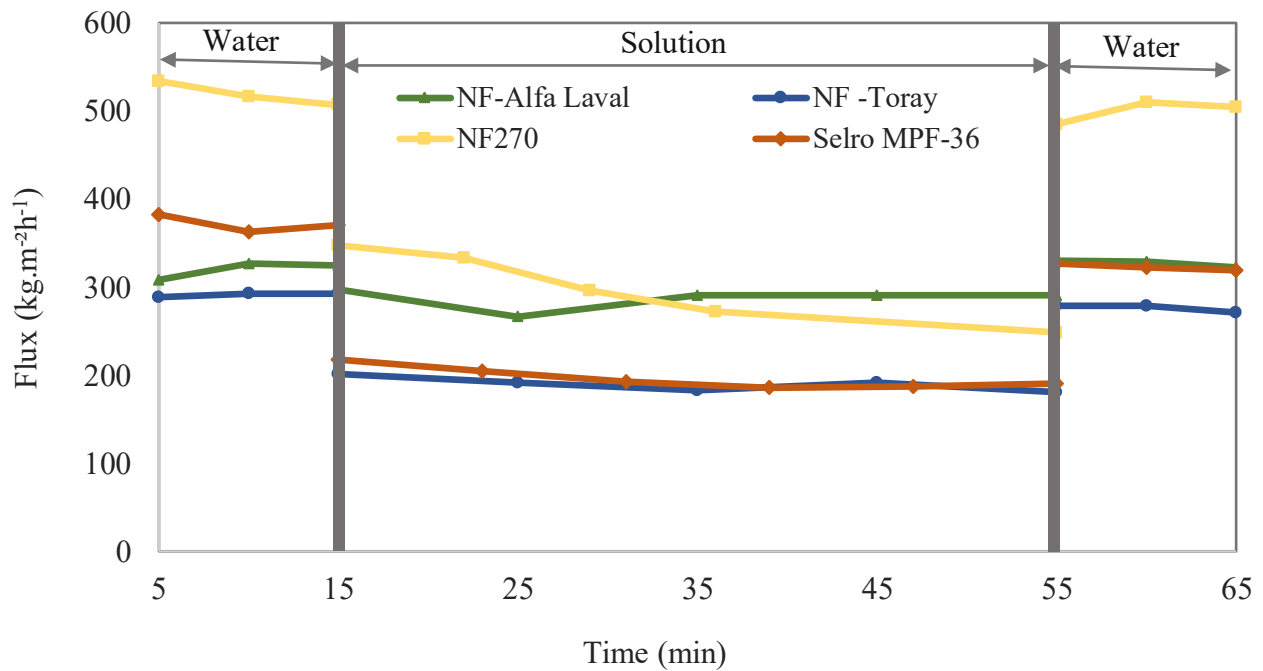


Figure 46. The flux variation with time for LA solution and deionized water before and after filtration for four commercially available NF membranes T = 40 °C, p = 32 bar, pH = 2.67.

The effect of applied temperature on the LA solution permeate flux and rejection is shown in Figures 47 and 48 for four commercially available NF membranes (Alfa Laval, NF Toray, NF270, and Selro MPF-36).

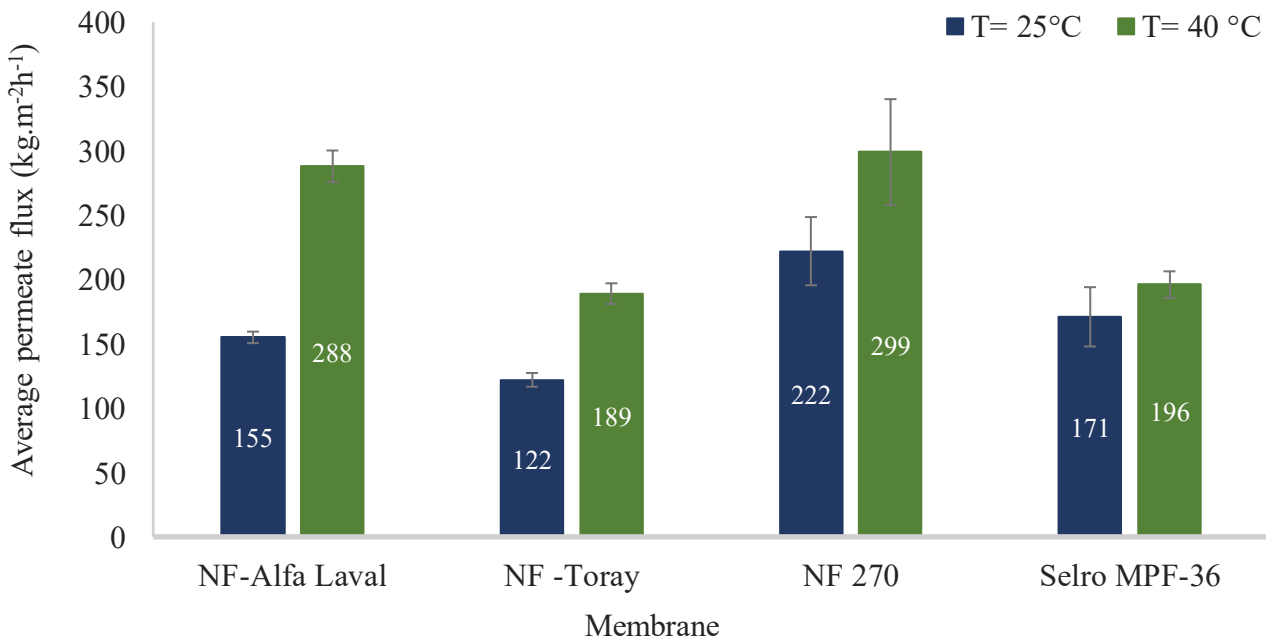


Figure 47. The effect of applied temperature on the LA solution permeate flux for four commercially available NF membranes at p = 32 bar, pH = 2.67.

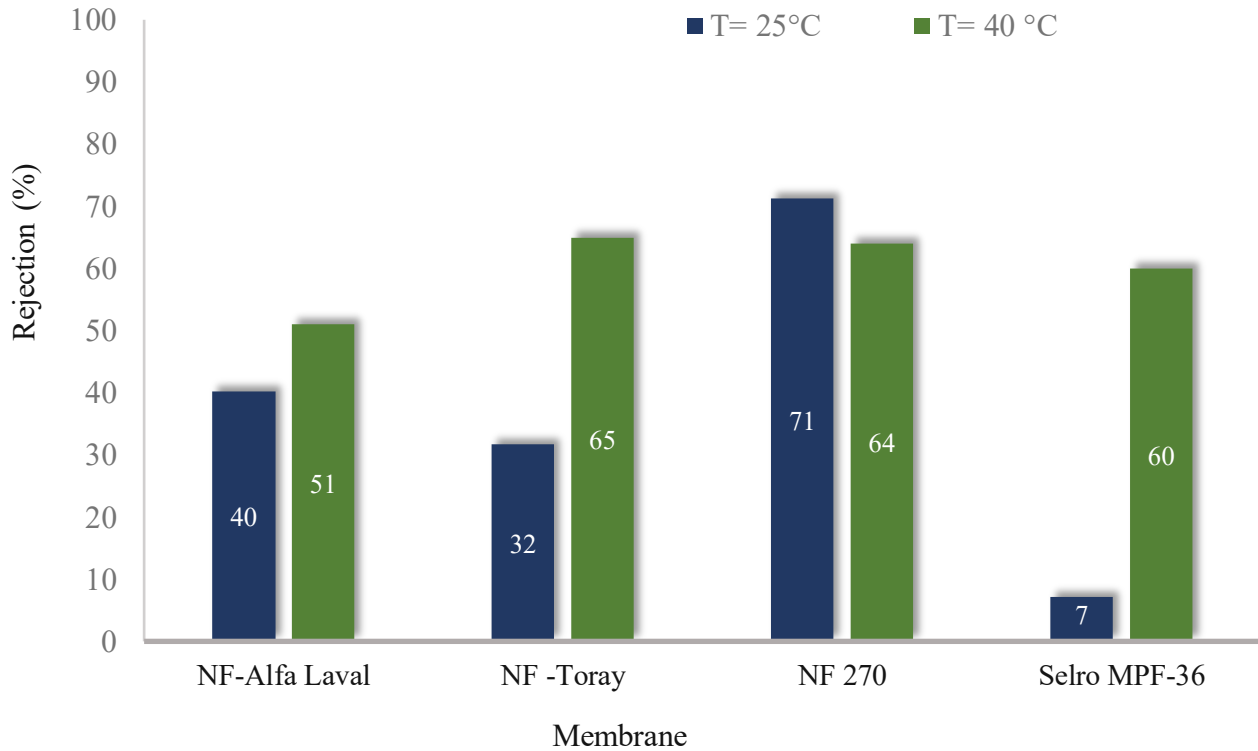


Figure 48. The effect of applied temperature on the LA solution rejection for four commercially available NF membranes at $p = 32$ bar, $pH = 2.67$.

It can be concluded from the variation with the temperature that the permeate flux always increases as the temperature increases and these effects occur due to the change in membrane structural parameters (effective pore radius, active layer thickness, membrane charge, and pore dielectric constant), solvent viscosity, and solute diffusivity due to temperature at each value of membrane charge. In addition, the solute rejection increased as applied temperature increased at constant pressure and pH for NF-Alfa Laval, NF Toray, and Selro MPF-36 membranes. In contrast, the solute rejection decreased as applied temperature increased for the NF270 membrane related to the expansion of the porous with rising temperature.

6.2. Determination of the optimal pH value for LA recovery

Fig 49 shows the flux variation with time for LA solution and deionized water before and after solution filtration using four commercially available NF membranes (Alfa Laval, NF Toray, NF270, and Selro MPF-36) at 25 °C and 32 bar, after adjusting the pH value to 3.8 using sodium hydroxide.

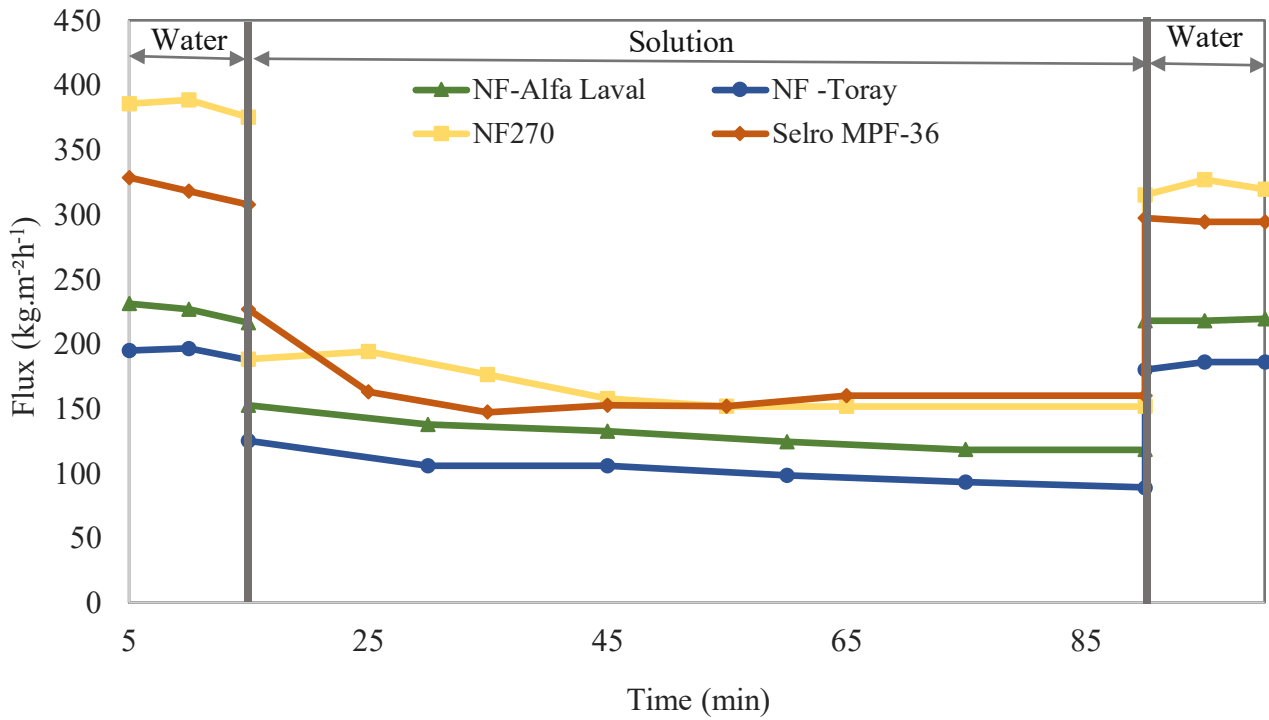


Figure 49. The flux variation with time for LA solution and deionized water before and after filtration for four commercially available NF membranes at T = 25 °C, p = 32 bar, pH = 3.8.

Fig 50 shows the flux variation with time for LA solution and deionized water before and after solution filtration using four commercially available NF membranes (Alfa Laval, NF Toray, NF270, and Selro MPF-36) at 25 °C and 32 bar, after adjusting the pH value to 6 using sodium hydroxide.

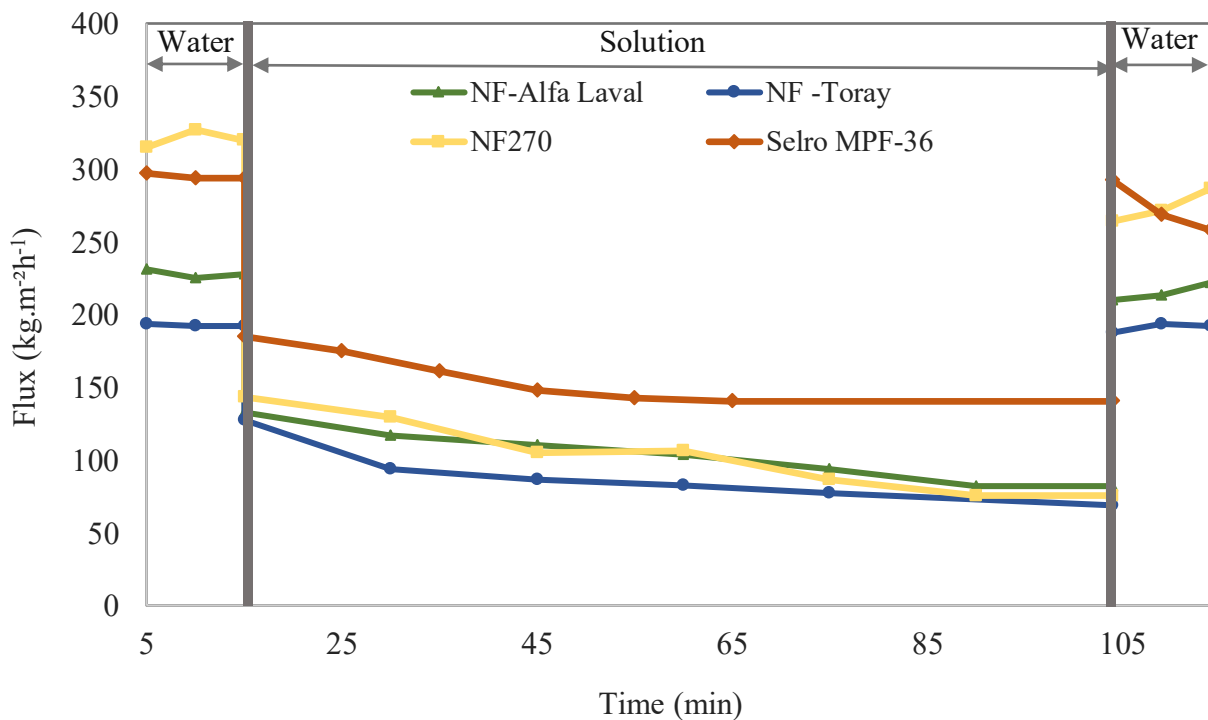


Figure 50. The flux variation with time for LA solution and deionized water before and after filtration for four commercially available NF membranes at T = 25 °C, p = 32 bar, pH = 6.

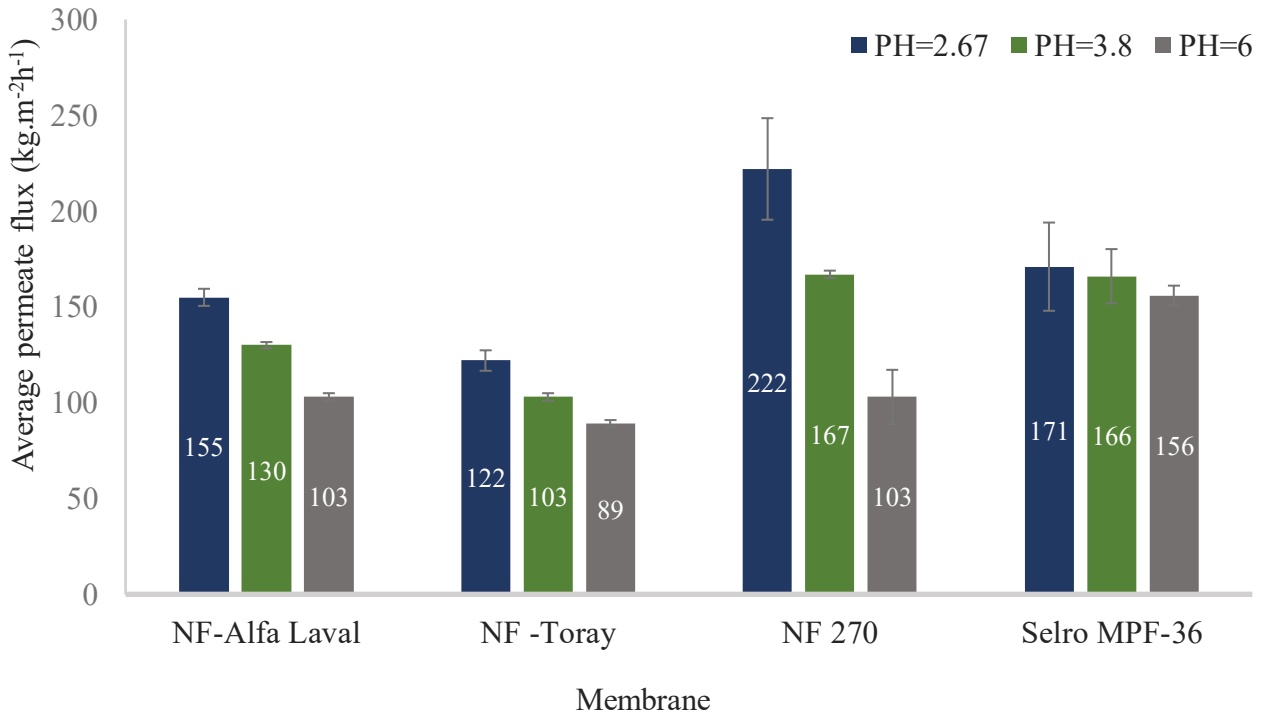


Figure 51. The effect of pH on the LA solution permeate flux for four commercially available NF membranes at p = 32 bar, T= 25 °C.

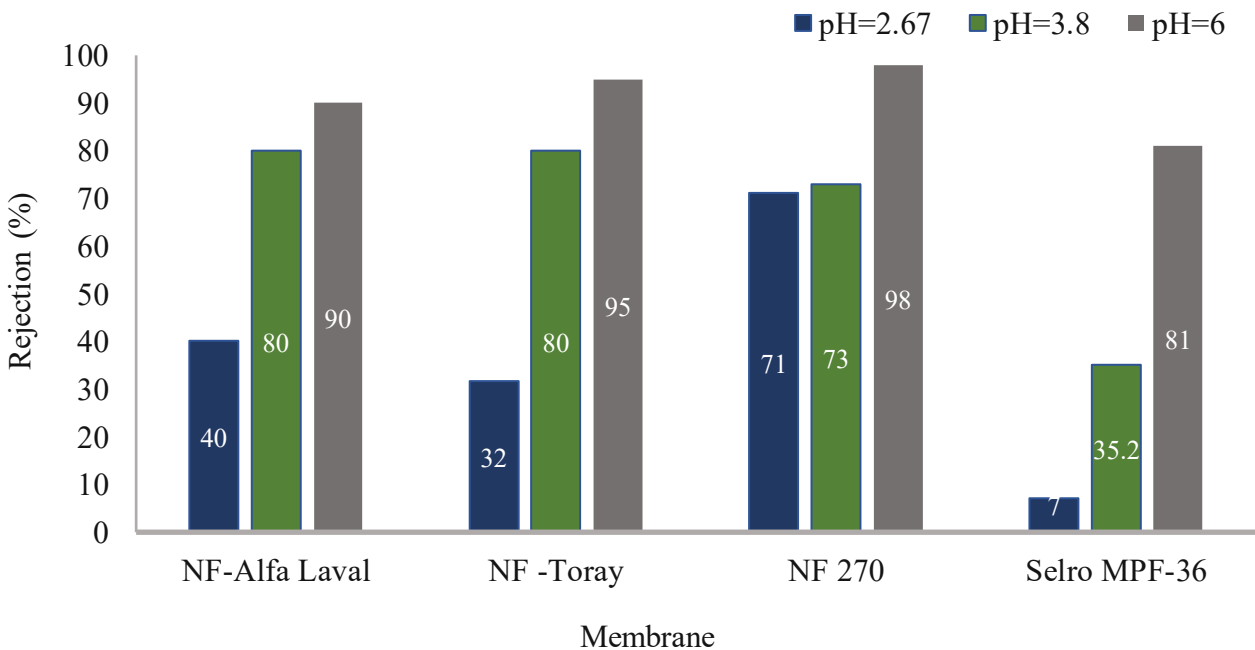


Figure 52. The effect of pH on the LA solution rejection for four commercially available NF membranes at p = 32 bar, T = 25 °C.

The effect of pH on the permeate flux and rejection of LA solution is shown in Fig 51 and Fig 52 for four commercially available NF membranes (Alfa Laval, NF Toray, NF270, and Selro MPF-36). Fig 51 and Fig 52 show that as pH increased at constant temperature and pressure, the LA permeate flux decreased, and LA's rejection increased. Regarding to the effect of pH on both selectivity and

performance of the NF process is related to the characteristic behavior of the used membranes, which is that electrolyte rejection increases as the pH of the feed solutions increases due to the change of membrane charge. In addition, the ratio of lactate ions to non-ionized (non-dissociated) LA in the feed stream, in particular, is an essential factor influencing LA permeability.

This ratio is highly influenced by the LA equilibrium at the system's operating temperature and can be determined using the Henderson–Hasselbalch equation Eq 6.1

$$pH = pK_a + \log \frac{[\text{lactate}]}{[\text{lactic acid}]} \quad (6.1)$$

Where pK_a is the dissociation constant of lactic acid, which is 3.86 at 25 °C.

6.3. Determination of the best membrane for LA recovery

A comparison between the separation performances of four commercially available NF membranes (Alfa Laval, NF Toray, NF270, and Selro MPF-36) for LA, AA, Glu, and Fru at a constant temperature, pressure, concentration, and pH is shown in Fig 53.

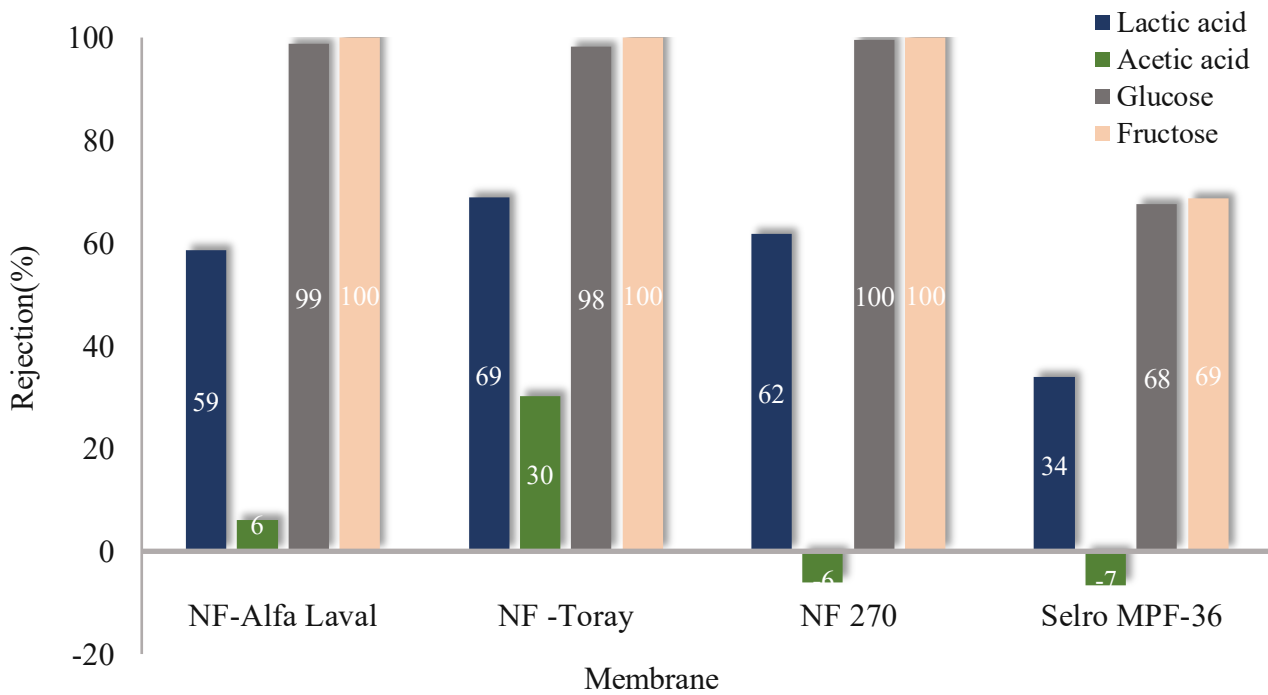


Figure 53. The separation performance of four commercially available NF membranes for LA, AA, Glu, and Fru at $p = 32$ bar, $T = 25$ °C, and $pH = 2.67$.

The NF-Alfa Laval membrane completely rejects Glu, and Fru, around 6 % AA and 59 % LA. The NF Toray membrane completely rejects Glu, and Fru, around 30 % AA and 69 % LA. Also the NF270 membrane rejects Glu, and Fru entirely and 62% of LA, but not AA. While, the Selro MPF-36 membrane rejects 68% of Glu, 69% of Fru, and 34% of LA, but not AA. The rejection difference between the four membranes is primarily due to differences in the chemical composition and structure

of the membranes' active layer. The process of selecting the best membrane among the four membranes is primarily constrained by several factors, including an acceptable permeate flux value, low LA retention, and high retention of accompanying LA components such as AA, Glu, and Fru. By evaluating the performance of the four membranes on the previously mentioned criteria, we conclude that the NF-Alfa Laval membrane most satisfies the desired purpose, and therefore was used in the Investigation of the effect of different minerals on LA recovery.

6.4. Investigation of the effect of different minerals on LA recovery

The separation performance of NF for solutions containing a mixture of neutral solutes such as organic acids and charged solutes such as salts, as well as their interactions have not been widely studied. Previous researches tried to improve the efficiency of recovering LA using membrane technology. However, no study has been published in the public domain that investigates the effect of various components such as minerals on LA recovery from synthetic grass silage employing NF membrane technology.

The separation performance of NF for solutions containing organic solutes (LA, AA, Glu, and Fru) with or without binary, ternary, quaternary, and octonary ionic systems were discussed. The following section will describe the permeate flux and rejection in how the presence of these various minerals can affect the LA recovery from the synthetic model solution.

NF-Alfa Laval Membrane is a three-layer, thin-film (TF) Polypiperazinamide (PPA) membrane that is a composite membrane in which the active PPA layer is attached to porous support. The porous support is often an ultrafiltration membrane, which is attached to a non-woven material, frequently made of polypropylene or polyester. The cross-linking of the active PPA layer stabilizes the structure. Separation in NF is determined by the Donnan effect (electrical charge) and the Sieving mechanism (size exclusion). The active PPA layer is an aromatic/aliphatic PPA. It can be thought of as a polyampholyte with both positive and negative charges due to the amine and carboxylate residual groups; the positive surface charge below the isoelectric point is caused by the protonation of the amine functional groups ($\equiv\text{NH}_2 \rightarrow \equiv\text{NH}_3^+$). The negative charge above the isoelectric point is caused by deprotonation of the carboxyl groups ($\equiv\text{COOH} \rightarrow \equiv\text{COO}^-$), which is pH feed solution dependant. Donnan exclusion relies on the charge of the membrane, the ionic strength, and the valence of the ions, with the latter two affecting both the membrane charge density and the isoelectric point. Finally, size exclusion is structure dependant; a more dense structure results in less permeation. Previous studies have found both increasing (Nyström et al. 1995) and decreasing (Kilduff et al. 2004) permeability in the presence of salts due to changes in the membrane structure.

A previous study for the PPA membrane's zeta potential as a function of pH change determined that the membrane surface is isoelectric at pH 4.5 (Zeta potential= 0 [mV]), positive at pH less than 4.5, and negative at pH more than 4.5 (Nyström et al. 1995).

Since the matrix of organic membranes is not rigid, many explanations have been suggested to describe the observed influence of salts on neutral solute rejection. These include the following:

1) Pore swelling/shrinking, defined as an increase/decrease in the average pore radius due to repulsion forces between counterions in the electrical double layer at the pore walls (Bargeman et al. 2005) .

2) Hofmeister effects, i.e., partial dehydration of neutral molecules in the presence of ions due to water's preferential solvation of ions, which decreases the Stokes radius of neutral solutes (salting-out phenomenon). Fig 54 shows the Hofmeister series of cations, anions, and the relative effect of some salts on promoting hydrophobic interactions. Inorganic ions have distinctive and irreplaceable roles in various physical, chemical, and biological processes occurring in aqueous solutions. For example, it was discovered that ions cause distinct changes in the water network, including altering the number of hydrogen bonds per water molecule and affecting the reorientation of individual water molecules. Both observables are affected more by higher valencies and smaller cations and follow a direct Hofmeister trend (Chen et al. 2017) .

3) Osmotic pressure of salts.

4) The existence of a distribution of pore sizes. When ions are present inside pores, the flux through small tiny pores is lowered more than through larger pores (electroviscous effect) (Bargeman et al. 2005) . Thus, the bigger pores would govern the rejection of neutral solutes, which would decrease with the addition of salt.

5) Compression of the electrical double layer is generated at the membrane surface, resulting in the opening of membrane pores, consequently increasing the transport area.

6) The molecules' polarizability results in interactions with charged membranes (Mandale and Jones 2008) .

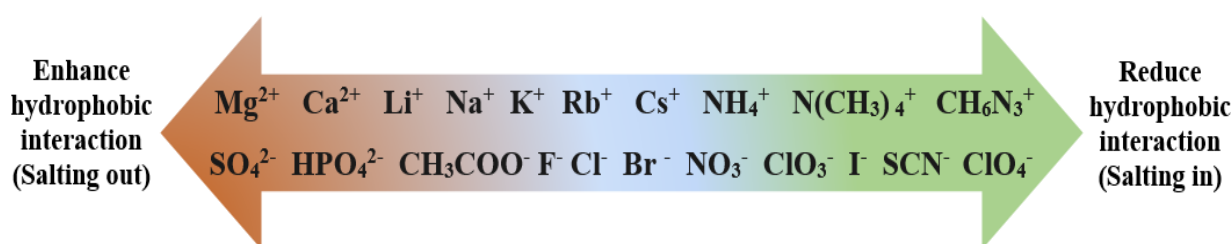


Figure 54. The Hofmeister series of cations, anions, and the relative effect of some salts on promoting hydrophobic interactions, adapted from (Liu et al. 2017) .

6.4.1 LA separation performance from the model solution with and without a binary ionic system

Fig 55 shows the Permeate flux and the rejection of LA, AA, Glu, and Fru with and without a binary ionic system using NF-Alfa Laval Membrane at a pressure equal to 32 bar and Temperature equal to 25 °C.

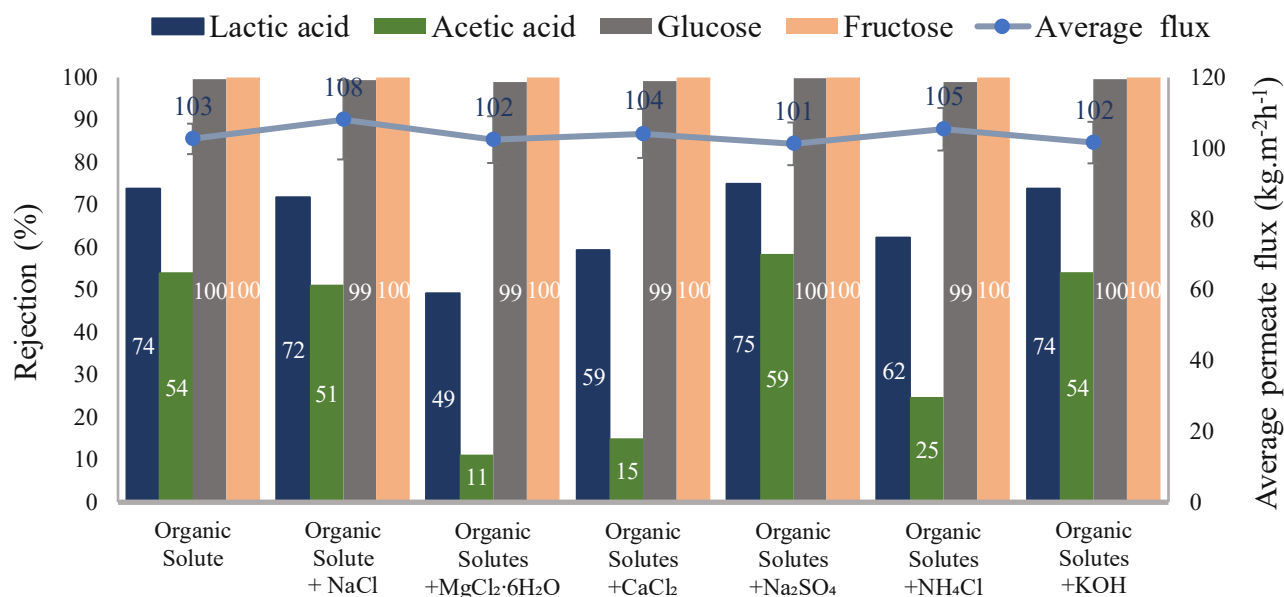


Figure 55. The permeate flux and the rejection of LA, AA, Glu, and Fru with and without a binary ionic system using NF-Alfa Laval Membrane at $p = 32$ bar, $T = 25$ °C.

Fig 55 shows the following results:

- The rejection of LA in the presence of NaCl decreased by 2.6% and the rejection of AA decreased by 4.8% while the rejection of Glu and Fru was not affected. On the other hand, the permeate flux of the solution increased by 4.9 % in the presence of NaCl.
- The rejection of LA in the presence of MgCl₂·6H₂O decreased by 33.4% and that the rejection of AA decreased by 79.3% while the rejection of Glu and Fru was not affected. On the other hand, the permeate flux of the solution decreased by 1% in the presence of MgCl₂·6H₂O.
- The rejection of LA in the presence of CaCl₂ decreased by 19.4% and that the rejection of AA decreased by 72.2% while the rejection of Glu and Fru was not affected. On the other hand, the permeate flux of the solution increased by 1% in the presence of CaCl₂.
- The rejection of LA in the presence of Na₂SO₄ increased by 1.7% and that the rejection of AA increased by 8.65% while the rejection of Glu and Fru was not affected. On the other hand, the permeate flux of the solution decreased by 2% in the presence of Na₂SO₄.

- The rejection of LA in the presence of NH_4Cl decreased by 15.4% and that the rejection of AA decreased by 53.9%, while the rejection of Glu and Fru was not affected. On the other hand, the permeate flux of the solution increased by 2% in the presence of NH_4Cl .
- The rejection of LA in the presence of KOH increased by 0.3% and that the rejection of AA increased by 0.5% while the rejection of Glu and Fru was not affected. On the other hand, the permeate flux of the solution decreased by 1% in the presence of KOH.

The rejection variation of LA and AA also the variation in solution permeate flux by adding binary ionic system ($(\text{Na}^+ + \text{Cl}^-)$, $(\text{NH}_4^+ + \text{Cl}^-)$, $(\text{Ca}^{2+} + \text{Cl}^-)$, $(\text{Mg}^{2+} + \text{Cl}^-)$, $(\text{K}^+ + \text{OH}^-)$ or $(\text{Na}^+ + \text{SO}_4^{2-})$) can be explained as a consequence of pore swelling /shrinking, Hofmeister effect, distribution of pore sizes, compression of the electrical double layer, the molecules' polarizability, and salt osmotic pressure. On the other hand, the rejection of glucose and fructose may be due to a steric hindrance effect since all membranes were compacted before the filtering procedure, which was unaffected by the adding binary ionic system.

6.4.1.1 Ionic rejection of NaCl with and without organic solutes

In NaCl binary ionic system solution the pH was equal to 6.27, at this pH the membrane is intended to be negatively charged. Therefore, Cl^- ions are subjected to electrostatic exclusion (Donnan exclusion) and are rejected from the membrane and Na^+ ions flow backward to maintain electroneutrality.

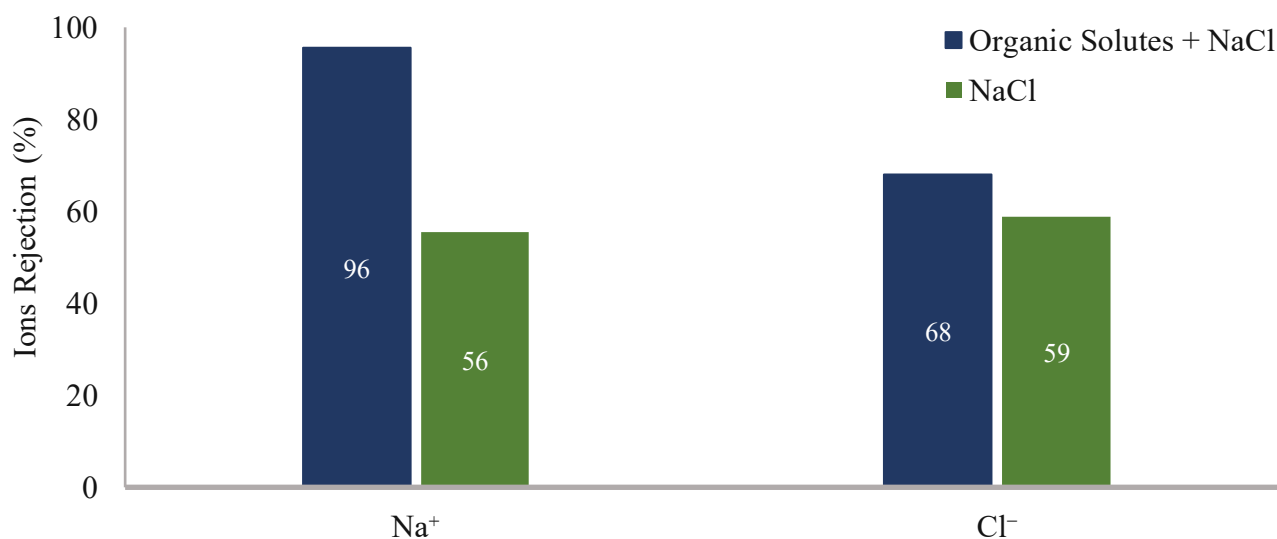


Figure 56. Ionic rejection of NaCl with and without organic solutes.

Adding the organic solutes to NaCl solution decrease pH to 2.04, the membrane became positively charged. In this case, Na^+ is repelled and rejected from the membrane due to Donnan exclusion. It was predicted that Cl^- which is in this case counter-ion to permeate through the membrane but it flows back to bulk feed for maintaining electroneutrality.

It is important to note that Cl^- has lower retention than Na^+ . Most studies agree on the qualitative interpretation of this phenomenon; that chloride adsorption is more abundant on the membrane than sodium adsorption since anions have smaller hydration radii than cations.

6.4.1.2 Ionic rejection of $\text{MgCl}_2 \cdot 6\text{H}_2\text{O}$ with and without organic solutes

Fig 57 shows the ionic rejection of $\text{MgCl}_2 \cdot 6\text{H}_2\text{O}$ with and without Organic solutes. In $\text{MgCl}_2 \cdot 6\text{H}_2\text{O}$ binary ionic system solution the pH was equal to 6.23, at this pH the membrane is intended to be negatively charged. Therefore, Cl^- ions are subjected to electrostatic exclusion (Donnan exclusion) and are rejected from the membrane and Mg^{+2} ions flow backward to maintain electroneutrality. Adding the organic solutes to $\text{MgCl}_2 \cdot 6\text{H}_2\text{O}$ solution decrease pH to 2.06, the membrane became positively charged. In this case, Mg^{+2} is repelled and rejected from the membrane due to Donnan exclusion. It was predicted that Cl^- which is in this case counter-ion to permeate through the membrane but it flows back to bulk feed for maintaining electroneutrality.

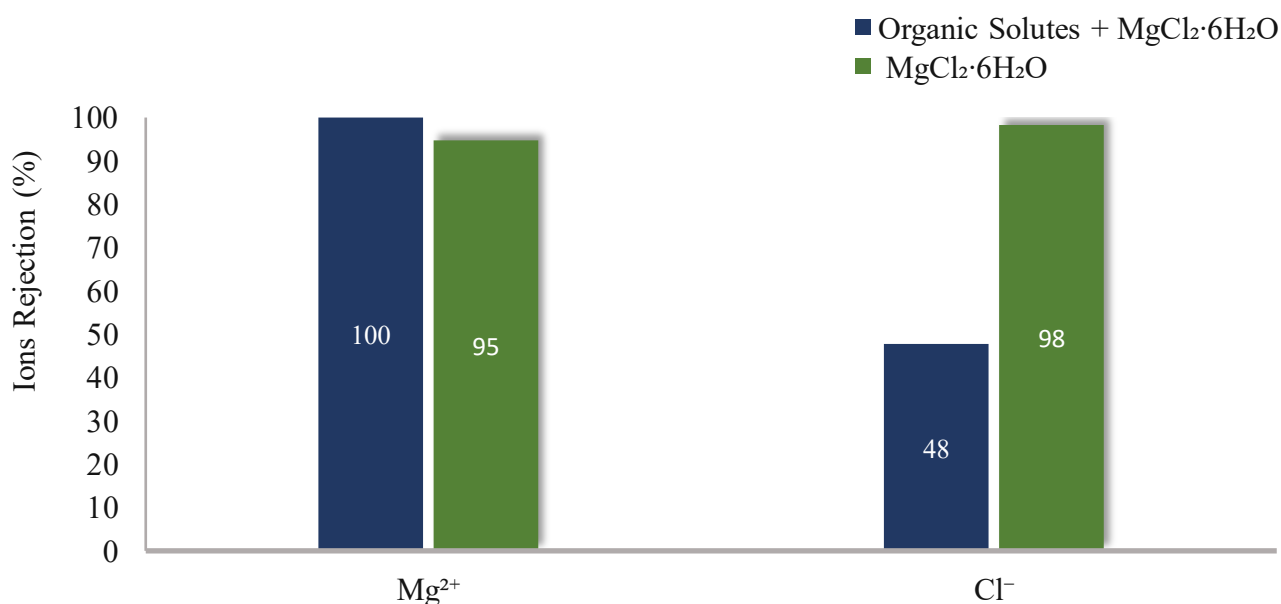


Figure 57. Ionic rejection of $\text{MgCl}_2 \cdot 6\text{H}_2\text{O}$ with and without organic solutes.

6.4.1.3 The ionic rejection of CaCl_2 with and without organic solutes

Fig 58 shows the ionic rejection of CaCl_2 with and without organic solutes. In CaCl_2 binary ionic system solution, the pH was equal to 6.7, at this pH the membrane is intended to be negatively charged. Therefore, Cl^- ions are subjected to electrostatic exclusion (Donnan exclusion) and are rejected from the membrane and Ca^{2+} ions flow backward to maintain electroneutrality. Adding the organic solutes to the CaCl_2 solution decrease pH to 2.09, the membrane became positively charged. In this case, Ca^{2+} is repelled and rejected from the membrane due to Donnan exclusion. As predicted Cl^- which is in this case counter-ion permeate through the membrane.

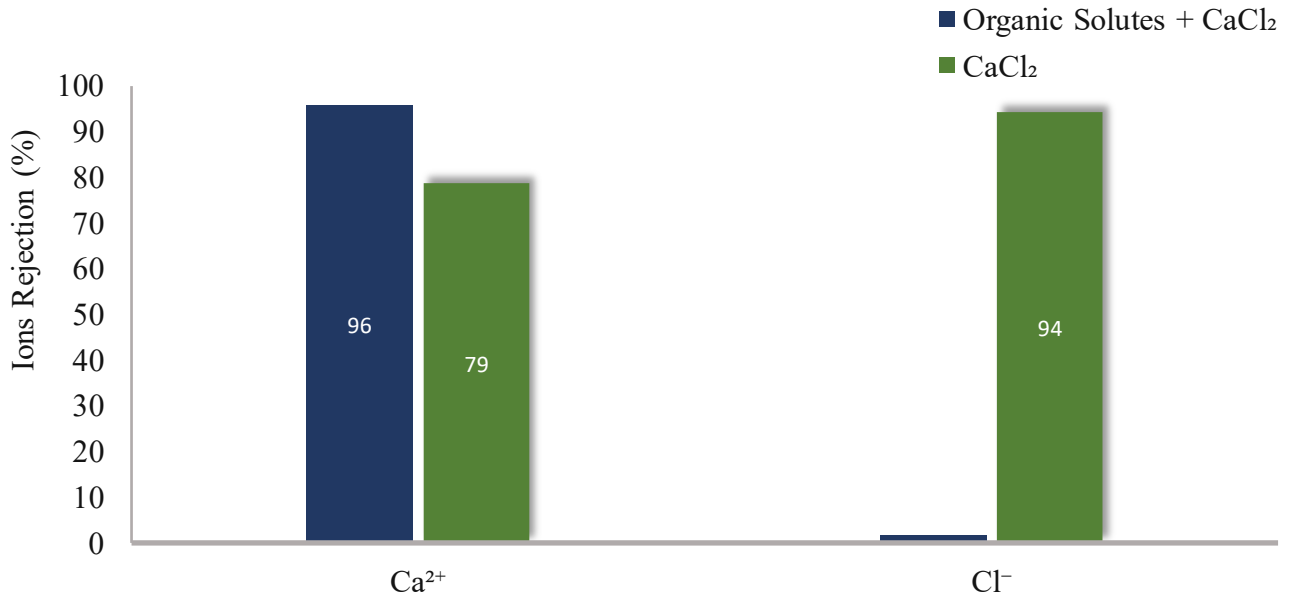


Figure 58. The ionic rejection of CaCl₂ with and without organic solutes.

6.4.1.4 The ionic rejection of Na₂SO₄ with and without organic solutes

Fig 59 confirms that cations with a greater charge density are rejected from similar charge membranes more than cations with a lower charge density, and anions are more adsorbed than cations on the surface of different charge membranes.

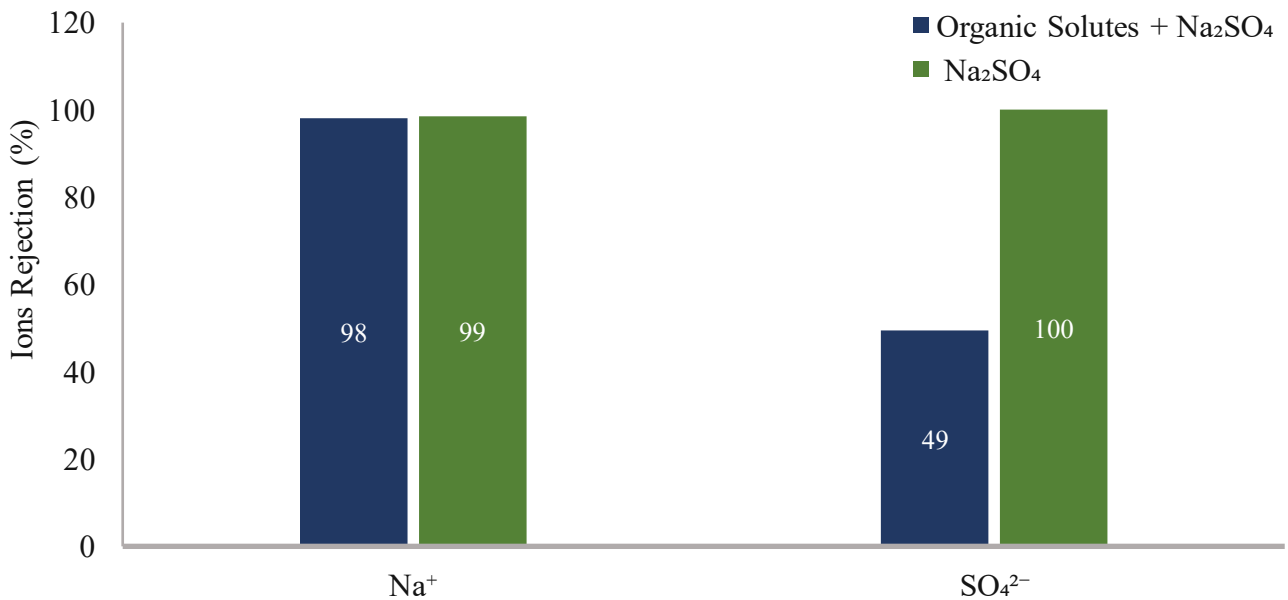


Figure 59. The ionic rejection of Na₂SO₄ with and without organic solutes.

6.4.1.5 The ionic rejection of NH₄Cl with and without organic solutes

Fig 60 shows the ionic rejection of NH₄Cl with and without Organic solutes.

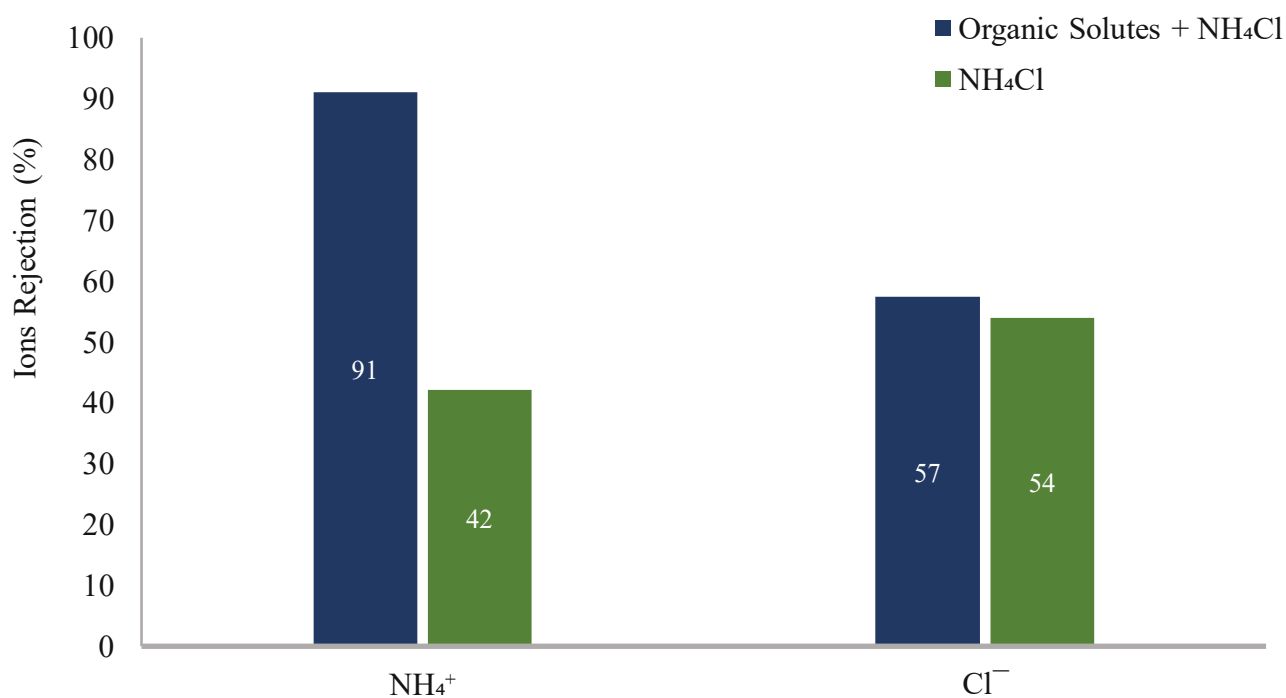


Figure 60. The ionic rejection of NH₄Cl with and without organic solutes.

In NH₄Cl binary ionic system solution, the pH was equal to 6.84, at this pH the membrane is intended to be negatively charged. Therefore, Cl⁻ ions are subjected to electrostatic exclusion (Donnan exclusion) and are rejected from the membrane and NH₄⁺ ions flow backward to maintain electroneutrality. Adding the organic solutes to NH₄Cl solution decrease pH to 2.1, the membrane became positively charged. In this case, NH₄⁺ is repelled and rejected from the membrane due to Donnan exclusion. It was predicted that Cl⁻ which is in this case counter-ion to permeate through the membrane but it flows back to bulk feed for maintaining electroneutrality.

6.4.1.6 The ionic rejection of KOH with and without organic solutes

Figure 61 shows the change of K⁺ rejection only because the Thermo Fisher Scientific's Dionex ICS-5000+ ion chromatography system does not measure the OH⁻ concentration.

Adding the organic solutes to KOH solution decrease pH to 2.44, the membrane became positively charged. In this case, K⁺ is repelled and rejected from the membrane due to Donnan exclusion.

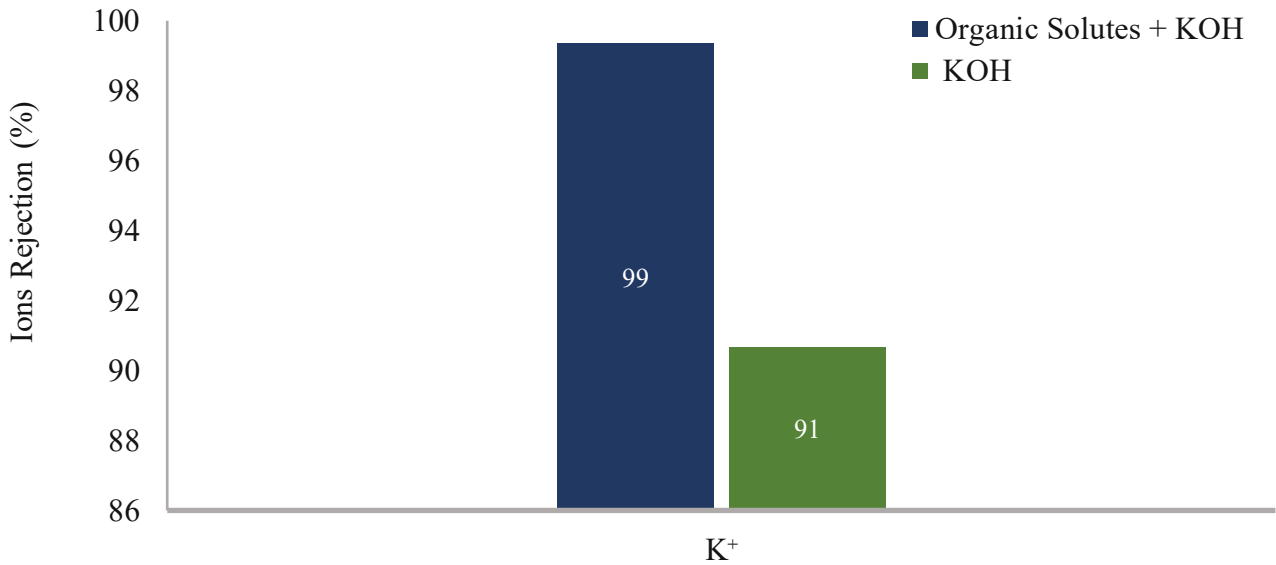


Figure 61. The ionic rejection of KOH with and without organic solutes.

6.4.2 LA separation performance from the model solution with and without a ternary ionic system

Fig 62 shows the following results:

- The rejection of LA in the presence of NaCl + MgCl₂·6H₂O increased by 14.8% and that the rejection of AA increased by 43.2% while the rejection of Glu and Fru was not affected. On the other hand, the permeate flux of the solution decreased by 3.9% in the presence of NaCl + MgCl₂·6H₂O.

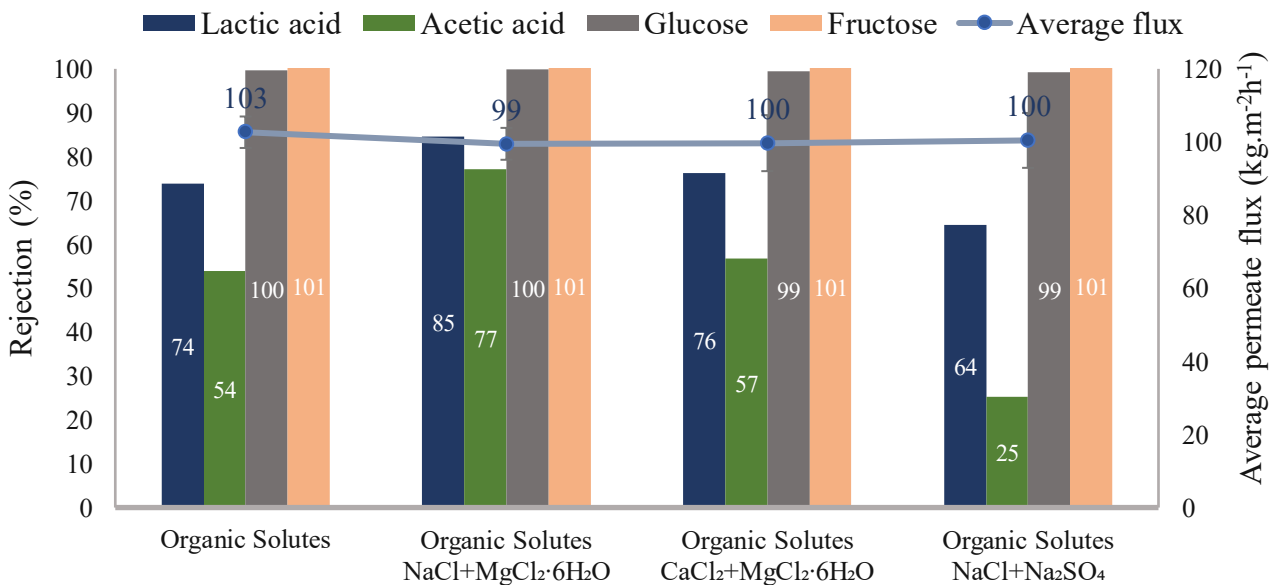


Figure 62. The permeate flux and the rejection of LA, AA, Glu, and Fru with and without a ternary ionic system using NF-Alfa Laval Membrane at p = 32 bar, T = 25 °C.

- The rejection of LA in the presence of CaCl₂ + MgCl₂·6H₂O decreased by 22.9% and that the rejection of AA increased by 5.4% while the rejection of Glu and Fru was not affected. On the

other hand, the permeate flux of the solution decreased by 2.9% in the presence of $\text{CaCl}_2 + \text{MgCl}_2 \cdot 6\text{H}_2\text{O}$.

- The rejection of LA in the presence of $\text{NaCl} + \text{Na}_2\text{SO}_4$ decreased by 12.8% and that the rejection of AA decreased by 53% while the rejection of Glu and Fru was not affected. On the other hand, the permeate flux of the solution decreased by 2.9% in the presence of $\text{NaCl} + \text{Na}_2\text{SO}_4$.

The rejection variation of LA and AA also the variation in solution permeate flux by adding ternary ionic system ($(\text{Mg}^{2+} + \text{Na}^+ + \text{Cl}^-)$, $(\text{Na}^+ + \text{Cl}^- + \text{SO}_4^{2-})$, or $(\text{Mg}^{2+} + \text{Ca}^{2+} + \text{Cl}^-)$) can be explained as a consequence of pore swelling /shrinking, Hofmeister effect, distribution of pore sizes, compression of the electrical double layer, the molecules' polarizability, and salt osmotic pressure. On the other hand, the rejection of Glu and Fru may be due to a steric hindrance effect since all membranes were compacted before the filtering procedure, which was unaffected by the adding ternary ionic system.

6.4.2.1 The ionic rejection of $\text{NaCl} + \text{MgCl}_2 \cdot 6\text{H}_2\text{O}$ with and without organic solutes

Figure 63 shows the ionic rejection of $\text{NaCl} + \text{MgCl}_2 \cdot 6\text{H}_2\text{O}$ with and without organic solutes. In $\text{NaCl} + \text{MgCl}_2 \cdot 6\text{H}_2\text{O}$ ternary ionic system solution the pH was equal to 6.88, at this pH the membrane is intended to be negatively charged. Therefore, Cl^- ions are subjected to electrostatic exclusion (Donnan exclusion) and are rejected from the membrane. Among all the ions, the rejection of monovalent counter-ion Na^+ in the presence of divalent counter-ion Mg^{2+} was the lowest. Mg^{2+} ions also flow backward to maintain electroneutrality.

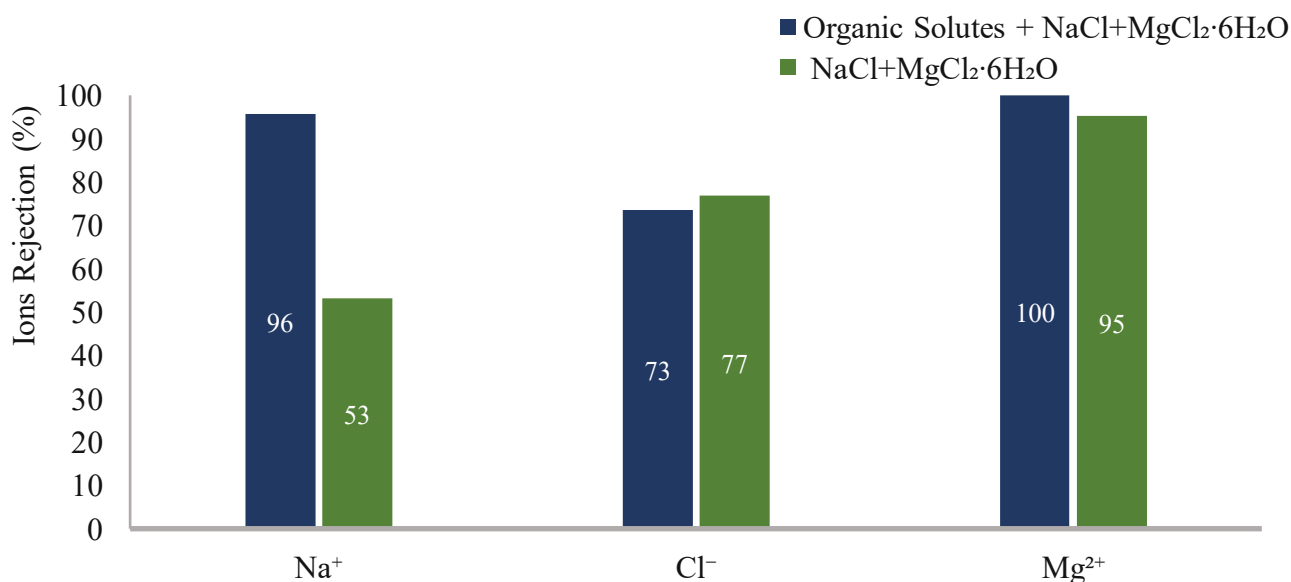


Figure 63. The ionic rejection of $\text{NaCl} + \text{MgCl}_2 \cdot 6\text{H}_2\text{O}$ with and without organic solutes.

Adding the organic solutes to the CaCl_2 solution decrease pH to 2.08, the membrane became positively charged. In this case, Mg^{2+} and Na^+ are repelled and rejected from the membrane due to

Donnan exclusion. It was predicted that Cl^- which is in this case counter-ion to permeate through the membrane but it flows back to bulk feed for maintaining electroneutrality.

6.4.2.2 The ionic rejection of $\text{CaCl}_2 + \text{MgCl}_2 \cdot 6\text{H}_2\text{O}$ with and without organic solutes

Fig 64 shows the ionic rejection of $\text{CaCl}_2 + \text{MgCl}_2 \cdot 6\text{H}_2\text{O}$ with and without organic solutes. In $\text{CaCl}_2 + \text{MgCl}_2 \cdot 6\text{H}_2\text{O}$ ternary ionic system solution the pH was equal to 6.3, at this pH the membrane is intended to be negatively charged. Therefore, Cl^- ions are subjected to electrostatic exclusion (Donnan exclusion) and are rejected from the membrane. Mg^{2+} , Ca^{2+} ions also flow backward to maintain electroneutrality. Adding the organic solutes to $\text{CaCl}_2 + \text{MgCl}_2 \cdot 6\text{H}_2\text{O}$ solution decrease pH to 2.08, the membrane became positively charged. In this case, Mg^{2+} and Ca^{2+} are repelled and rejected from the membrane due to Donnan exclusion. It was predicted that Cl^- which is in this case counter-ion to permeate through the membrane but it flows back to bulk feed for maintaining electroneutrality.

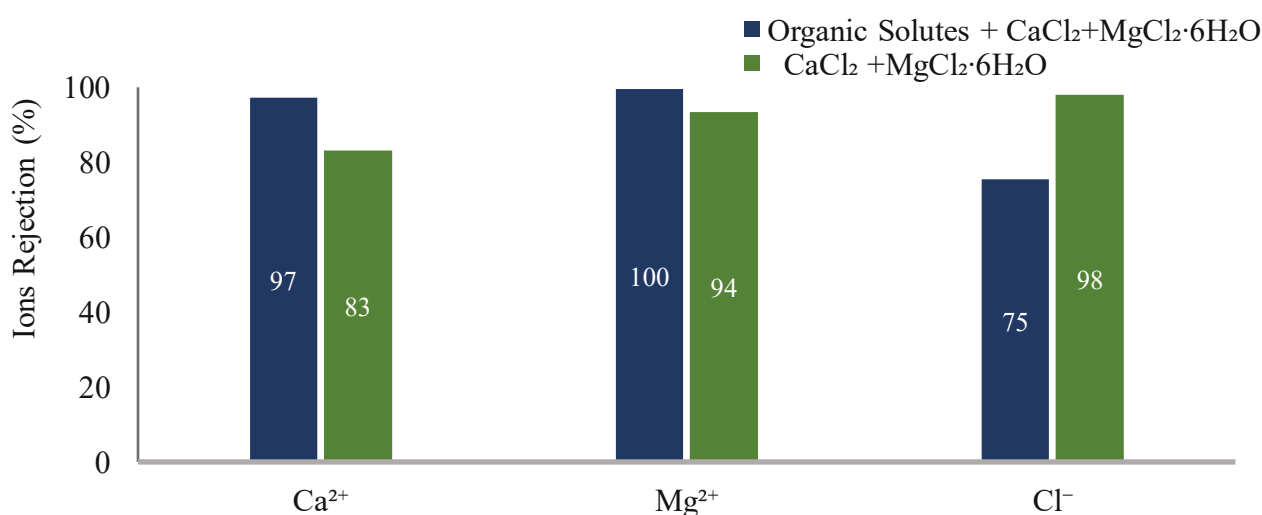


Figure 64. The ionic rejection of $\text{CaCl}_2 + \text{MgCl}_2 \cdot 6\text{H}_2\text{O}$ with and without organic solutes.

6.4.2.3 The ionic rejection of $\text{NaCl} + \text{Na}_2\text{SO}_4$ with and without organic solutes

Fig 65 shows the ionic rejection of $\text{NaCl} + \text{Na}_2\text{SO}_4$ with and without Organic solutes. In $\text{NaCl} + \text{Na}_2\text{SO}_4$ ternary ionic system solution the pH was equal to 6.7, at this pH the membrane is intended to be negatively charged. Therefore, SO_4^{2-} ions are subjected to electrostatic exclusion (Donnan exclusion) and are rejected entirely from the membrane. The retention of Na^+ ions was 68 percent and is strongly dependent on the electroneutrality-induced rejection of SO_4^{2-} ions. Since SO_4^{2-} ion could not permeate the membrane due to its divalent charge and relatively higher hydrated radii, Cl^- ions were forced to penetrate with Na^+ ions to maintain electroneutrality on both sides of the membrane.

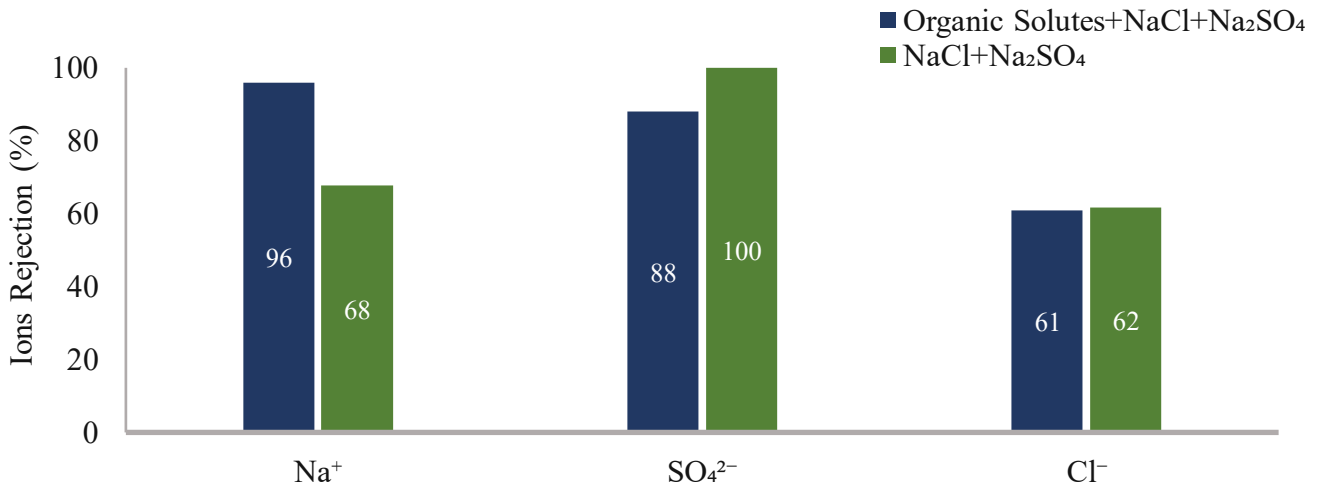


Figure 65. The ionic rejection of NaCl + Na₂SO₄ with and without organic solutes.

Adding the organic solutes to NaCl + Na₂SO₄ solution decrease pH to 2.08, the membrane became positively charged. In this case, Na⁺ is repelled and rejected from the membrane due to Donnan exclusion. It was predicted that Cl⁻ which is in this case counter-ion to permeate through the membrane but it flows back to bulk feed for maintaining electroneutrality.

6.4.3 LA separation performance from the model solution with and without a quaternary ionic system.

Fig 66 shows the following results:

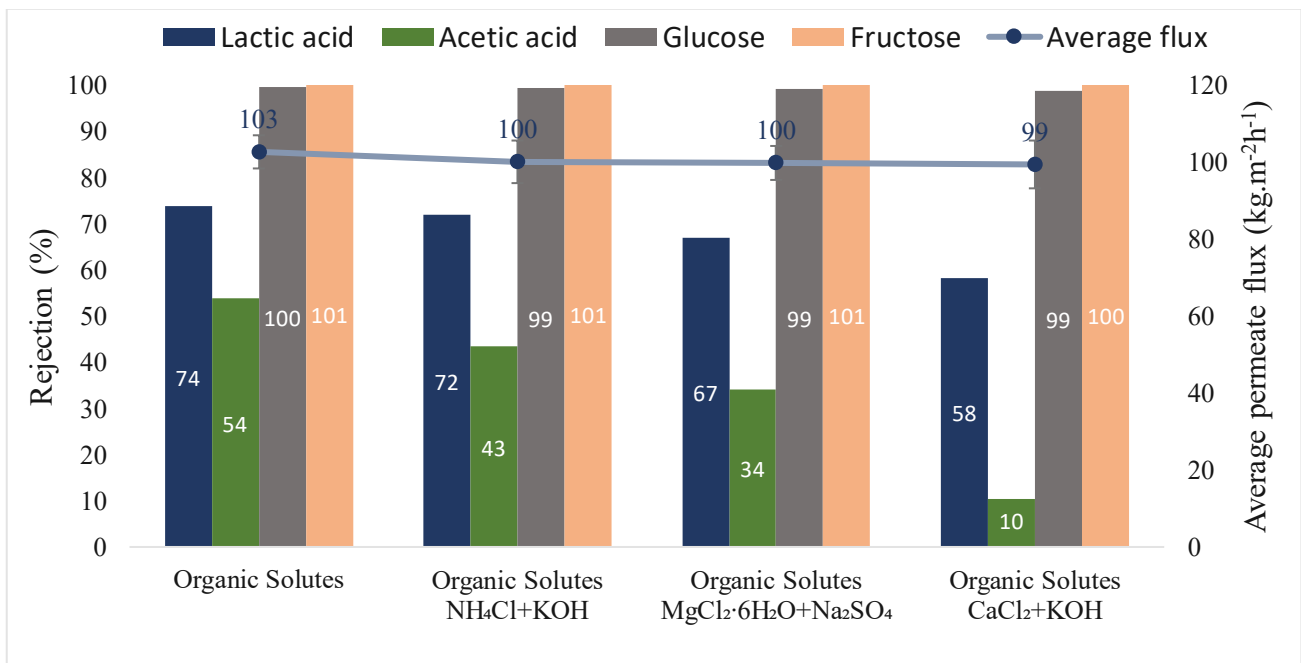


Figure 66. The permeate flux and the rejection of LA, AA, Glu, and Fru with and without a quaternary ionic system using NF-Alfa Laval Membrane at p = 32 bar, T = 25 °C.

- The rejection of LA in the presence of $\text{NH}_4\text{Cl} + \text{KOH}$ decreased by 2.6% and that the rejection of AA decreased by 19.5% while the rejection of Glu and Fru was not affected. On the other hand, the permeate flux of the solution decreased by 2.9% in the presence of $\text{NH}_4\text{Cl} + \text{KOH}$.
- The rejection of LA in the presence of $\text{MgCl}_2 \cdot 6\text{H}_2\text{O} + \text{Na}_2\text{SO}_4$ decreased by 9.2% and that the rejection of AA decreased by 36.7% while the rejection of Glu and Fru was not affected. On the other hand, the permeate flux of the solution decreased by 3% in the presence of $\text{MgCl}_2 \cdot 6\text{H}_2\text{O} + \text{Na}_2\text{SO}_4$.
- The rejection of LA in the presence of $\text{CaCl}_2 + \text{KOH}$ decreased by 21% and that the rejection of AA decreased by 80.8% while the rejection of Glu and Fru was not affected. On the other hand, the permeate flux of the solution decreased by 3.5% in the presence of $\text{CaCl}_2 + \text{KOH}$.

The rejection variation of LA and AA also the variation in solution permeate flux by adding quaternary ionic system ($(\text{NH}_4^+ + \text{Cl}^- + \text{K}^+ + \text{OH}^-)$, $(\text{Na}^+ + \text{Cl}^- + \text{Mg}^{2+} + \text{SO}_4^{2-})$, or $(\text{Ca}^{2+} + \text{Cl}^- + \text{K}^+ + \text{OH}^-)$) can be explained as a consequence of pore swelling /shrinking, Hofmeister effect, distribution of pore sizes, compression of the electrical double layer, the molecules' polarizability, and salt osmotic pressure. On the other hand, the rejection of Glu and Fru may be due to a steric hindrance effect since all membranes were compacted before the filtering procedure, which was unaffected by the adding quaternary ionic system.

6.4.3.1 The ionic rejection of $\text{NH}_4\text{Cl} + \text{KOH}$ with and without organic solutes

Fig 67 shows the ionic rejection of NH_4^+ , Cl^- , K^+ with and without Organic solutes because the Thermo Fisher Scientific's Dionex ICS-5000+ ion chromatography system does not measure the OH^- concentration.

In $\text{NH}_4\text{Cl} + \text{KOH}$ quaternary ionic system solution the pH was equal to 9.8, at this pH the membrane is intended to be negatively charged. Therefore, Cl^- ions are subjected to electrostatic exclusion (Donnan exclusion) and are rejected from the membrane. K^+ ions also flow backward to maintain electroneutrality. While NH_4^+ permeates through the membrane. Adding the organic solutes to $\text{NH}_4\text{Cl} + \text{KOH}$ solution decrease pH to 2.45, the membrane became positively charged. In this case, K^+ , and NH_4^+ are repelled and rejected from the membrane due to Donnan exclusion. It was predicted that Cl^- which is in this case counter-ion to permeate through the membrane but it flows back to bulk feed for maintaining electroneutrality.

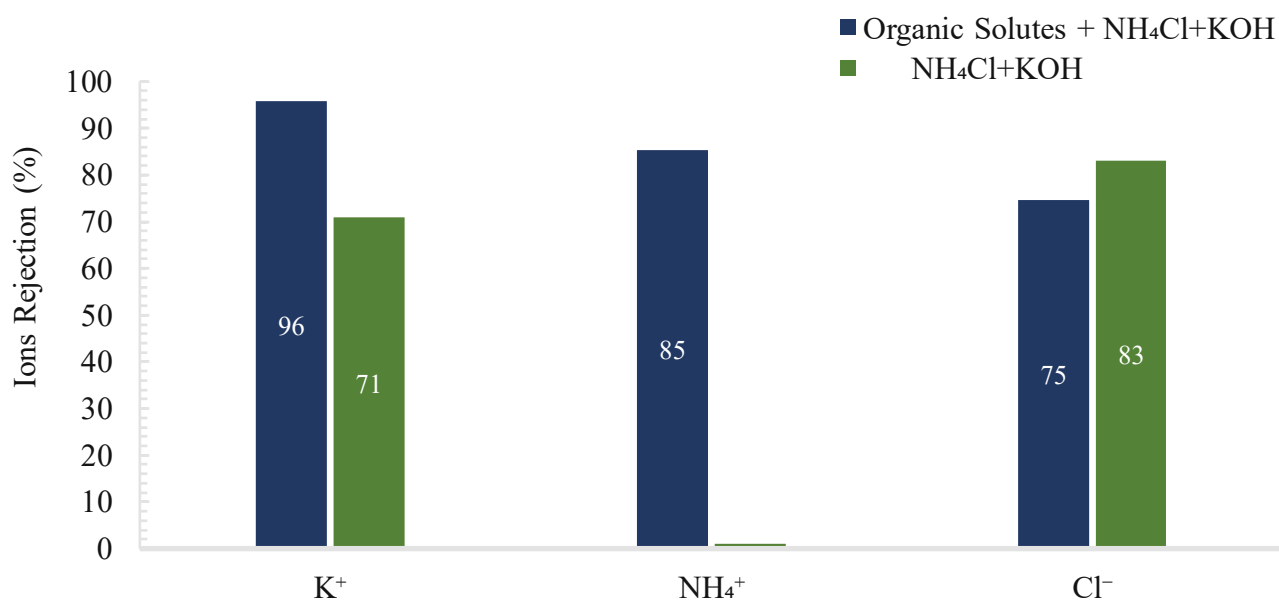


Figure 67. The ionic rejection of $\text{NH}_4\text{Cl} + \text{KOH}$ with and without organic solutes.

6.4.3.2 The ionic rejection of $\text{MgCl}_2 \cdot 6\text{H}_2\text{O} + \text{Na}_2\text{SO}_4$ with and without organic solutes

Fig 68 shows the ionic rejection of $\text{MgCl}_2 \cdot 6\text{H}_2\text{O} + \text{Na}_2\text{SO}_4$ with and without Organic solutes.

In $\text{MgCl}_2 \cdot 6\text{H}_2\text{O} + \text{Na}_2\text{SO}_4$ quaternary ionic system solution the pH was equal to 7, at this pH the membrane is intended to be negatively charged. Therefore, SO_4^{2-} being divalent co-ions showed extreme electrostatic exclusion with membrane resulting in high rejection (100%), Mg^{2+} ions also flow backward to maintain electroneutrality.

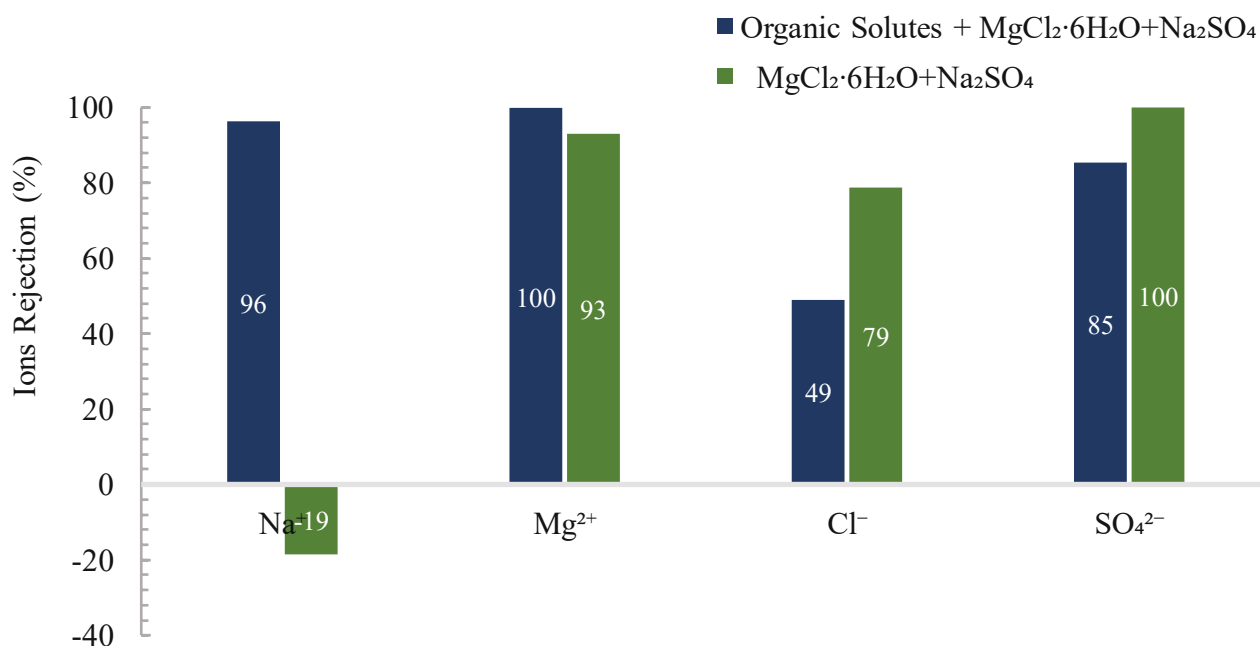


Figure 68. The ionic rejection of $\text{MgCl}_2 \cdot 6\text{H}_2\text{O} + \text{Na}_2\text{SO}_4$ with and without organic solutes.

Na⁺ ions shield the membrane charge to offer Cl⁻ ions a reduced electrostatic exclusion from the membrane. Adding the organic solutes to MgCl₂·6H₂O + Na₂SO₄ solution decrease pH to 2.08, the membrane became positively charged. In this case, Mg²⁺, and Na⁺ are repelled and rejected from the membrane due to Donnan exclusion. . SO₄²⁻ ions also flow backward to maintain electroneutrality. It is important to note that Cl⁻ has lower retention than SO₄²⁻.

6.4.3.3 The ionic rejection of CaCl₂ + KOH with and without organic solutes

Fig 69 shows the ionic rejection of Ca²⁺, Cl⁻, and K⁺ only with and without Organic solutes because the Thermo Fisher Scientific's Dionex ICS-5000+ ion chromatography system does not measure the OH⁻ concentration.

In CaCl₂+ KOH quaternary ionic system solution the pH was equal to 12.06, at this pH the membrane is intended to be negatively charged. Therefore, Cl⁻ ions are exposed to Donnan exclusion and are rejected from the membrane, K⁺ ions also flow backward to maintain electroneutrality. Simultaneously, since Ca²⁺ is a divalent ion, it cannot pass through the membrane. Adding the organic solutes to CaCl₂+ KOH solution decrease pH to 2.43, the membrane became positively charged. In this case, Ca²⁺, K⁺ are repelled and rejected from the membrane due to Donnan exclusion, and Cl⁻ has lower retention than K⁺, Ca²⁺.

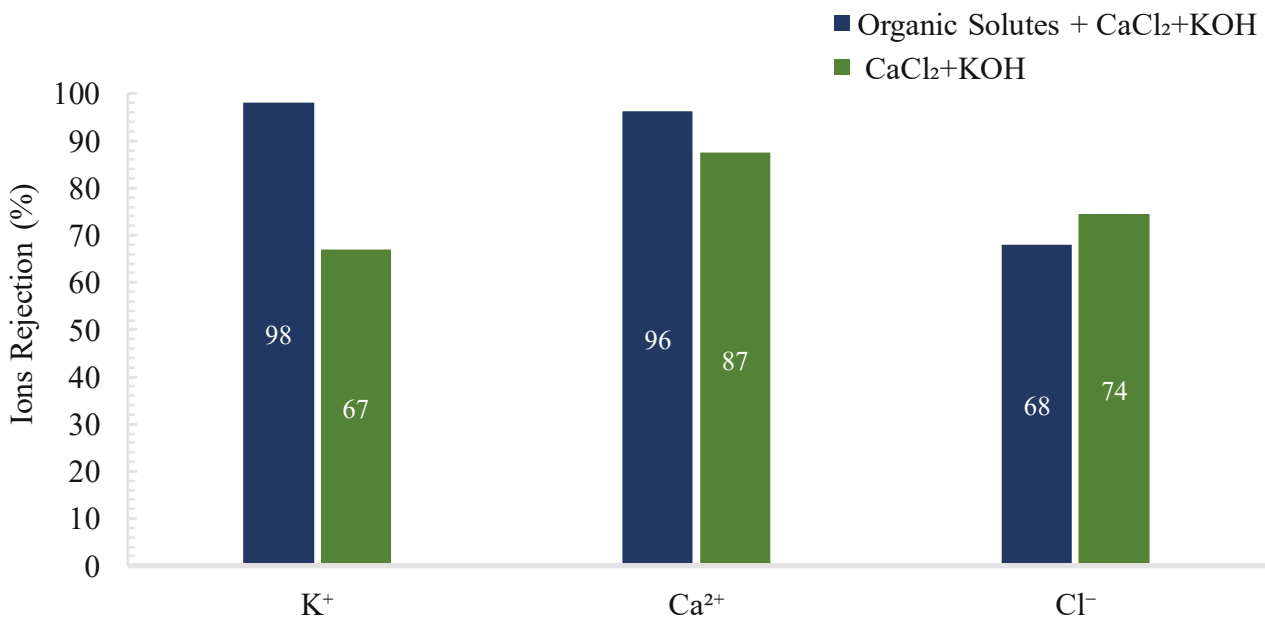


Figure 69. The ionic rejection of CaCl₂ + KOH with and without organic solutes.

6.4.4 LA separation performance from the model solution with and without an octonary ionic system

Fig 70 shows that the rejection of LA in the presence of $\text{NaCl} + \text{MgCl}_2 \cdot 6\text{H}_2\text{O} + \text{CaCl}_2 + \text{Na}_2\text{SO}_4 + \text{NH}_4\text{Cl} + \text{KOH}$ decreased by 22.6% and that the rejection of AA decreased by 98% while the rejection of Glu and Fru was not affected.

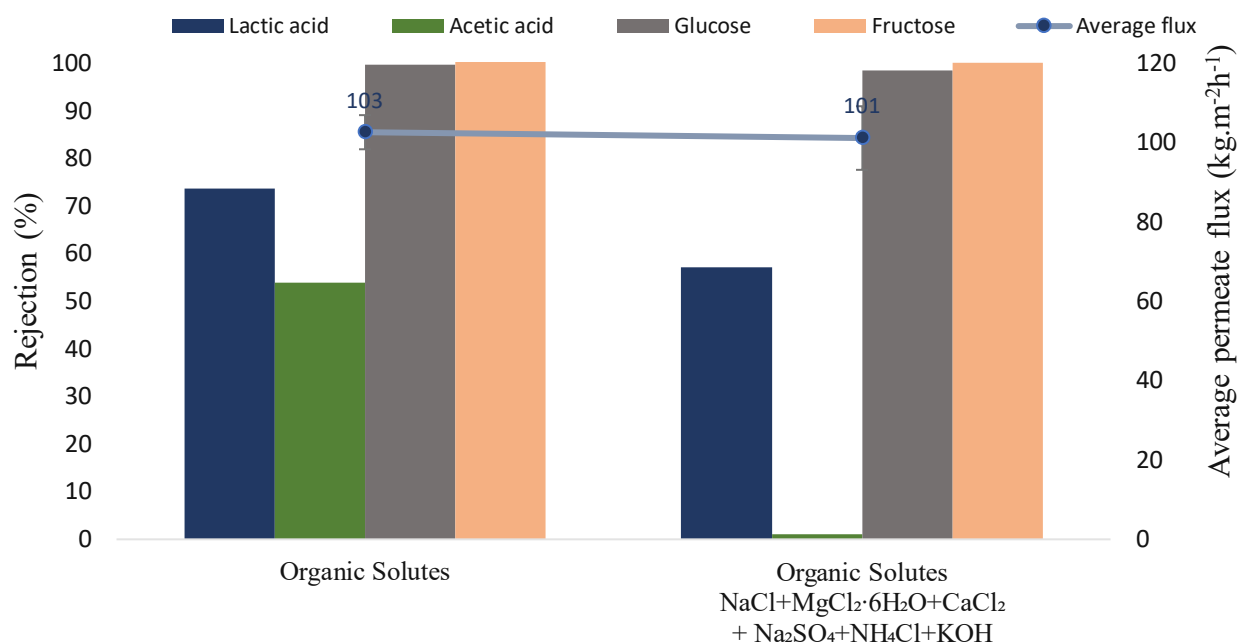


Figure 70. The permeate flux and the rejection of LA, AA, Glu, and Fru with and without an octonary ionic system using NF-Alfa Laval Membrane at $p = 32$ bar, $T = 25$ °C.

On the other hand, the permeate flux of the solution decreased by 1.7% in the presence of $\text{NaCl} + \text{MgCl}_2 \cdot 6\text{H}_2\text{O} + \text{CaCl}_2 + \text{Na}_2\text{SO}_4 + \text{NH}_4\text{Cl} + \text{KOH}$.

The rejection variation of LA and AA also the variation in solution permeate flux by adding octonary ionic system ($\text{Na}^+ + \text{K}^+ + \text{NH}_4^+ + \text{Mg}^{2+} + \text{Ca}^{2+} + \text{OH}^- + \text{Cl}^- + \text{SO}_4^{2-}$) can be explained as a consequence of pore swelling /shrinking, Hofmeister effect, distribution of pore sizes, compression of the electrical double layer, the molecules' polarizability, and salt osmotic pressure. On the other hand, the rejection of Glu and Fru may be due to a steric hindrance effect since all membranes were compacted before the filtering procedure, which was unaffected by the adding octonary ionic system.

6.4.4.1 The ionic rejection of $\text{NaCl} + \text{MgCl}_2 \cdot 6\text{H}_2\text{O} + \text{CaCl}_2 + \text{Na}_2\text{SO}_4 + \text{NH}_4\text{Cl} + \text{KOH}$ with and without organic solutes

Figure 71 shows the ionic rejection of Na^+ , K^+ , NH_4^+ , Ca^{2+} , Mg^{2+} , Cl^- , SO_4^{2-} only with and without Organic solutes because the Thermo Fisher Scientific's Dionex ICS-5000+ ion chromatography system does not measure the OH^- concentration.

In $\text{NaCl} + \text{MgCl}_2 \cdot 6\text{H}_2\text{O} + \text{CaCl}_2 + \text{Na}_2\text{SO}_4 + \text{NH}_4\text{Cl} + \text{KOH}$ octonary ionic system solution the pH was equal to 9.91, at this pH, the membrane is intended to be negatively charged, SO_4^{2-} being divalent co-ions showed extreme electrostatic exclusion with membrane resulting in high rejection. The Cl^- ions are exposed to Donnan exclusion and are rejected 67.07% from the membrane; Na^+ , K^+ , NH_4^+ ions also flow backward to maintain electroneutrality. Simultaneously, Ca^{2+} and Mg^{2+} are divalent ions and have a high rejection rate because they cannot pass through the membrane.

Adding the organic solutes to $\text{NaCl} + \text{MgCl}_2 \cdot 6\text{H}_2\text{O} + \text{CaCl}_2 + \text{Na}_2\text{SO}_4 + \text{NH}_4\text{Cl} + \text{KOH}$ solution decrease pH to 2.31, the membrane became positively charged. In this case, Na^+ , K^+ , NH_4^+ , Ca^{2+} , Mg^{2+} are repelled and rejected from the membrane due to Donnan exclusion, Cl^- flows backward to keep the electroneutrality.

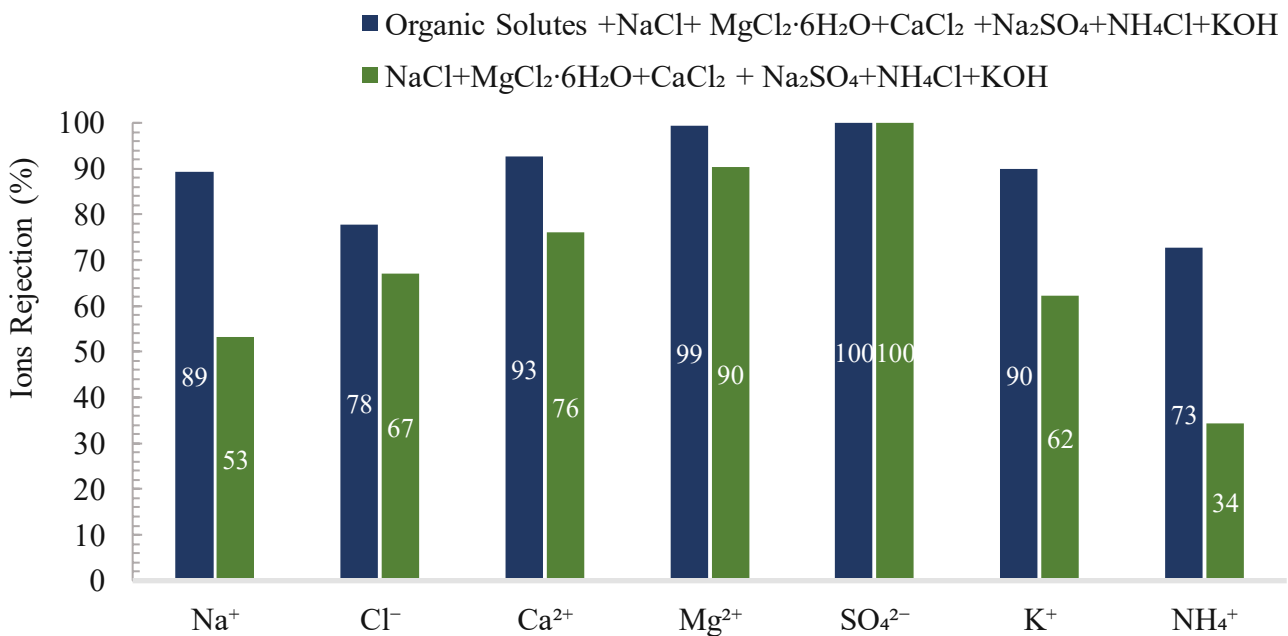


Figure 71. The ionic rejection of $\text{NaCl} + \text{MgCl}_2 \cdot 6\text{H}_2\text{O} + \text{CaCl}_2 + \text{Na}_2\text{SO}_4 + \text{NH}_4\text{Cl} + \text{KOH}$ with and without organic solutes.

7. Summary and conclusions

In the present work, various experiments were conducted initially on four commercially available NF membranes (NF-Alfa Laval, NF Toray, NF270, and Selro MPF-36) using pure LA solution with change the operating temperature and pH values to determine the optimal operating temperature and pH value for LA recovery. Furthermore, additional experiments were conducted using these four different commercially available NF membranes using the synthetic grass silage (Model solution) at the determined optimal operating temperature and pH value to determine the best membrane performance. After determining the optimal temperature, pH, and best membrane, additional experiments were conducted to investigate the effect of different minerals on the LA separation process. To accomplish this, synthetic grass silage (Model solution) was made that closely resembles the chemical composition of real grass silage juice. Complex mixtures composed entirely of minerals with and without Organic solutes were produced, and solutions containing octonary ionic, quaternary ionic, ternary ionic, or binary ionic systems were obtained. The experiments showed that:

1. The permeate flux increases with temperature increase for all four commercially available NF membranes. In addition, the LA rejection increases with the temperature increase at constant pressure and pH for NF-Alfa Laval, NF Toray, and Selro MPF-36 membranes. In contrast, the NF270 membrane's LA rejection decreases with the temperature increase. These effects may be attributed to temperature-dependent changes in membrane structural characteristics (effective pore radius, active layer thickness, membrane charge, and pore dielectric constant), solvent viscosity, and solute diffusivity.
2. The permeate flux decrease and the LA rejection increases with pH increase at constant pressure and temperature for all four commercially available NF membranes. These effects may be attributed to pH-dependent changes in membrane structural characteristics, especially membrane charge, and the ratio of lactate ions to non-dissociated LA in the feed stream.
3. The NF-Alfa Laval membrane was chosen for the subsequent investigation because it achieves a high LA recovery at room temperature and a pH value of around 2.
4. The permeate flux and the LA rejection rate by an NF-Alfa Laval membrane were changed remarkably when minerals (NaCl, $MgCl_2 \cdot 6H_2O$, $CaCl_2$, Na_2SO_4 , NH_4Cl , and KOH) were added to the organic solution.

- The rejection rate of LA and AA increased when a binary ionic system ($(K^+ + OH^-)$, or $(Na^+ + SO_4^{2-})$) were added to the solution, in opposition to; the rejection rate of LA and AA decreased when a binary ionic system ($(Na^+ + Cl^-)$, $(NH_4^+ + Cl^-)$, $(Ca^{2+} + Cl^-)$, or $(Mg^{2+} + Cl^-)$) were added to the solution.
- When ternary ionic system ($(Mg^{2+} + Na^+ + Cl^-)$, or $(Mg^{2+} + Ca^{2+} + Cl^-)$) were added to the solution, the rejection rate of LA and AA increased, in opposition to, the rejection rate of LA and AA decreased when the ternary ionic system $(Na^+ + Cl^- + SO_4^{2-})$ was added to the solution.
- When quaternary ionic systems ($(NH_4^+ + Cl^- + K^+ + OH^-)$, $(Na^+ + Cl^- + Mg^{2+} + SO_4^{2-})$, or $(Ca^{2+} + Cl^- + K^+ + OH^-)$) were added to the solution, the rejection rate of LA and AA decreased.
- When the octonary ionic system $(Na^+ + K^+ + NH_4^+ + Mg^{2+} + Ca^{2+} + OH^- + Cl^- + SO_4^{2-})$ was added to the solution, the rejection rate of LA and AA decreased.
- The addition of an ionic system (binary, ternary, quaternary, or octonary ionic system) did not affect the rejection of Glu and Fru. Since all membranes were compressed before the filtering operation, the rejection of Glu and Fru may be attributed to the steric hindrance effect.

The LA and AA rejections variation by adding minerals depending on its ionic strength as a result of Hofmeister's effects, pore swelling, the difference in the osmotic pressures of minerals, the electro-viscous effect, the compression of the electrical double layer generated at the membrane surface, and the molecules' polarizability.

On the other hand, our investigation confirmed that the membrane is positively charged when the feed solution's pH is less than 4.5 and negatively charged when the feed solution's pH is more than 4.5, as shown by the co-ions rejection behavior when they are subjected to the Donnan exclusion.

Because divalent co-ions are exposed to a stronger Donnan exclusion, they have a higher rejection rate, which may explain why salts containing divalent co-ions have a more significant impact on reducing LA and AA rejection.

Because the minerals present in grass silage juice have a positive effect on LA recovery by reducing its rejection, there is no need to separate the minerals using an ion exchanger before the NF process, especially since NF separates most of the divalent ions.

Minerals having divalent co-ions with a charge similar to that of the membrane can also be added to reduce LA rejection.

Using these four NF membranes (NF-Alfa Laval, NF Toray, NF270, and Selro MPF-36), we were unable to remove AA from grass silage juice. As a result, more studies into removing AA from grass silage juice using alternative membranes is recommended.

Minerals with constant concentrations, similar to those present in grass silage juice, were employed in this research. Therefore, in the future, the effect of varying mineral concentrations on LA recovery can be investigated.

Fig 76 shows a graphic summary of the Investigation of the presence of minerals on the LA recovery using NF membrane technology.

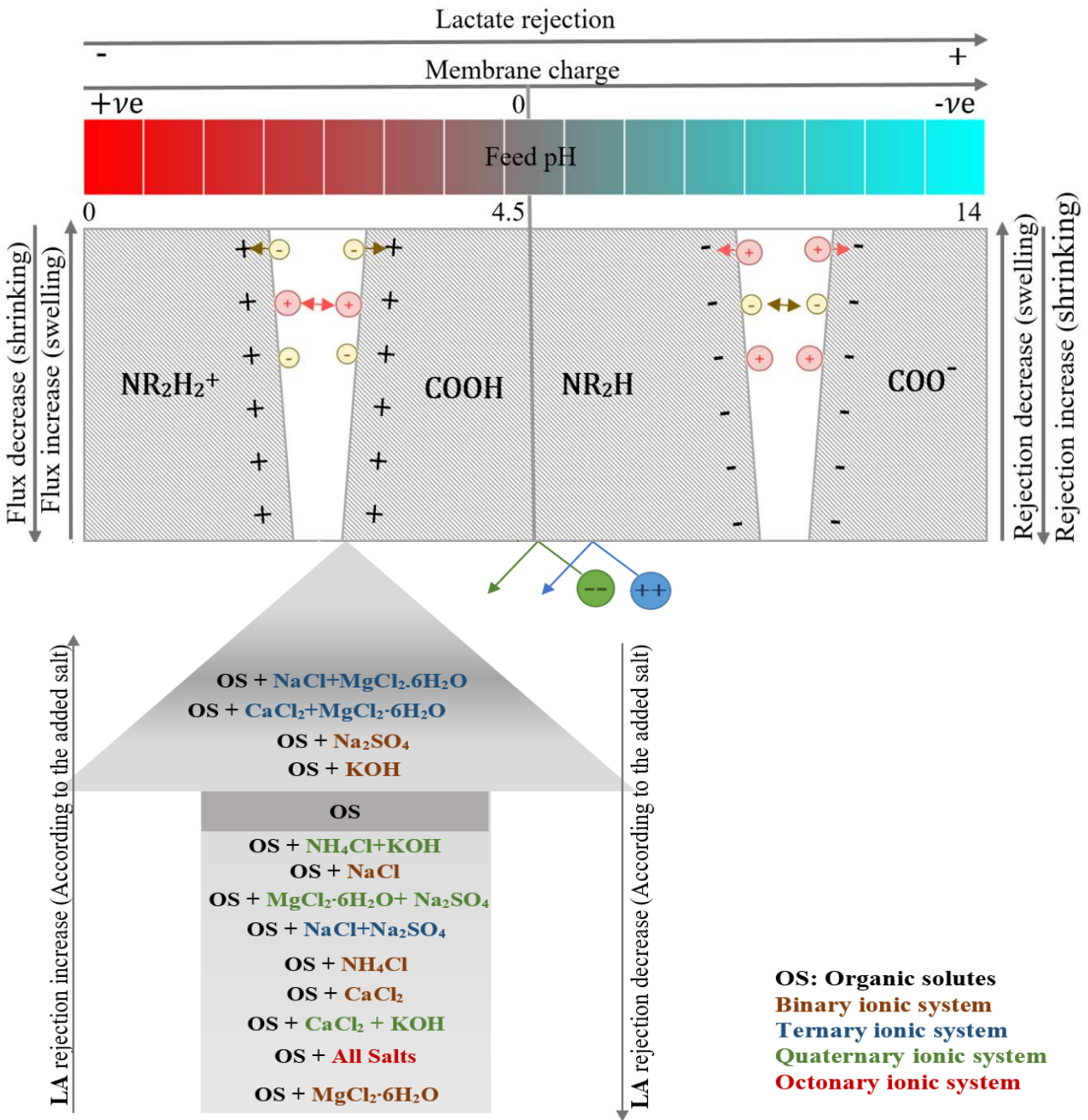


Figure 72. A graphic summary of the investigation of the presence of minerals on the LA recovery using NF membrane technology.

8. References

1. Abdullatif Tay (2000): Production of L (+)-Lactic Acid from Glucose and Starch by fermentations with immobilized cells of *Rhizopus Oryzae*. In.
2. Abedi, Elahe; Hashemi, Seyed Mohammad Bagher (2020): Lactic acid production - producing microorganisms and substrates sources-state of art. In *Heliyon* 6 (10), e04974. DOI: 10.1016/j.heliyon.2020.e04974.
3. Agler, Matthew T.; Wrenn, Brian A.; Zinder, Stephen H.; Angenent, LARGUS T. (2011): Waste to bioproduct conversion with undefined mixed cultures: the carboxylate platform. In *Trends in biotechnology* 29 (2), pp. 70–78. DOI: 10.1016/j.tibtech.2010.11.006.
4. Alves de Oliveira, Regiane; Komesu, Andrea; Vaz Rossell, Carlos Eduardo; Maciel Filho, Rubens (2018): Challenges and opportunities in lactic acid bioprocess design—from economic to production aspects. In *Biochemical Engineering Journal* 133, pp. 219–239. DOI: 10.1016/j.bej.2018.03.003.
5. Anderson, William F.; Akin, Danny E. (2008): Structural and chemical properties of grass lignocelluloses related to conversion for biofuels. In *Journal of Industrial Microbiology & Biotechnology* 35 (5), pp. 355–366. DOI: 10.1007/s10295-007-0291-8.
6. Auras, Rafael (2010): Poly (lactic acid). Synthesis, structures, properties, processing, and applications edited by Rafael Auras ... [et al.]. Hoboken N.J.: Wiley (Wiley series on polymer engineering and technology).
7. Baker, R. W. (2012): Membrane technology and applications. 3rd ed (Online-Ausg.). Chichester, U.K.: Wiley. Available online at <http://site.ebrary.com/lib/alltitles/Doc?id=10582602>.
8. Bargeman, G.; Vollenbroek, J. M.; Straatsma, J.; Schroën, C.G.P.H.; Boom, R. M. (2005): Nanofiltration of multi-component feeds. Interactions between neutral and charged components and their effect on retention. In *Journal of Membrane Science* 247 (1), pp. 11–20. DOI: 10.1016/j.memsci.2004.05.022.
9. Basile, Angelo; Figoli, Alberto; Khayet, Mohamed (Eds.) (2015): Pervaporation, Vapour Permeation and Membrane Distillation: Woodhead Publishing Series in Energy. Oxford: Woodhead Publishing.
10. BeMiller, James; Whistler, Roy (Eds.) (2009): Starch (Third Edition): Food Science and Technology. San Diego: Academic Press.
11. Big Chemical Encyclopedia (2021): Chemical substances, components, reactions, process design. Available online at <https://chempedia.info/info/dcfrr/>.

References

12. Castillo Martínez, Fabio Andres; Balciunas, Eduardo Marcos; Salgado, José Manuel; Domínguez González, José Manuel; Converti, Attilio; Oliveira, Ricardo Pinheiro de Souza (2013): Lactic acid properties, applications and production: A review. In *Trends in Food Science & Technology* 30 (1), pp. 70–83. DOI: 10.1016/j.tifs.2012.11.007.
13. Cavaco Morão, A. I.; Szymczyk, A.; Fievet, P.; Brites Alves, A. M. (2008): Modelling the separation by nanofiltration of a multi-ionic solution relevant to an industrial process. In *Journal of Membrane Science* 322 (2), pp. 320–330. DOI: 10.1016/j.memsci.2008.06.003.
14. Charcosset, Catherine (Ed.) (2012): *Membrane Processes in Biotechnology and Pharmaceutics*. Amsterdam: Elsevier.
15. Chen, Yixing; Okur, Halil I.; Liang, Chungwen; Roke, Sylvie (2017): Orientational ordering of water in extended hydration shells of cations is ion-specific and is correlated directly with viscosity and hydration free energy. In *Physical Chemistry Chemical Physics* 19 (36), 11. 24678–24688. DOI: 10.1039/c7cp03395h.
16. Choi, Jong-il; Hong, Won Hi (1999): Recovery of Lactic Acid by Batch Distillation with Chemical Reactions Using Ion Exchange Resin. In *Journal of Chemical Engineering of Japan* 32, pp. 184–189.
17. Compounds Identification (2021): D-Lactic acid (YMDB00287),L-Lactic acid (YMDB00247). Available online at <http://www.ymdb.ca/compounds/YMDB00287>.
18. Corona, Andrea; Ambye-Jensen, Morten; Vega, Giovanna Croxatto; Hauschild, Michael Zwicky; Birkved, Morten (2018): Techno-environmental assessment of the green biorefinery concept: Combining process simulation and life cycle assessment at an early design stage. In *The Science of the total environment* 635, pp. 100–111. DOI: 10.1016/j.scitotenv.2018.03.357.
19. Dai, Zhongde; Ansaloni, Luca; Deng, Liyuan (2016): Recent advances in multi-layer composite polymeric membranes for CO₂ separation: A review. In *Green Energy & Environment* 1 (2), pp. 102–128. DOI: 10.1016/j.gee.2016.08.001.
20. Danner, H.; Madzingaidzo, L.; Holzer, M.; Mayrhuber, L.; Braun, R. (2000): Extraction and purification of lactic acid from silages. In *Bioresource Technology* 75 (3), pp. 181–187. DOI: 10.1016/S0960-8524(00)00068-7.
21. Ecker, J.; Raab, T.; Harasek, M. (2012): Nanofiltration as key technology for the separation of LA and AA. In *Journal of Membrane Science* 389, pp. 389–398. DOI: 10.1016/j.memsci.2011.11.004.
22. Eş, Ismail; Mousavi Khaneghah, Amin; Barba, Francisco J.; Saraiva, Jorge A.; Sant'Ana, Anderson S.; Hashemi, Seyed Mohammad Bagher (2018): Recent advancements in lactic acid

References

23. production - a review. In *Food research international* (Ottawa, Ont.) 107, pp. 763–770. DOI: 10.1016/j.foodres.2018.01.001.
24. Evangelista, Roque L.; Nikolov, Zivko L. (1996): Recovery and purification of lactic acid from fermentation broth by adsorption. In *Applied Biochemistry and Biotechnology* 57 (1), p. 471. DOI: 10.1007/BF02941727.
25. Factory of Tomorrow (2001): Green Biorefinery - Separation of Lactic Acid from Grass Silage Juice (Brown Juice). Available online at <https://nachhaltigwirtschaften.at/en/fdz/projects/green-biorefinery-separation-of-lactic-acid-from-grass-silage-juice-brown-juice.php>.
26. Gao, Chao; Ma, Cuiqing; Xu, Ping (2011): Biotechnological routes based on lactic acid production from biomass. In *Biotechnology advances* 29 (6), pp. 930–939. DOI: 10.1016/j.biotechadv.2011.07.022.
27. Goeweil (2021): Grass silage bale. Available online at <https://www.goeweil.com/en/round-bale-silage-or-bunker-silo/>.
28. González, M. Isabel; Alvarez, Silvia; Riera, Francisco A.; Álvarez, Ricardo (2008): Lactic acid recovery from whey ultrafiltrate fermentation broths and artificial solutions by nanofiltration. In *Desalination* 228 (1), pp. 84–96. DOI: 10.1016/j.desal.2007.08.009.
29. Handojo, L.; Wardani, A. K.; Regina, D.; Bella, C.; Kresnowati, M. T. A. P.; Wenten, I. G. (2019): Electro-membrane processes for organic acid recovery. In *RSC Adv* 9 (14), pp. 7854–7869. DOI: 10.1039/C8RA09227C.
30. Heriban, V.; Škára, J.; Šturdík, E.; Ilavský, J. (1993): Isolation of free lactic acid using electro dialysis. In *Biotechnology Techniques* 7 (1), pp. 63–68. DOI: 10.1007/BF00151092.
31. Kellogg, E. A. (2001): Evolutionary history of the grasses. In *Plant physiology* 125 (3), pp. 1198–1205. DOI: 10.1104/pp.125.3.1198.
32. Kern (2020): What Are the Chemical Structure of Lactic Acid and Lactate and How Is Lactic Acid Made? Available online at <https://www.acne.org/what-are-the-chemical-structure-of-lactic-acid-and-lactate-and-how-is-lactic-acid-made.html>.
33. Kilduff, James E.; Mattaraj, Supatpong; Belfort, Georges (2004): Flux decline during nanofiltration of naturally-occurring dissolved organic matter: effects of osmotic pressure, membrane permeability, and cake formation. In *Journal of Membrane Science* 239 (1), pp. 39–53. DOI: 10.1016/j.memsci.2003.12.030.
34. Koros, William (2001): Membrane Technology in the Chemical Industry: S.P. Nunes and K.V. Peinemann (Eds.), Wiley-VCH, Weinheim, 2001, 299 pp. In *Journal of Membrane Science* 194, p. 277.

References

35. Kromus, Stefan; Wachter, B.; Koschuh, Werner; Mandl, M.; Krotscheck, Christian; Narodoslowsky, Michael (2004): The Green Biorefinery Austria - Development of an Integrated System for Green Mass Utilization. In *Nature* 18.
36. Labbez, C.; Fievet, P.; Szymczyk, A.; Vidonne, A.; Foissy, A.; Pagetti, J. (2002): Analysis of the salt retention of a titania membrane using the “DSPM” model: effect of pH, salt concentration and nature. In *Journal of Membrane Science* 208 (1), pp. 315–329. DOI: 10.1016/S0376-7388(02)00310-1.
37. Lawson, Kevin W.; Lloyd, Douglas R. (1997): Membrane distillation. In *Journal of Membrane Science* 124 (1), pp. 1–25. DOI: 10.1016/S0376-7388(96)00236-0.
38. Lee, Hee Dae; Lee, Min Yong; Hwang, Yoon Sung; Cho, Young Hoon; Kim, Hyo Won; Park, Ho Bum (2017): Separation and Purification of Lactic Acid from Fermentation Broth Using Membrane-Integrated Separation Processes. In *Industrial & Engineering Chemistry Research* 56 (29), pp. 8301–8310. DOI: 10.1021/acs.iecr.7b02011.
39. Liu, Lvdan; Kou, Ran; Liu, Guangming (2017): Ion specificities of artificial macromolecules. In *Soft Matter* 13 (1), pp. 68–80. DOI: 10.1039/C6SM01773H.
40. Mandale, Stephen; Jones, Meirion (2008): Interaction of electrolytes and non-electrolytes in nanofiltration. In *Desalination* 219 (1), pp. 262–271. DOI: 10.1016/j.desal.2007.06.005.
41. Market Analysis Report (2021): Lactic Acid Market Size, Share & Trends Analysis Report By Raw Material (Sugarcane, Corn, Cassava), By Application (PLA, Food & Beverages), By Region, And Segment Forecasts. Available online at <https://www.grandviewresearch.com/industry-analysis/lactic-acid-and-poly-lactic-acid-market>.
42. Matsumoto, Michiaki; Takahashi, Toru; Fukushima, Kenji (2003): Synergistic extraction of lactic acid with alkylamine and tri-n-butylphosphate: effects of amines, diluents and temperature. In *Separation and Purification Technology* 33 (1), pp. 89–93. DOI: 10.1016/S1383-5866(03)00002-9.
43. Melin, Thomas (2004): Membranverfahren. Grundlagen der Modul- und Anlagenauslegung. With assistance of Robert Rautenbach. 2nd ed. Berlin, Heidelberg: Springer Berlin / Heidelberg (VDI-Buch Ser). Available online at <https://ebookcentral.proquest.com/lib/kxp/detail.action?DocID=6287544>.
44. Melin, Thomas; Rautenbach, R. (2007): Membranverfahren. Grundlagen der Modul- und Anlagenauslegung. 3., aktualisierte und erw. Aufl. Berlin, New York: Springer (Chemische Technik/Verfahrenstechnik).
45. Harasek.M (2018): Membrantechnik-VO-2018-Teil1.

References

46. Mikhaylin, Sergey; Bazinet, Laurent (2016): Fouling on ion-exchange membranes: Classification, characterization and strategies of prevention and control. In *Advances in colloid and interface science* 229, pp. 34–56. DOI: 10.1016/j.cis.2015.12.006.
47. Muley, Pranjali; Boldor, Dorin (2017): *Advances in Biomass Pretreatment and Cellulosic Bioethanol Production Using Microwave Heating*.
48. Nagy, Endre (2019a): Mass Transport in the Presence of a Fouling Layer. In: *Basic Equations of Mass Transport Through a Membrane Layer*: Elsevier, pp. 317–336.
49. Nagy, Endre (2019b): Membrane Materials, Characterization, and Transport Properties. In: *Basic Equations of Mass Transport Through a Membrane Layer*: Elsevier, pp. 1–10.
50. Nyström, Marianne; Kaipia, Lena; Luque, Susana (1995): Fouling and retention of nanofiltration membranes. In *Journal of Membrane Science* 98 (3), pp. 249–262. DOI: 10.1016/0376-7388(94)00196-6.
51. Ooi, B. S.; Sum, J. Y.; Beh, J. J.; Lau, Woei Jye; Lai, S. O. (2019): Chapter 2 - Materials and Engineering Design of Interfacial Polymerized Thin Film Composite Nanofiltration Membrane for Industrial Applications. In Ahmad Fauzi Ismail, Mukhlis A. Rahman, Mohd Hafiz Dzarfan Othman, Takeshi Matsuura (Eds.): *Membrane Separation Principles and Applications: Handbooks in Separation Science*: Elsevier, pp. 47–83. Available online at <https://www.sciencedirect.com/science/article/pii/B9780128128152000028>.
52. Richard E. Muck; Brian J. Holmes (2000): FACTORS AFFECTING BUNKER SILO DENSITIES. In *Applied Engineering in Agriculture* 16, pp. 613–619.
53. Roy, Yagnaseni; Warsinger, David M.; Lienhard, John H. (2017): Effect of temperature on ion transport in nanofiltration membranes: Diffusion, convection and electromigration. In *Desalination* 420, pp. 241–257. DOI: 10.1016/j.desal.2017.07.020.
54. Schaep, Johan; Vandecasteele, Carlo (2001): Evaluating the charge of nanofiltration membranes. In *Journal of Membrane Science* 188 (1), pp. 129–136. DOI: 10.1016/S0376-7388(01)00368-4.
55. Sharma, H. S. S.; Carmichael, E.; Muhamad, M.; McCall, D.; Andrews, F.; Lyons, G. et al. (2012): Biorefining of perennial ryegrass for the production of nanofibrillated cellulose. In *RSC Advances* 2 (16), pp. 6424–6437. DOI: 10.1039/C2RA20716H.
56. Sirkar (1992): Part X Chapter 46 Other New Membrane Processes. Sirkar K K (eds) *Membrane Handbook*. New York.
57. Synder-filtration (2021): Hollow Fiber Membranes. Available online at <https://synderfiltration.Com/learning-center/articles/module-configurations-process/hollow-fiber-membranes/>.

References

58. Szymczyk, A.; Labbez, C.; Fievet, P.; Vidonne, A.; Foissy, A.; Pagetti, J. (2003): Contribution of convection, diffusion and migration to electrolyte transport through nanofiltration membranes. In *Advances in colloid and interface science* 103 (1), pp. 77–94. DOI: 10.1016/S0001-8686(02)00094-5.
59. Talebi, Sahar; Suarez, Francisco; Chen, George Q.; Chen, Xia; Bathurst, Karren; Kentish, Sandra E. (2020): Pilot Study on the Removal of Lactic Acid and Minerals from Acid Whey Using Membrane Technology. In *ACS Sustainable Chem. Eng.* 8 (7), pp. 2742–2752. DOI: 10.1021/acssuschemeng.9b06561.
60. Tan, Xiaoyao; Li, Kang (2015): *Inorganic Membrane Reactors: Fundamentals and Applications*.
61. Vezzani, Daniele; Bandini, Serena (2002): Donnan equilibrium and dielectric exclusion for characterization of nanofiltration membranes. In *Desalination* 149 (1), pp. 477–483. DOI: 10.1016/S0011-9164(02)00784-1.
62. Way Cern Khor (2017): Production of lactic acid and derivatives from grass using mixed populations. In.
63. Zhang, Li; Li, Xin; Yong, Qiang; Yang, Shang-Tian; Ouyang, Jia; Yu, Shiyuan (2015): Simultaneous saccharification and fermentation of xylo-oligosaccharides manufacturing waste residue for l-lactic acid production by *Rhizopus oryzae*. In *Biochemical Engineering Journal* 94, pp. 92–99. DOI: 10.1016/j.bej.2014.11.020.